

1-1-2007

# Optimal control of a bleed air temperature regulation system

Lan Shang  
*Ryerson University*

Follow this and additional works at: <http://digitalcommons.ryerson.ca/dissertations>



Part of the [Mechanical Engineering Commons](#)

---

## Recommended Citation

Shang, Lan, "Optimal control of a bleed air temperature regulation system" (2007). *Theses and dissertations*. Paper 303.

This Thesis is brought to you for free and open access by Digital Commons @ Ryerson. It has been accepted for inclusion in Theses and dissertations by an authorized administrator of Digital Commons @ Ryerson. For more information, please contact [bcameron@ryerson.ca](mailto:bcameron@ryerson.ca).

---

# **OPTIMAL CONTROL OF A BLEED AIR TEMPERATURE REGULATION SYSTEM**

---

by

**Lan Shang, B. Eng. (Mechanical)**  
**Beijing University of Technology, 2004**

A thesis  
presented to Ryerson University  
in partial fulfillment of the requirement for the degree of  
Master of Applied Science  
in the Program of  
Mechanical Engineering

Toronto, Ontario, Canada, 2007

©Lan Shang, 2007

## **AUTHOR'S DECLARATION**

I hereby declare that I am the sole author of this thesis.

I authorize Ryerson University to lend this thesis to other institutions or individuals for the purpose of scholarly research.

I further authorize Ryerson University to reproduce this thesis by photocopying or by other means, in total or in part, at the request of other institutions or individuals for the purpose of scholarly research.

# **ABSTRACT**

## *Optimal Control of Bleed Air Temperature Regulation System*

© Lan Shang, 2007

Master of Applied Science

in the Program of

Mechanical Engineering

**RYERSON UNIVERSITY**

This thesis investigates temperature control of an aircraft engine bleed air system, aiming at reducing ram air usage to reduce fuel consumption while maintaining fast temperature control response. To achieve both of the objectives, a system configuration is designed to control both ram air and bypass flows. The analytical equations describing the system dynamics are derived and utilized in developing the overall bleed air system model. Optimal state feedback control and output feedback control are applied in the temperature control system. Computer simulations and experiments have been conducted, and the proposed configuration and control strategy are shown to be effective in minimizing ram air usage and maintaining fast temperature control response in the meantime.



## **ACKNOWLEDGEMENT**

The author would like to express her gratitude to her supervisor, Dr. Guangjun Liu, for his guidance before, during and after the process of this thesis work.

Special thanks to Dr. C. H. Lam of Honeywell, who offered very helpful and invaluable suggestions throughout the research work.

Special thanks also to Mr. Primoz Cresnik for his helpful work on the experiment setup and very beneficial discussions.

Thanks are also due to my colleagues at the Systems and Control Laboratory of Ryerson University: Xiaojia He, Sajan Abdul, Jing Yuan, Hirmand Nouraei, Richard Mohamed, Sung Koh and Yugang Liu for their beneficial discussions on control theories and contributions in developing the test rig setup.

# TABLE OF CONTENTS

<b>ABSTRACT.....</b>	<b>III</b>
<b>ACKNOWLEDGEMENT.....</b>	<b>IV</b>
<b>TABLE OF CONTENTS .....</b>	<b>V</b>
<b>LIST OF FIGURES .....</b>	<b>VII</b>
<b>LIST OF TABLES .....</b>	<b>X</b>
<b>NOMENCLATURE.....</b>	<b>XI</b>
<b>CHAPTER 1 INTRODUCTION.....</b>	<b>1</b>
1.1 Motivations .....	1
1.1.1 <i>Use of Bleed Air</i> .....	1
1.1.2 <i>Environmental Control System</i> .....	1
1.1.3 <i>Optimization for Bleed Air System</i> .....	2
1.2 Background of LQ Control on Temperature Control System.....	4
1.3 Contributions.....	6
1.4 Organization of Thesis.....	6
<b>CHAPTER 2 MODELING OF A BLEED AIR SYSTEM .....</b>	<b>8</b>
2.1 System Configuration and Modeling Assumption.....	8
2.2 Nonlinear Dynamic Model of an Engine Bleed Air System.....	9
2.2.1 <i>Heat Exchanger</i> .....	9
2.2.2 <i>Pressure Calculation</i> .....	12
2.2.3 <i>Control Valves and Flow Rate</i> .....	13
2.2.4 <i>Temperature Calculation</i> .....	15
2.3 System Model Linearization .....	16
2.3.1 <i>Linearization of Heat Exchanger Model</i> .....	16
2.3.2 <i>Linear Open-loop System Model</i> .....	19
2.4 Simulations of Open-loop System Model.....	22
<b>CHAPTER 3 TEMPERATURE CONTROL OF BLEED AIR SYSTEM.....</b>	<b>27</b>
3.1 Ram-Air-Plus-Bypass Control Strategy.....	27

3.2 Linear Quadratic Regulator (LQR) with Output Feedback .....	28
3.2.1 <i>Optimal Controller Design</i> .....	28
3.2.2 <i>Selection of Weighting Matrix</i> .....	30
3.3 Simulations .....	32
3.4 Discussions and Conclusions .....	37
<b>CHAPTER 4 DEVELOPMENT OF TEST FACILITY AND EXPERIMENTS .....</b>	<b>38</b>
4.1 Test Rig Design.....	38
4.2 Main Components.....	40
4.2.1 <i>Heat Exchanger</i> .....	40
4.2.2 <i>Heater and Control Systems</i> .....	41
4.2.3 <i>Control Valve</i> .....	42
4.2.4 <i>Temperature Sensor</i> .....	43
4.2.5 <i>Flow Sensor</i> .....	43
4.2.6 <i>Pressure Sensor</i> .....	44
4.3 Operating Conditions of Experiments .....	44
4.4 Experiment with PI Controller.....	47
4.4.1 <i>Result of Ram Air Control Configuration</i> .....	47
4.4.2 <i>Result of Bypass Control Configuration</i> .....	48
4.4.3 <i>Result of Ram-Air-Plus-Bypass Control Configuration</i> .....	50
4.5 Experiment with LQ Output Feedback Controller.....	51
4.6 Conclusions and Discussions.....	55
<b>CHAPTER 5 CONCLUSIONS AND FUTURE WORK .....</b>	<b>57</b>
5.1 Conclusions.....	57
5.2 Future Work .....	58
<b>REFERENCES.....</b>	<b>59</b>
<b>APPENDIX.....</b>	<b>62</b>
<b>CURRICULUM VITAE.....</b>	<b>80</b>

## LIST OF FIGURES

Fig. 1.1 Environmental control system (Moir and Seabridge, 2001).....	2
Fig. 1.2 Ram-air-plus-bypass control configuration .....	3
Fig. 1.3 Temperature control configurations: (a) ram air channel control; (b) bypass channel control.....	4
Fig. 2.1 Ram-air-plus-bypass control configuration .....	8
Fig. 2.2 Plate-fin cross-flow heat exchanger core.....	10
Fig. 2.3 Partitioning of the heat exchanger plate .....	11
Fig. 2.4 Airflow through a ball valve.....	14
Fig. 2.5 Linear open-loop model for bleed air system.....	22
Fig. 2.6 Step response to a 20°F step increase in bleed air inlet temperature $T_{hi}$ : (a) nonlinear model simulation; (b) linear model simulation.....	23
Fig. 2.7 Step response to a 5 psig step increase in bleed air inlet pressure $P_{hin}$ : (a) nonlinear model simulation; (b) linear model simulation.....	23
Fig. 2.8 Step response to a 20 °F step increase in ambit temperature $T_{amb}$ : (a) nonlinear model simulation; (b) linear model simulation.....	23
Fig. 2.9 Step response to a 5 psig step increase in ambit pressure $P_{amb}$ : (a) nonlinear model simulation; (b) linear model simulation.....	24
Fig. 2.10 Step response to a 1% step increase in bypass valve opening $u_{bypass}$ : (a) nonlinear model simulation; (b) linear model simulation.....	24
Fig. 2.11 Step response to a 1% step increase in ram air valve opening $u_{ram}$ : (a) nonlinear model simulation; (b) linear model simulation.....	24
Fig. 2.12 Errors of the temperature time response of the nonlinear and linearized models: (a) 20°F step increase in bleed air inlet temperature $T_{hi}$ ; (b) 5 psig step increase in bleed air inlet pressure $P_{hin}$ ; (c) 20°F step increase in ambit temperature $T_{amb}$ ; (d) 5 psig step increase in bleed air inlet pressure $P_{amb}$ ; (e) 1% step increase in bypass valve opening $u_{bypass}$ ; (f) 1% step increase in bypass valve opening $u_{ram}$ .....	25
Fig. 3.1 Ram-air-plus-bypass control strategy.....	27
Fig. 3.2 Load temperature response under different $q$ and $r$ : (a) $r = 1$ ; (b) $q = 1$ .....	31

Fig. 3.3 Load temperature response under small range of $q$ and $r$ : (a) $r = 1$ , $q = 0.01\sim 0.5$ ; (b) $r = 1$ , $q = 0.5\sim 1$ ; (c) $q = 1$ , $r = 10\sim 100$ ; (d) $q = 1$ , $r = 1\sim 10$ .....	32
Fig. 3.4 Simulink program for optimal output feedback control .....	33
Fig. 3.5 System response to input 1: (a) load temperature; (b) bypass valve opening; (c) ram-air valve opening; (d) ram-air mass flow rate .....	34
Fig. 3.6 System response to input 2: (a) load temperature; (b) bypass valve opening; (c) ram-air valve opening; (d) ram-air mass flow rate .....	35
Fig. 3.7 System response to input 3: (a) load temperature; (b) bypass valve opening; (c) ram-air valve opening; (d) ram-air mass flow rate .....	35
Fig. 3.8 System response to input 4: (a) load temperature; (b) bypass valve opening; (c) ram-air valve opening; (d) ram-air mass flow rate .....	36
Fig. 3.9 System response to input 5: (a) load temperature; (b) bypass valve opening; (c) ram-air valve opening; (d) ram-air mass flow rate .....	36
Fig. 3.10 System response to input 6: (a) load temperature; (b) bypass valve opening; (c) ram-air valve opening; (d) ram-air mass flow rate .....	37
Fig. 4.1 Bleed air temperature control test fig configuration.....	39
Fig. 4.2 Picture of the test rig.....	39
Fig. 4.3 Air to air plate-fin heat exchanger, manufactured by Bell Intercoolers .....	41
Fig. 4.4 Air heater control system, manufactured by SYLANVIA .....	42
Fig. 4.5 Control valve manufactured by BI-TORQ, CARBO-BOND, Inc.....	42
Fig. 4.6 RTD temperature sensor, supplied by Honeywell.....	43
Fig. 4.7 Air velocity transducer, manufactured by OMEGA Inc.....	43
Fig. 4.8 Pressure sensors, manufactured by OMEGA Inc.: (a) PX303; (b) PX209.....	44
Fig. 4.9 Operating condition for ram air control configuration (to be continued).....	46
Fig. 4.10 System response to a 5 °F load temperature set point increase using ram air control .....	48
Fig. 4.11 System response to a 5 °F load temperature set point increase using bypass control .....	49
Fig. 4.12 System response to a 5 °F load temperature set point increase using ram-air-plus-bypass control .....	50

Fig. 4.13 System response to Input A .....	52
Fig. 4.14 System response to Input B .....	53
Fig. 4.15 System response to Input C .....	54

## **LIST OF TABLES**

Table 2.1 Operating conditions and corresponding mission data selected for simulation	22
Table 3.1 Initial steady-state conditions .....	34
Table 4.1 Main components of the test rig .....	40
Table 4.2 Initial steady-state conditions and controller parameters for ram air control configuration .....	47
Table 4.3 Initial steady-state condition for optimal feedback control .....	51

# NOMENCLATURE

## Roman

$c_p$	specific heat of fluid
$d$	valve diameter; pipe diameter
$dt$	nonlinear model time step
$e_{bypass}$	bypass valve opening error
$e_{temp}$	load temperature error
$g$	gravity constant
$mc_s$	lump-level heat exchanger core thermal mass
$t$	time
$A$	state-space model system matrix; valve opening area
$B$	state-space model matrix
$BR$	bypass flow ratio
$C$	state-space model matrix
$C_c$	cold flow specific heat
$C_h$	hot flow specific heat
$D$	state-space model matrix
$E$	error matrix
$F_{rec}$	pressure recovery factor
$G$	state-space model matrix
$H$	total heat transfer coefficient for heat exchanger hot/cold side; state-space model matrix
$J$	LQ-optimal performance index function
$K$	gain constant
$Mach$	aircraft speed
$MC_s$	heat exchanger core thermal mass
$N$	heat exchanger plate partitioning dimension
$P$	pressure
$P_{drop}$	pressure drop
$Q$	heat transfer; states-deviation penalty weight



$R$	universal gas constant; control effort penalty weight
$T$	temperature
$U$	state-space input vector
$W$	fluid mass flow rate
$X$	state vector
$Y$	state-space model output
$Y'$	heat exchanger state-space model intermediate output vector

### **Greek**

$\beta$	control valve angle opening
$\phi$	pressure ratio
$\gamma$	ratio of specific heats
$\tau$	time constant

### **Subscript**

$amb$	ambient (atmospheric) condition
$bleed$	total bleed air
$bleedbypass$	bypass-channel bleed air
$bleedmain$	main-channel bleed air
$bypass$	bypass channel valve
$c$	cold side
$ci$	cold-side fluid inlet
$co$	cold-side fluid outlet
$d$	valve downstream location
$h$	hot side
$hi$	hot-side fluid inlet
$ho$	hot-side fluid outlet
$i$	heat exchanger plate row index
$in$	inlet
$I_{bypass}$	integral bypass control
$I_{ram}$	integral ram air control

<i>j</i>	heat exchanger plate column index
<i>load</i>	load
<i>load_m</i>	measured at the load
<i>lq</i>	LQ-optimal
<i>m</i>	measured by sensor
<i>o</i>	operating point
<i>out</i>	outlet
<i>P<sub>bypass</sub></i>	proportional bypass control
<i>P<sub>ram</sub></i>	proportional ram-air control
<i>ram</i>	ram-air channel valve
<i>s</i>	heat transfer surface; heat exchanger core
<i>sp</i>	set-point
<i>ts</i>	temperature sensor
<i>u</i>	valve upstream location
<i>v</i>	control valve

### **Superscript**

<i>ci</i>	lump cold-side fluid inlet
<i>co</i>	lump cold-side fluid outlet
<i>hi</i>	lump hot-side fluid inlet
<i>ho</i>	lump hot-side fluid outlet
<i>s</i>	lump surface

# CHAPTER 1 INTRODUCTION

## 1.1 Motivations

### 1.1.1 *Use of Bleed Air*

Bleed air in gas turbine engines is compressed air taken from within the engine, after the compressor stage(s) and before the fuel is injected in the burners. This high-pressure and high-temperature engine bleed air is commonly used within the aircraft in many different ways, including de-icing (Yeoman, 1994), pressurizing the cabin (Newman et al., 1980), and air conditioning for passengers and avionics equipment (Ensign and Gallman, 2006). However, engine bleed air can be quite hot and, when being used in the cabin or other low temperature areas, it must be cooled to a desired temperature, in order to be utilized appropriately. For some bleed air applications, it is critical to control the temperature of the supply air with fast transient response and high steady-state accuracy.

In civil aircraft, bleed air's primary use is to provide pressure for the aircraft cabin by supplying air to the environmental control system (ECS) (Hunt et al., 1995). Additionally, bleed air is used to keep critical parts of the aircraft (such as the wing leading edges) ice-free. When used for cabin pressurization, the air from the engine must first be cooled by passing the bleed air through an air-to-air heat exchanger cooled by cold outside air. It is then fed to an air cycle machine unit which regulates the temperature and flow of air into the cabin, keeping the environment comfortable.

### 1.1.2 *Environmental Control System*

The environmental control system in today's jetliners is designed to provide a safe and comfortable cabin environment at cruising altitudes that can reach 40,000 feet. At those altitudes, the cabin must be pressurized to enable passengers and crew to breathe

normally. By government regulation, the cabin pressure cannot be less, at maximum cruise altitude, than the equivalent of outside air pressure at 8,000 feet. In addition to pressurization, the environmental control system controls air flow, air filtration and temperature.

Fig. 1.1 shows the environmental control system of an aircraft. The turbine drives the compressor which is used to increase the air pressure with a corresponding increase in temperature. The bleed air temperature is then reduced in the ram air cooled heat exchanger. This reduction in temperature may lead to water being condensed out of the air. A water extractor at the turbine inlet is used to remove most of the free water. A bypass line is used to vary the turbine outlet temperature to the required value. The volume of air flowing round the bypass is varied by a temperature control valve.

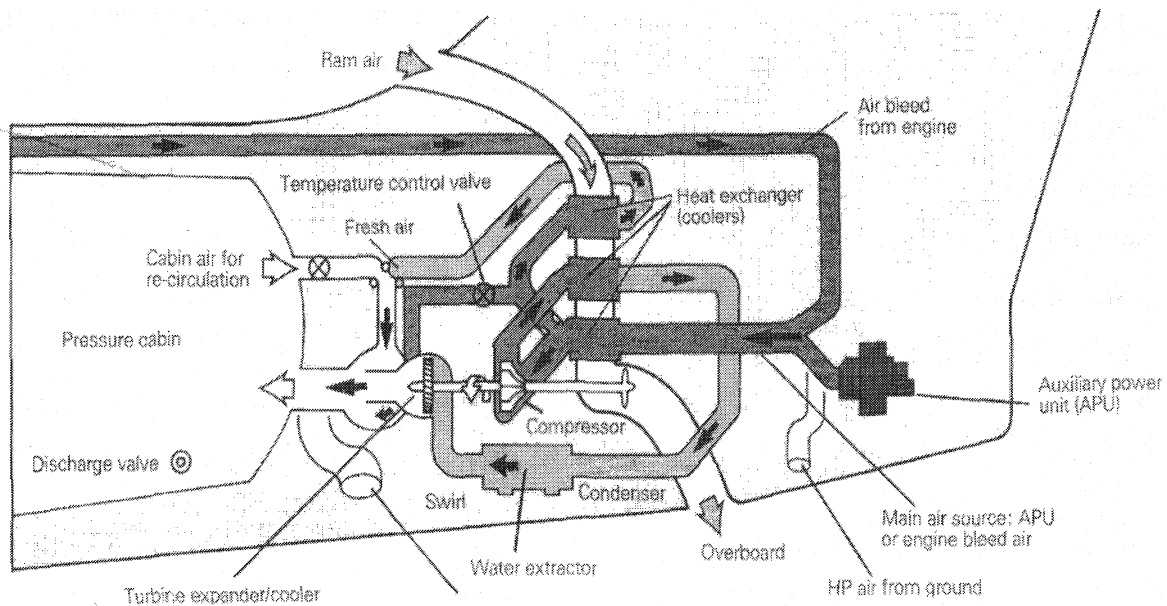


**Fig. 1.1 Environmental control system (Moir and Seabridge, 2001)**

### **1.1.3 Optimization for Bleed Air System**

The bleed air system is the heart of ECS. For a business jet, optimization of the bleed air system offers the largest potential for improvements in performance, useful load, reliability, and purchase price. Ensign and Gallman, 2006, explored the benefits of

an electrically driven ice protection and environmental control system, which can alleviate energy waste. Newman et al., 1980, stated a design of the cabin air conditioning systems for the DC-10, an American three-engine airliner, which was aimed to reduce the bleed air extracted from the engine.

Ram air is used to cool the engine bleed air and is scooped from the aircraft boundary layer or close to it. The air is forced through a scoop, which faces into the external air flow, through a heat exchanger matrix and then rejected overboard by forward motion of the aircraft. A large ram air flow rate will increase the aircraft drag because of the resistance of the scoop, pipe work and the heat exchanger matrix.

A ram-air-plus-bypass control configuration (Hodal and Liu, 2005) is studied in this thesis with emphasis on low ram air usage. As shown in Fig. 1.2, the source of the supply air stream is the aircraft's engine, from which the hot bleed air is extracted. To cool the hot bleed air, cold air is collected from the aircraft's boundary layer and is employed for heat exchange between the air streams. This air stream is referred to as the ram air flow. A heat exchanger device is used to exchange thermal energy between the two air streams. Bleed air flows through the hot side of the heat exchanger, while ram air flows through the cold side. With a bypass placed on the bleed air channel, the bleed air leaving the heat exchanger first mixes with the bypassed flow and then is fed to the load. A control valve is placed in the ram air channel, as well as in the bypass channel. In order to obtain fast time response and low overshoot, optimal control is designed and applied to the bypass valve control.

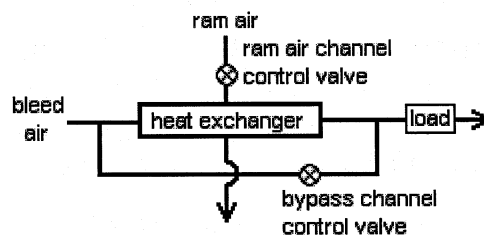


**Fig. 1.2 Ram-air-plus-bypass control configuration**

## 1.2 Background of LQ Control on Temperature Control System

Temperature control is a process in which the temperature at the load is measured and the passage of heat energy into or out of the load is adjusted to achieve a desired temperature. In order to keep it at a desired temperature, a control system must be designed and implemented accordingly. When speaking of a temperature control system, one is referring to the physical and mathematical combination of the structures that contain the temperature-controlled mass, the disturbances to which they are subjected, as well as the components used to regulate its temperature (Kutz, 1968, Levis and Syrmos, 1995, Mikles and Fikar, 2000).

For the bleed air temperature regulation system studied in this thesis, the temperature of the supply bleed air at the load is to be controlled at a set-point value of 190 °F. A temperature sensor is located at the load to measure the temperature for feedback purposes. Control valves play the role of final control element, by manipulating the flow rate in their respective channels, and thus effectively changing the thermal energy carried by the airflow.

The engine bleed air temperature varies significantly under idle, take-off and cruise operating conditions. Ram air temperature and humidity can also vary largely with changes in atmospheric and aircraft flight conditions. Feedback control is thus required for the temperature regulation.

In Hodal and Liu, 2005, the load temperature is controlled with a traditional PI controller. Some simulations were performed to demonstrate the advantage of ram-air-plus-bypass control configuration, compared to ram air channel control and bypass channel control, as shown in Fig. 1.3.

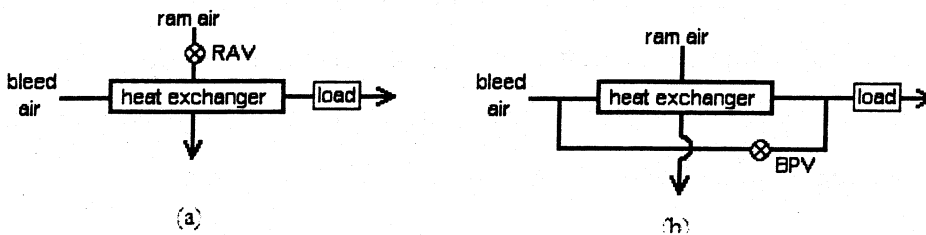


Fig. 1.3 Temperature control configurations: (a) ram air channel control; (b) bypass channel control

The theory of optimal control is concerned with operating dynamic systems at minimum cost. The case where the system dynamics are described by a set of linear differential equations and the cost is described by a quadratic functional is called the linear quadratic (LQ) problem. One of the main results in the theory is that the solution is provided by the linear-quadratic regulator (LQR).

The cost (function) is often defined as a sum of the deviations of key measurements from their desired values. In effect, this algorithm therefore finds those controller settings that minimize the undesired deviations, like deviations from desired altitude or process temperature. Often the magnitude of the control action itself is included in this sum as to keep the energy expended by the control action itself limited.

The LQR algorithm is at its core just an automated way of finding an appropriate state-feedback controller. But the user needs to specify the weighting factors and compare the results with the specified design goals. A large number of designing approaches for selecting weighting matrices have been put forward. Kalman, 1964, first presented a method acquiring the weighting matrices according to the given closed-loop poles. Zhang and Mao, 2002, demonstrated a new method that the weighting matrices can be found by genetic algorithms to satisfy given performance.

LQR optimal control theory is an important part of modern control theory, and it is applied in a broad range of temperature control systems and other applications. Forrest et al., 1993, implemented a primary LQ controller in their study of super-heater control, proposing periodic plant sampling and controller self-tuning for their outer loop controller. Katayama et al., 1990 investigated an optimal tracking control of a heat exchanger with load change, and derived an optimal tracking controller with integral, state feedback plus preview actions. Orzylowski et al., 1999, discussed optimal and suboptimal control, based on the linear quadratic (LQ) performance index, for their furnace batch temperature control system.

## 1.3 Contributions

The contributions of this thesis are as follows:

1. A nonlinear model for the bleed air system is developed, which can be used for linearization and simulation.
2. A linearized model of a simplified engine bleed air temperature control system is developed. These models are used to verify the effectiveness of the control strategies.
3. An optimal controller of ram-air-plus-bypass control configuration is developed, based on the linearized state space model of the multi-input and multi-output (MIMO) system. Simulations are conducted, and the results are analyzed.
4. A computer-controlled bleed air temperature control test rig has been designed and constructed. The ram air plus bypass temperature control approach is investigated experimentally. The experimental results are presented and discussed.

## 1.4 Organization of Thesis

This thesis consists of five chapters. They are organized as follows:

- Chapter 2: The nonlinear mathematical model of a bleed air temperature control system is developed. Then, the nonlinear model is linearized around an operating point. Based on the linear model, a state-space representation of the system is also derived.
- Chapter 3: The optimal controller is designed based on the simplified linear state-space system equation. Simulations of ram-air-plus-bypass control strategy for the engine bleed air system are conducted and simulation results are given.



**Chapter 4:** An experimental setup for demonstrating the effectiveness of the ram air plus bypass bleed air temperature control strategy is designed. The experimental results of the temperature control are presented. Some comments on the experimental results are drawn.

**Chapter 5:** Conclusions of the thesis work and potential future research topics are provided.

# CHAPTER 2 MODELING OF A BLEED AIR SYSTEM

This chapter presents bleed air system models that will be used for temperature control. The nonlinear dynamic model of the bleed air system is developed first. Then, the nonlinear model is linearized around an operating point. To validate the model accuracy, MATLAB/Simulink simulations are carried out and the simulation results are discussed.

## 2.1 System Configuration and Modeling Assumption

The ram-air-plus-bypass control configuration is shown in Fig. 2.1.

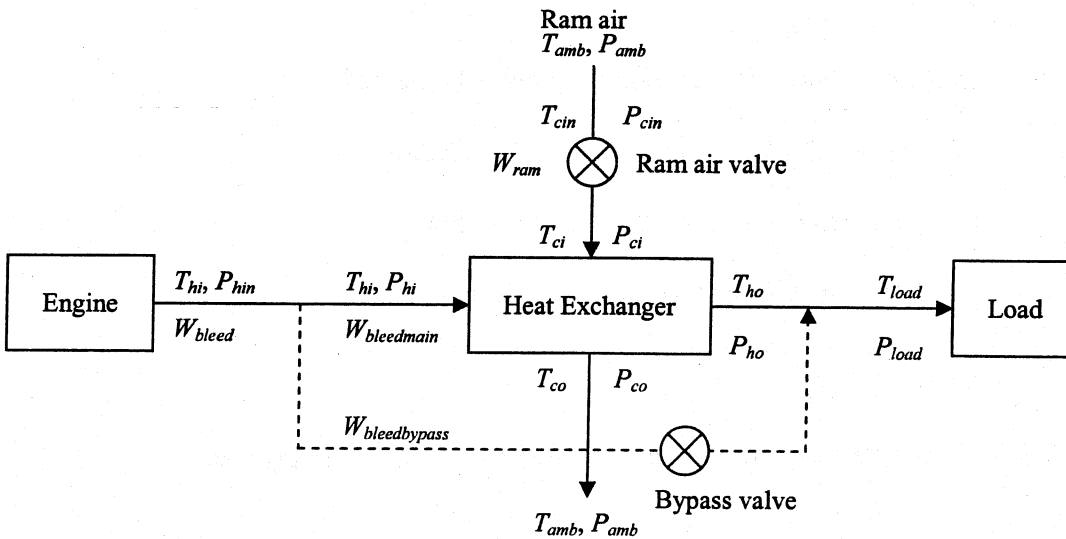


Fig. 2.1 Ram-air-plus-bypass control configuration

The hot bleed air comes from aircraft engine, at a temperature of  $T_{hi}$  (°F), pressure  $P_{hi}$  (psia), and a mass flow rate  $W_{bleed}$  (lb/s). Ram air is from the atmosphere at a mass

flow rate  $W_{ram}$ . Inlet pressure  $P_{cin}$  (psi) and temperature  $T_{cin}$  (°F) are determined from the ambient temperature  $T_{amb}$  and ambient pressure  $P_{amb}$  (Hodal and Liu, 2005):

$$T_{cin} = (T_{amb} + 460) \left( 1 + 0.2 Mach^2 \right) - 460 \quad (2.1)$$

$$P_{cin} = F_{rec} \left( P_{amb} \left( 1 + 0.2 Mach^2 \right)^{3.5} - P_{amb} \right) + P_{amb} \quad (2.2)$$

where  $F_{rec}$  is the pressure recovery factor.

Before entering the heat exchanger, the hot bleed air is divided into two channels, main bleed air and bypass channel, which are at mass flow rates  $W_{bleedmain}$  and  $W_{bleedbypass}$ , respectively. The main bleed air will be cooled by ram air through the heat exchanger and mixed with bypass flow at load. Control valves are placed in the ram air channel and the bypass channel which can be controlled to achieve fast temperature response and efficient ram air usage.

To simplify the system, some assumptions are made as follows (Hodal and Liu, 2005):

- (a). transport delay between components is neglected;
- (b). there is no heat loss from the pipes to surrounding air;
- (c). pressure loss due to pipe flow is negligible; and
- (d). the flow is assumed to be fully developed.

## 2.2 Nonlinear Dynamic Model of an Engine Bleed Air System

### 2.2.1 Heat Exchanger

The heat exchanger presented in this thesis is a plate-fin heat exchanger (PFHE). As shown in Fig. 2.2, the PFHE are made by the stacking of corrugated sheets (fins) separated by planar sheets and closed on the sides by lateral bars. The gaps between

constitute a fluid layer. A core is made of a great number of layers. The exchanger can be made of one or more cores. The number of plate and fin layers, the size of the plates and fin, the height of the fin and the type of fin are engineered for optimum performance.

The plate-fin heat exchangers are increasingly being used in industry where weight and compactness are of importance, as in the case of automobiles, aerospace vehicles, and electronic equipment. Some special types of the plate-fin exchangers are known as compact heat exchangers. They are characterized by the high ratio of heat transfer surface to heat exchanger volume, which gives them excellent compactness and heat transfer characteristics.

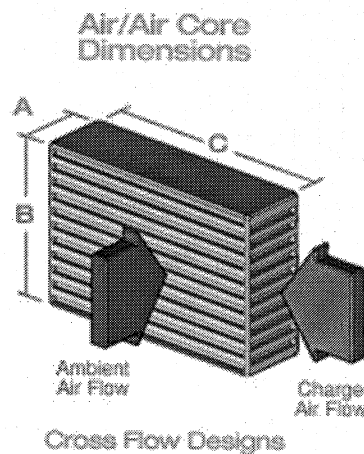


**Fig. 2.2 Plate-fin cross-flow heat exchanger core<sup>1</sup>**

The heat exchanger is modeled using the “direct lumping procedure” (Hodal and Liu, 2005), where the heat exchanger is divided into a finite number of lumps as shown in Fig. 2.3. Each of these lumps is considered as a control volume over which the relevant heat transfer equations are applied. For simplicity, the heat exchanger core is modeled as a thin plate. The temperature is distributed over the plate, in two dimensions.

In modeling,  $T_s$  (°F) denotes the surface temperature of heat exchanger core of each cell,  $T_{hi}$  and  $T_{ho}$  are inlet and outlet temperatures of heat exchanger hot side, respectively.  $W_{bleedmain}$  (lb/s) and  $C_h$  (Btu/lb·°F) are the flow rate and specific heat of hot

<sup>1</sup> Taken from <http://www.bellintercoolers.com/pages/AAMain.html>

side fluid (bleed air) flow, respectively.  $W_{ram}$  and  $C_c$  are the cold side fluid (ram air) flow rate and specific heat, respectively. The inlet and outlet temperatures of ram air are  $T_{ci}$  and  $T_{co}$ , respectively.  $H_h$  and  $H_c$  (Btu/s·°F) are the hot and cold side overall heat transfer coefficients, respectively.  $mc_s$  (Btu/°F) is the thermal mass of each lump.  $N$  is the number of rows/columns, and  $i=1, 2, \dots, N, j=1, 2, \dots, N$ .

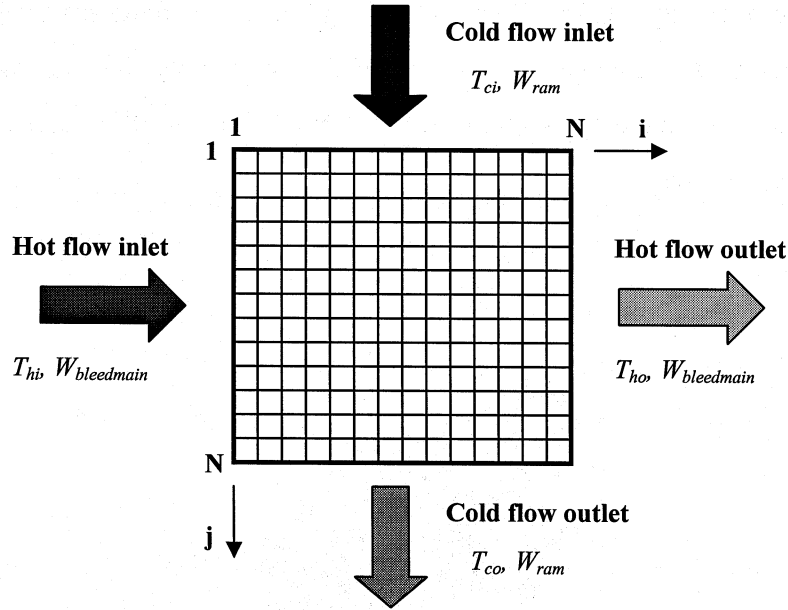


Fig. 2.3 Partitioning of the heat exchanger plate

From Hodal and Liu, 2005, the state equation of heat exchanger on a ‘per cell’ is

$$\dot{T}_{i,j}^s = \psi T_{i,j}^s + \theta T_{i,j}^{hi} + \phi T_{i,j}^{ci} \quad (2.3)$$

where

$$\psi = \frac{-W_{bleedmain}C_h a - W_{ram}C_c b}{Nmc_s}, \quad \theta = \frac{W_{bleedmain}C_h a}{Nmc_s}, \quad \text{and} \quad \phi = \frac{W_{ram}C_c b}{Nmc_s}$$

$$a = 1 - e^{-\frac{H_h}{W_{bleedmain}c_h}}, \quad b = 1 - e^{-\frac{H_c}{W_{ram}c_c}}$$

Two algebraic equations representing the convection heat transfer relate the hot/cold cell output temperatures to the cell core temperature and cell inlet temperatures:

$$T_{i,j}^{ho} = (1 - a)T_{i,j}^{hi} + aT_{i,j}^s \quad (2.4-a)$$

$$T_{i,j}^{co} = (1 - b)T_{i,j}^{ci} + bT_{ij}^s. \quad (2.4-b)$$

By geometry, lump inlet temperatures are related to the outlet temperatures of adjacent lumps,

$$T_{i,j}^{hi} = T_{i-1,j}^{ho}, \text{ and } T_{i,j}^{ci} = T_{i,j-1}^{co} \quad (2.5)$$

### 2.2.2 Pressure Calculation

When air flows through the heat exchanger, the pressure drop caused by heat exchanger is a function of flow rate. The bleed air and ram air side heat exchanger pressure drops are given as follows:

$$P_{drop_h} = P_{hi} - P_{ho} = K_1 W_{bleedmain}^2 + K_2 W_{bleedmain} \quad (2.6)$$

$$P_{drop_c} = P_{ci} - P_{co} = K_3 W_{ram}^2 + K_4 W_{ram} \quad (2.7)$$

where  $P_{hi}$  and  $P_{ci}$  are the hot and cold side pressures upstream of the heat exchanger, and  $P_{ho}$  and  $P_{co}$  are hot and cold side pressures downstream of the heat exchanger, respectively. The constants  $K_1$ ,  $K_2$ ,  $K_3$ , and  $K_4$  come from empirical data of a real-life heat exchanger<sup>2</sup>.

The pressure at load is:

$$P_{load} = K_{load} W_{bleed}^2 + P_{amb} \quad (2.8)$$

where  $K_{load}$  is the load impedance constant, and  $W_{bleed}$  is the total bleed air flow rate.

---

<sup>2</sup> The author is bound by a confidentiality agreement not to release the exact values of these parameters

As a result of neglecting the pressure drop due to the pipe flow, some equivalency statements can be drawn between the pressures at some positions of the system:

- the heat exchanger hot-side inlet pressure is equal to the bleed-air pressure leaving the source,  $P_{hi} \equiv P_{hin}$
- the pressure at the hot-side heat exchanger outlet is equivalent to the pressure upstream of the load,  $P_{ho} \equiv P_{load}$
- since ram air is dumped directly into the atmosphere, pressure at the cold-side heat exchanger outlet is equivalent to ambient pressure,  $P_{co} \equiv P_{amb}$

### 2.2.3 Control Valves and Flow Rate

Control valves are placed at ram air channel and bypass channel to regulate the system. Ball valves are used and manipulate the flow rate by changing their opening angle  $\beta_v$ , and thus the opening area  $A_v$ . Neglecting valve hysteresis and backlash, the valve dynamics are modeled as a first-order lag.

$$\beta_v(s) = u_v(s)G_v(s) = u_v(s) \frac{K_v}{\tau_v s + 1} \quad (2.9)$$

where  $u_v$  is the opening-command input to the valve (0%-100%),  $\beta_v$  is the valve opening angle (rad),  $K_v$  is the valve gain, and  $\tau_v$  is the valve time constant (s).

Fig. 2.4 shows airflow through a ball valve. Valve opening angles  $\beta_v=0$  rad and  $\beta_v = \pi/2$  correspond to a fully-closed and fully-opened valve. Between these two limits, a given angle will produce a valve opening area of

$$A_v = \frac{\pi d^2}{4} (1 - \cos \beta_v) \quad (2.10)$$

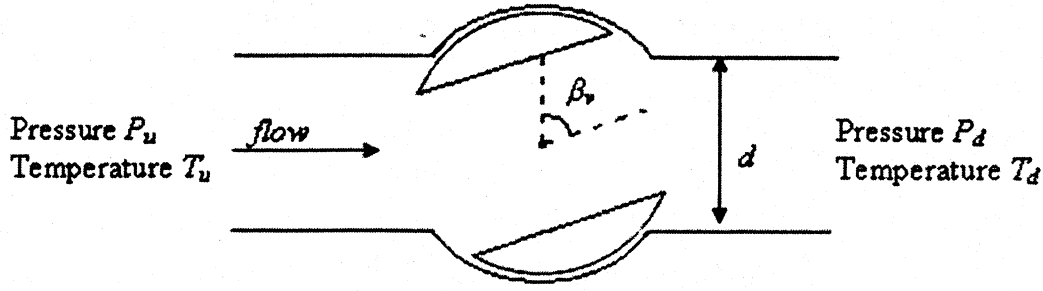


Fig. 2.4 Airflow through a ball valve

The airflow rate  $W_v$  going through a valve or orifice with an opening area  $A_v$  is calculated by the following equation:

$$W_v = \frac{A_v P_u}{\sqrt{T_u}} \left[ \frac{2\gamma g}{(\gamma - 1)R} \left( \phi^{\frac{2}{\gamma}} - \phi^{\frac{(1+\gamma)}{\gamma}} \right) \right]^{\frac{1}{2}} \quad (2.11)$$

where

$$\phi = \frac{P_d}{P_u} \text{ for } \frac{P_d}{P_u} \geq 0.5283, \quad \phi = 0.5283 \text{ for } \frac{P_d}{P_u} < 0.5283$$

$P_u$  and  $P_d$  are the upstream and downstream pressures (psia), respectively;  $T_u$  is the upstream temperature ( $^{\circ}\text{R}$ );  $A_v$  is the valve opening area ( $\text{in}^2$ );  $g = 32.174 \text{ ft/s}^2$  is the acceleration of gravity;  $R = 1717 \text{ ft}^2/(\text{s}^2 \cdot ^{\circ}\text{R})$  is the gas constant for air; and  $\gamma = 1.4$  (for air) is the ratio of specific heat at constant pressure and specific heat at constant volume. In the ram air channel,  $W_v = W_{ram}$ , and with  $P_u \equiv P_{cin}$ ,  $P_d \equiv P_{ci}$ ,  $T_u \equiv T_{ci}$ . And for the bypass channel,  $W_v = W_{bleedmain}$ , with  $P_u \equiv P_{hin}$ ,  $P_d \equiv P_{load}$ ,  $T_u \equiv T_{hi}$ . Eq. (2.11) can be rewritten as:

for the ram air channel

$$W_{ram} = \frac{A_{ram} P_{cin}}{\sqrt{T_{cin}}} \left[ \frac{2\gamma g}{(\gamma - 1)R} \left( \phi^{\frac{2}{\gamma}} - \phi^{\frac{(1+\gamma)}{\gamma}} \right) \right]^{\frac{1}{2}} \quad (2.12)$$



where  $\phi = \frac{P_{ci}}{P_{cin}}$  for  $\frac{P_{ci}}{P_{cin}} \geq 0.5283$ ,  $\phi = 0.5283$  for  $\frac{P_{ci}}{P_{cin}} < 0.5283$

and for the bypass channel

$$W_{bleedbypass} = \frac{A_{bypass} P_{hin}}{\sqrt{T_{hi}}} \left[ \frac{2\gamma g}{(\gamma-1)R} \left( \frac{2}{\phi^\gamma} - \frac{(1+\gamma)}{\phi} \right) \right]^{\frac{1}{2}} \quad (2.13)$$

where  $\phi = \frac{P_{load}}{P_{hin}}$  for  $\frac{P_{load}}{P_{hin}} \geq 0.5283$ ,  $\phi = 0.5283$  for  $\frac{P_{load}}{P_{hin}} < 0.5283$

Since the pressure ratio  $\phi$  is limited in case the flow becomes choked, Eq. (2.11-2.13) is valid only for subsonic flow calculation.

#### 2.2.4 Temperature Calculation

For an isentropic flow, pressures and temperatures are related through the following equation:

$$\frac{P_2}{P_1} = \left( \frac{T_2}{T_1} \right)^{\frac{\gamma}{\gamma-1}} \quad (2.14)$$

where  $P_1$  and  $T_1$ ,  $P_2$  and  $T_2$  are upstream pressure and temperature, downstream pressure and temperature, respectively. The temperature in Eq. (2.14) is in Rankine.

From Eq. (2.14), the down stream temperature of the ram air valve is calculated as:

$$T_{ci} = T_{cin} \left( \frac{P_{ci}}{P_{cin}} \right)^{\frac{\gamma-1}{\gamma}} \quad (2.15)$$

The load temperature is a mixture of bypass flow and cooled main bleed flow, and is given by:

$$T_{load} = \frac{T_{ho}W_{bleedmain} + T_{hi}W_{bleedbypass}}{W_{bleed}} \quad (2.16)$$

The temperature sensor is to measure the temperature at load, which is denoted as  $T_{load\_m}$ . The measured temperature is fed back to the controller. The dynamics of the sensor are modeled by a simple first-order transfer function:

$$T_{load\_m}(s) = T_{load}(s) \frac{K_{ts}}{\tau_{ts}s + 1} \quad (2.17)$$

where,  $T_{load}$  is the actual temperature at the load,  $K_{ts}$  is the sensor gain, and the sensor time constant  $\tau_{ts}$  (sec) is a function of the flow being sensed/measured:

$$\tau_{ts} = f(W_m) \quad (2.18)$$

## 2.3 System Model Linearization

### 2.3.1 Linearization of Heat Exchanger Model

To derive a linear state space model for the heat exchanger, relevant differential and algebraic equations describing the heat transfer must be written in the state space format:

$$\dot{\hat{X}} = f(\hat{X}, \hat{U}) \quad (2.19)$$

$$\hat{Y} = g(\hat{X}, \hat{U}) \quad (2.20)$$

Define the state variable as core temperatures of each cell:

$$\hat{X} = [T_{11}^s, \dots, T_{1N}^s, T_{21}^s, \dots, T_{N1}^s, \dots, T_{NN}^s]^T \quad (2.21)$$

The input vector consists of the hot and cold inlet temperatures as well as the total hot and cold side mass flow rates:

$$\hat{U} = [T_{hi}, T_{ci}, W_{bleedmain}, W_{ram}]^T \quad (2.22)$$

There are thus  $N \times N$  equations of state (one for each cell), or  $N \times N$  functions,

$$\dot{\hat{X}}_k = f_k(\hat{X}_1, \hat{X}_2, \dots, \hat{X}_{N \times N}, \hat{U}_1, \hat{U}_2, \hat{U}_3, \hat{U}_4) \quad (2.23)$$

where  $k=1 \dots N \times N$ .

The linearized state equation takes the following form:

$$\begin{aligned} \Delta \dot{\hat{X}}_k = & \left. \frac{\partial f_k}{\partial \hat{X}_1} \right|_{\hat{X}_{1_o}} \Delta \hat{X}_1 + \left. \frac{\partial f_k}{\partial \hat{X}_2} \right|_{\hat{X}_{2_o}} \Delta \hat{X}_2 + \dots + \left. \frac{\partial f_k}{\partial \hat{X}_{N \times N}} \right|_{\hat{X}_{N \times N_o}} \Delta \hat{X}_{N \times N} \\ & + \left. \frac{\partial f_k}{\partial \hat{U}_1} \right|_{\hat{U}_{1_o}} \Delta \hat{U}_1 + \left. \frac{\partial f_k}{\partial \hat{U}_2} \right|_{\hat{U}_{2_o}} \Delta \hat{U}_2 + \left. \frac{\partial f_k}{\partial \hat{U}_3} \right|_{\hat{U}_{3_o}} \Delta \hat{U}_3 + \left. \frac{\partial f_k}{\partial \hat{U}_4} \right|_{\hat{U}_{4_o}} \Delta \hat{U}_4 \end{aligned} \quad (2.24)$$

The partial derivative terms appearing in the above equation are evaluated at an operating point  $o$ . Eq. (2.24) can be rewritten in matrix form:

$$\Delta \dot{\hat{X}} = \hat{A} \Delta \hat{X} + \hat{B} \Delta \hat{U} \quad (2.25)$$

where

$$\hat{A} = \begin{bmatrix} \left. \frac{\partial f_1}{\partial \hat{X}_1} \right|_{\hat{X}_{1_o}} & 0 & \dots & 0 \\ \left. \frac{\partial f_2}{\partial \hat{X}_1} \right|_{\hat{X}_{1_o}} & \left. \frac{\partial f_2}{\partial \hat{X}_2} \right|_{\hat{X}_{2_o}} & \dots & 0 \\ \vdots & \vdots & \ddots & \vdots \\ \left. \frac{\partial f_{N \times N}}{\partial \hat{X}_1} \right|_{\hat{X}_{1_o}} & \left. \frac{\partial f_{N \times N}}{\partial \hat{X}_2} \right|_{\hat{X}_{2_o}} & \dots & \left. \frac{\partial f_{N \times N}}{\partial \hat{X}_{N \times N}} \right|_{\hat{X}_{N \times N_o}} \end{bmatrix} \quad (2.26)$$

$$\hat{B} = \begin{bmatrix} \left. \frac{\partial f_1}{\partial \hat{U}_1} \right|_{\hat{U}_{1o}} & \left. \frac{\partial f_1}{\partial \hat{U}_2} \right|_{\hat{U}_{2o}} & \left. \frac{\partial f_1}{\partial \hat{U}_3} \right|_{\hat{U}_{3o}} & \left. \frac{\partial f_1}{\partial \hat{U}_4} \right|_{\hat{U}_{4o}} \\ \left. \frac{\partial f_2}{\partial \hat{U}_1} \right|_{\hat{U}_{1o}} & \left. \frac{\partial f_2}{\partial \hat{U}_2} \right|_{\hat{U}_{2o}} & \left. \frac{\partial f_2}{\partial \hat{U}_3} \right|_{\hat{U}_{3o}} & \left. \frac{\partial f_2}{\partial \hat{U}_4} \right|_{\hat{U}_{4o}} \\ \vdots & \vdots & \vdots & \vdots \\ \left. \frac{\partial f_{N \times N}}{\partial \hat{U}_1} \right|_{\hat{U}_{1o}} & \left. \frac{\partial f_{N \times N}}{\partial \hat{U}_2} \right|_{\hat{U}_{2o}} & \left. \frac{\partial f_{N \times N}}{\partial \hat{U}_3} \right|_{\hat{U}_{3o}} & \left. \frac{\partial f_{N \times N}}{\partial \hat{U}_4} \right|_{\hat{U}_{4o}} \end{bmatrix} \quad (2.27)$$

For the heat exchanger model the output  $\hat{Y}$  is the outlet temperature of the hot side (bleed air)  $T_{ho}$ .

$$\hat{Y} = T_{ho} = \begin{bmatrix} \frac{1}{N} & \frac{1}{N} & \dots & \frac{1}{N} \end{bmatrix} [Y'] \quad (2.28)$$

$$\text{where } Y' = \begin{bmatrix} T_{N1}^{ho} \\ T_{N2}^{ho} \\ \vdots \\ T_{NN}^{ho} \end{bmatrix} = \begin{bmatrix} g_1 \\ g_2 \\ \vdots \\ g_N \end{bmatrix}$$

Linearizing Eq. (2.28) at the operating point, the linearized output equation is:

$$\Delta \hat{Y} = \Delta T_{ho} = \hat{C} \Delta \hat{X} + \hat{D} \Delta \hat{U} \quad (2.29)$$

the  $\hat{C}$  and  $\hat{D}$  matrices are as follows:

$$\hat{C} = \begin{bmatrix} \frac{1}{N} & \frac{1}{N} & \dots & \frac{1}{N} \end{bmatrix} \begin{bmatrix} \left. \frac{\partial g_1}{\partial \hat{X}_1} \right|_{\hat{X}_{1o}} & 0 & \dots & 0 \\ \left. \frac{\partial g_2}{\partial \hat{X}_1} \right|_{\hat{X}_{1o}} & \left. \frac{\partial g_2}{\partial \hat{X}_2} \right|_{\hat{X}_{2o}} & \dots & 0 \\ \vdots & \vdots & \ddots & \vdots \\ \left. \frac{\partial g_N}{\partial \hat{X}_1} \right|_{\hat{X}_{1o}} & \left. \frac{\partial g_N}{\partial \hat{X}_2} \right|_{\hat{X}_{2o}} & \dots & \left. \frac{\partial g_N}{\partial \hat{X}_{N \times N}} \right|_{\hat{X}_{N \times N o}} \end{bmatrix} \quad (2.30)$$

$$\hat{D} = \begin{bmatrix} \frac{1}{N} & \frac{1}{N} & \dots & \frac{1}{N} \end{bmatrix} \begin{bmatrix} \frac{\partial g_1}{\partial \hat{U}_1} \Big|_{\hat{U}_{1o}} & \frac{\partial g_1}{\partial \hat{U}_2} \Big|_{\hat{U}_{2o}} & \frac{\partial g_1}{\partial \hat{U}_3} \Big|_{\hat{U}_{3o}} & \frac{\partial g_1}{\partial \hat{U}_4} \Big|_{\hat{U}_{4o}} \\ \frac{\partial g_2}{\partial \hat{U}_1} \Big|_{\hat{U}_{1o}} & \frac{\partial g_2}{\partial \hat{U}_2} \Big|_{\hat{U}_{2o}} & \frac{\partial g_2}{\partial \hat{U}_3} \Big|_{\hat{U}_{3o}} & \frac{\partial g_2}{\partial \hat{U}_4} \Big|_{\hat{U}_{4o}} \\ \vdots & \vdots & \vdots & \vdots \\ \frac{\partial g_N}{\partial \hat{U}_1} \Big|_{\hat{U}_{1o}} & \frac{\partial g_N}{\partial \hat{U}_2} \Big|_{\hat{U}_{2o}} & \frac{\partial g_N}{\partial \hat{U}_3} \Big|_{\hat{U}_{3o}} & \frac{\partial g_N}{\partial \hat{U}_4} \Big|_{\hat{U}_{4o}} \end{bmatrix} \quad (2.31)$$

### 2.3.2 Linear Open-loop System Model

For the bleed air system, the control valve dynamics must be considered. So the bypass valve opening angle and ram air valve opening angle,  $\beta_{bypass}$  and  $\beta_{ram}$ , respectively, are denoted as additional state variables. And from Eq. (2.9), additional state equations are derived as below:

$$\dot{\beta}_{bypass} = -\frac{1}{\tau_v} \beta_{bypass} + \frac{K_v}{\tau_v} u_{bypass} = f_{(N \times N + 1)}(X, U) \quad (2.32)$$

$$\dot{\beta}_{ram} = -\frac{1}{\tau_v} \beta_{ram} + \frac{K_v}{\tau_v} u_{ram} = f_{(N \times N + 2)}(X, U) \quad (2.33)$$

where  $u_{bypass}$  and  $u_{ram}$  are opening-command inputs to the bypass valve and ram air valve, respectively.

The state variable is a vector with  $(N \times N + 2)$  elements:

$$\begin{aligned} X &= \left[ T_{11}^s, \dots, T_{1N}^s, T_{21}^s, \dots, T_{N1}^s, \dots, T_{NN}^s, \beta_{bypass}, \beta_{ram} \right]^T \\ &= \left[ \hat{X} \quad \beta_{bypass} \quad \beta_{ram} \right]^T \end{aligned} \quad (2.34)$$

The valve opening-command  $u_{bypass}$  and  $u_{ram}$  compose the system input vector:

$$U = \begin{bmatrix} u_{bypass} & u_{ram} \end{bmatrix}^T = \begin{bmatrix} U_1 & U_2 \end{bmatrix}^T \quad (2.35)$$

There are some disturbances that affect the system output, and are denoted as

$$Z = [W_{bleed} \quad T_{hi} \quad T_{ci} \quad P_{hi} \quad P_{load} \quad P_{cin} \quad P_{ci}]^T \quad (2.36)$$

The system state equation can be written as

$$\dot{X} = f(X, U, Z) \quad (2.37)$$

To linearize Eq. (2.37) at an operating point, a linear state equation is driven as below:

$$\Delta \dot{X} = A \Delta X + B \Delta U + H \Delta Z \quad (2.38)$$

where

$$A = \begin{bmatrix} A_{11} & A_{12} \\ 0 & A_{22} \end{bmatrix} \quad (2.39)$$

in which  $A_{11} = \hat{A}$ ,

$$A_{12} = \begin{bmatrix} \left. \frac{\partial f_1}{\partial \beta_{bypass}} \right|_{\beta_{bypass0}} & \left. \frac{\partial f_1}{\partial \beta_{ram}} \right|_{\beta_{ram0}} \\ \left. \frac{\partial f_2}{\partial \beta_{bypass}} \right|_{\beta_{bypass0}} & \left. \frac{\partial f_2}{\partial \beta_{ram}} \right|_{\beta_{ram0}} \\ \vdots & \vdots \\ \left. \frac{\partial f_{N \times N}}{\partial \beta_{bypass}} \right|_{\beta_{bypass0}} & \left. \frac{\partial f_{N \times N}}{\partial \beta_{ram}} \right|_{\beta_{ram0}} \end{bmatrix}$$

$$A_{22} = \begin{bmatrix} -\frac{1}{\tau_v} & 0 \\ 0 & -\frac{1}{\tau_v} \end{bmatrix}$$

$$B = \begin{bmatrix} 0 \\ 0 \\ \frac{K_v}{\tau_v} & 0 \\ 0 & \frac{K_v}{\tau_v} \end{bmatrix} = [B_1 \quad B_2] \quad (2.40)$$

$$H = \begin{bmatrix} \left. \frac{\partial f_1}{\partial Z_1} \right|_{Z_{1o}} & \left. \frac{\partial f_1}{\partial Z_2} \right|_{Z_{2o}} & \dots & \left. \frac{\partial f_1}{\partial Z_7} \right|_{Z_{7o}} \\ \left. \frac{\partial f_2}{\partial Z_1} \right|_{Z_{1o}} & \left. \frac{\partial f_2}{\partial Z_2} \right|_{Z_{2o}} & \dots & \left. \frac{\partial f_2}{\partial Z_7} \right|_{Z_{7o}} \\ \vdots & \vdots & \ddots & \vdots \\ \left. \frac{\partial f_{N \times N}}{\partial Z_1} \right|_{Z_{1o}} & \left. \frac{\partial f_{N \times N}}{\partial Z_2} \right|_{Z_{2o}} & \dots & \left. \frac{\partial f_{N \times N}}{\partial Z_7} \right|_{Z_{7o}} \\ 0 & 0 & \dots & 0 \\ 0 & 0 & \dots & 0 \end{bmatrix} \quad (2.41)$$

There are two outputs for the bleed air system: one is the load temperature  $T_{load}$ , another is the bypass valve opening angle  $\beta_{bypass}$ . Hence, the output equations are

$$Y_1 = T_{load} = h(X, Z) \quad (2.42-a)$$

$$Y_2 = \beta_{bypass} = X_{N \times N + 1} \quad (2.40-b)$$

To linearize at an operating point, the output equation is:

$$\Delta Y = C \Delta X + G \Delta Z \quad (2.43)$$

where  $C = \begin{bmatrix} C_1 \\ C_2 \end{bmatrix}$ , and  $G = \begin{bmatrix} G_1 \\ 0 \end{bmatrix}$ ,

in which  $C_1 = \begin{bmatrix} \left. \frac{\partial h}{\partial X_1} \right|_{X_{1o}} & \left. \frac{\partial h}{\partial X_2} \right|_{X_{2o}} & \dots & \left. \frac{\partial h}{\partial X_{N \times N + 2}} \right|_{X_{N \times N + 2o}} \end{bmatrix}$ ,

$$C_2 = [0 \quad \dots \quad 0 \quad 1 \quad 0]$$

$$G_1 = \begin{bmatrix} \left. \frac{\partial h}{\partial Z_1} \right|_{Z_{1o}} & \left. \frac{\partial h}{\partial Z_2} \right|_{Z_{2o}} & \dots & \left. \frac{\partial h}{\partial Z_{N \times N}} \right|_{Z_{N \times N o}} \end{bmatrix}$$

## 2.4 Simulations of Open-loop System Model

To validate the effectiveness of the linearized model, simulations for certain operating conditions are conducted using both nonlinear and linearized models. Fig. 2.5 shows the Simulink program for the linear open-loop model for the bleed air system.

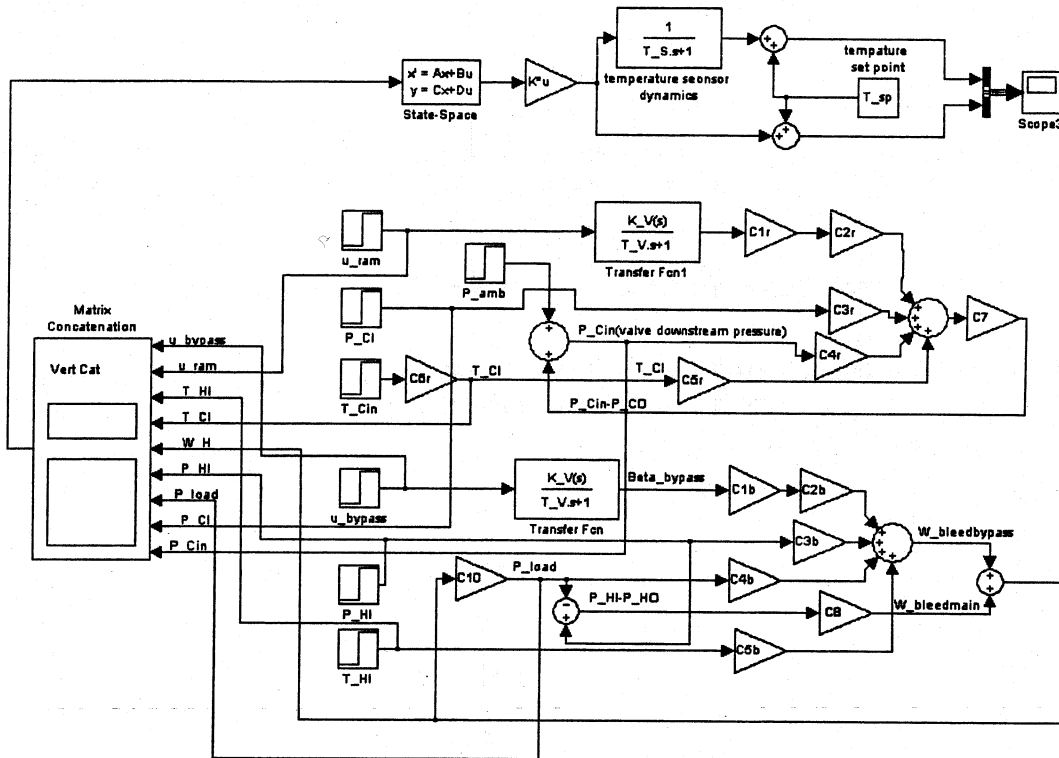


Fig. 2.5 Linear open-loop model for bleed air system

An operating condition, which is at certain engine loading and atmospheric conditions, as shown in Table 2.1, is chosen to represent the system simulations.

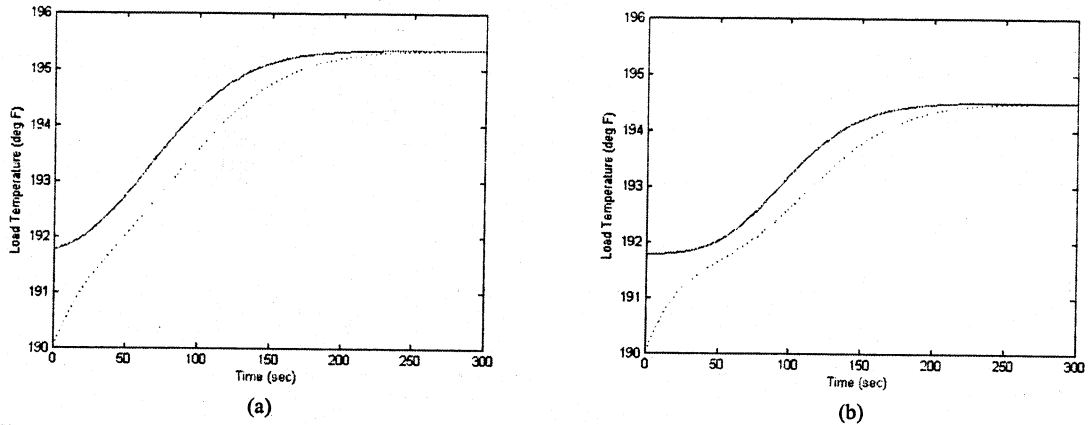
Altitude (kft)	Mach Number	Bleed Air Mass Flow $W_{bleed}$ (lb/s)	Bleed Air Pressure $P_{hin}$ (psig)	Bleed Air Temperature $T_{hi}$ (°F)	Ambient Pressure $P_{amb}$ (psia)	Ambient Temperature $T_{amb}$ (°F)
10	0.5	0.018333	35	380	10.11	90

Table 2.1 Operating conditions and corresponding mission data selected for simulation

The following figures (Fig. 2.6 to Fig. 2.11) show the load temperature step response of nonlinear and linear model, with respect to the step change of engine loading conditions ( $T_{hi}$ ,  $P_{hin}$ ), atmospheric conditions ( $T_{amb}$ ,  $P_{amb}$ ), bypass valve opening  $u_{bypass}$  and ram air valve opening  $u_{ram}$ . For the simulation, the pipe size of the bleed air channel



and ram air channel is 1.5-inch diameter, and the heat exchanger partitioning dimension  $N$  is 10. The load temperature set point is 190 °F. In the following figures, the solid line is the load temperature and the dashed line is the load temperature measured by a temperature sensor.



**Fig. 2.6 Step response to a 20°F step increase in bleed air inlet temperature  $T_{hi}$ : (a) nonlinear model simulation; (b) linear model simulation**

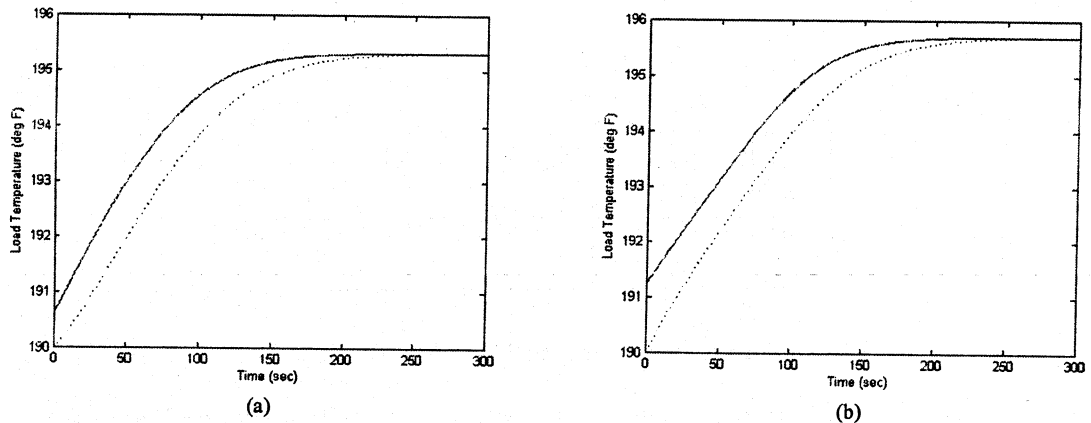


**Fig. 2.7 Step response to a 5 psig step increase in bleed air inlet pressure  $P_{hin}$ : (a) nonlinear model simulation; (b) linear model simulation**

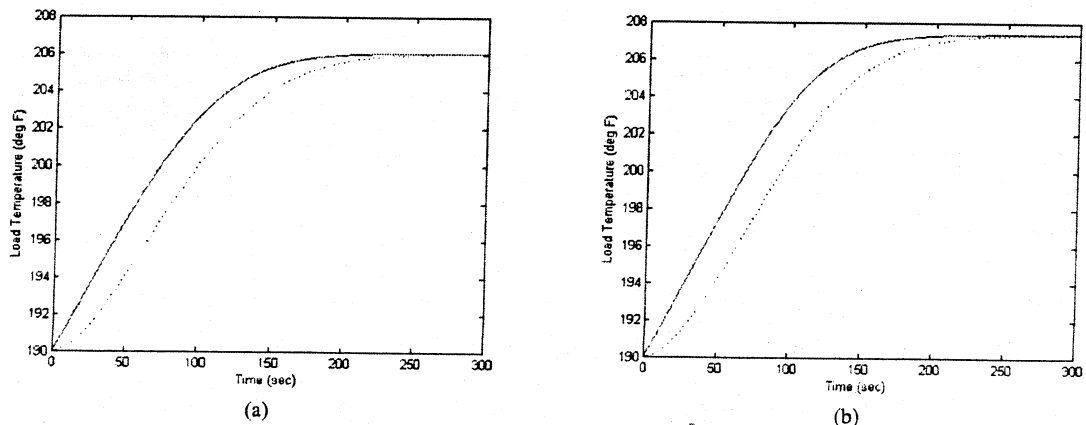
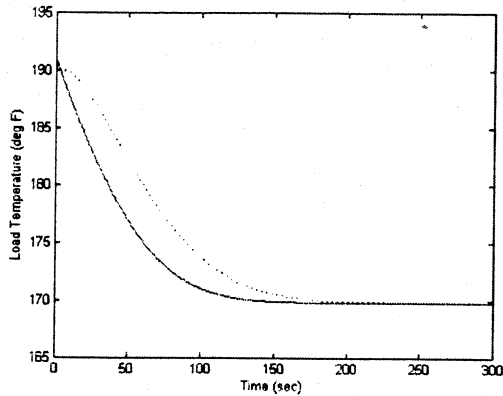
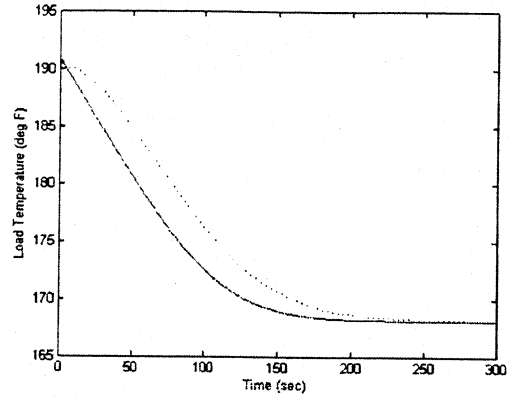


**Fig. 2.8 Step response to a 20 °F step increase in ambit temperature  $T_{amb}$ : (a) nonlinear model simulation; (b) linear model simulation**

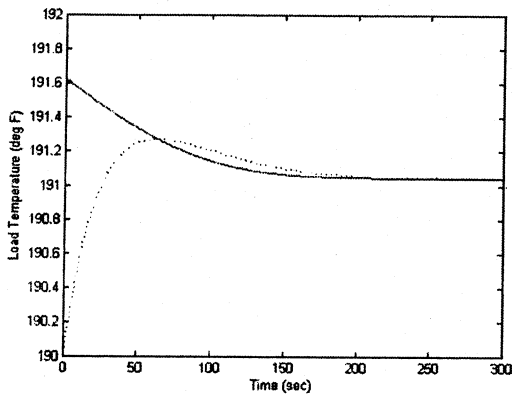


(a)

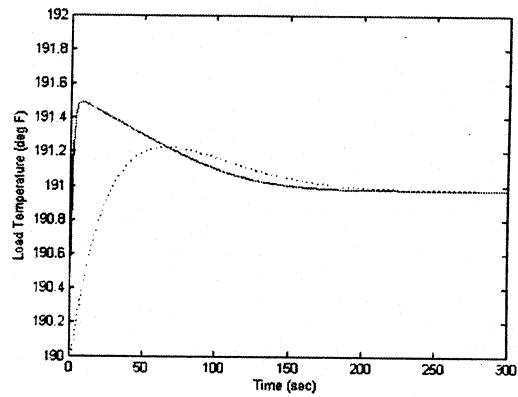


(b)

**Fig. 2.9 Step response to a 5 psig step increase in ambient pressure  $P_{amb}$ : (a) nonlinear model simulation; (b) linear model simulation**

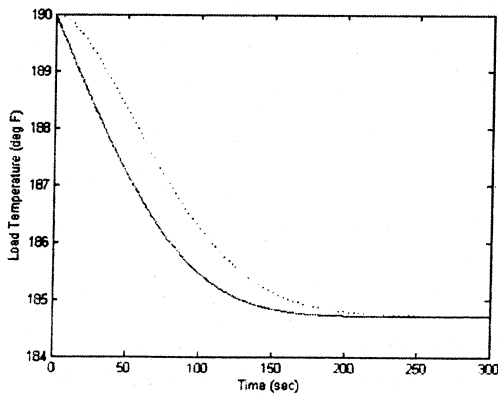


(a)

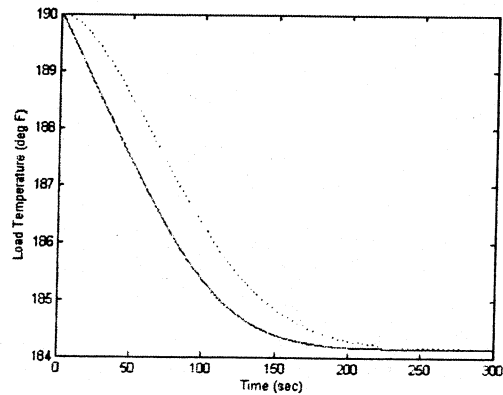


(b)

**Fig. 2.10 Step response to a 1% step increase in bypass valve opening  $u_{bypass}$ : (a) nonlinear model simulation; (b) linear model simulation**



(a)



(b)

**Fig. 2.11 Step response to a 1% step increase in ram air valve opening  $u_{ram}$ : (a) nonlinear model simulation; (b) linear model simulation**

Since the linearized model is a first order Taylor series expansion of the nonlinear model, as shown in Fig. 2.12, it may cause errors as a result of eliminating the high order term of the Taylor series expansion.

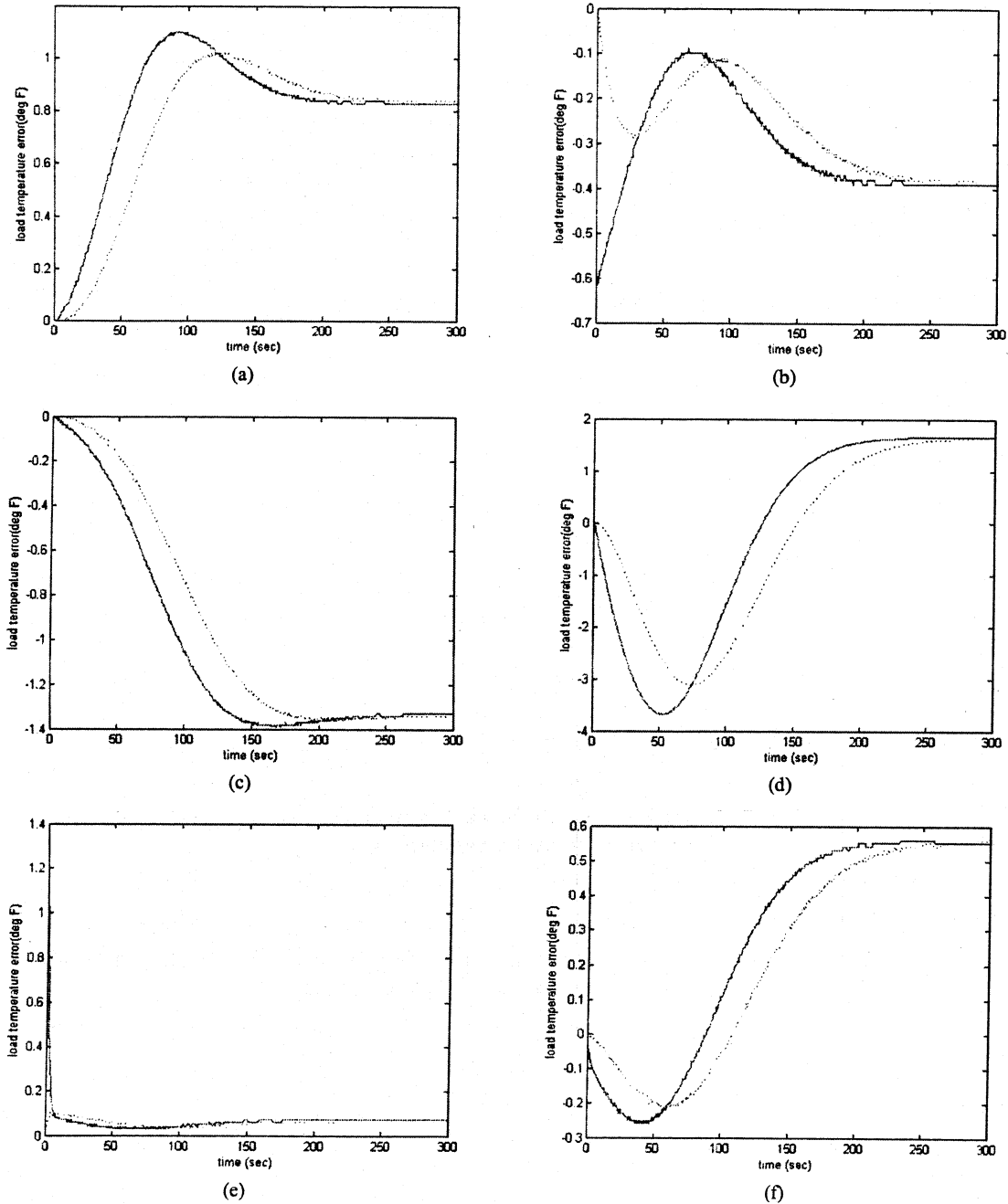


**Fig. 2.12 Errors of the temperature time response of the nonlinear and linearized models: (a) 20°F step increase in bleed air inlet temperature  $T_{hi}$ ; (b) 5 psig step increase in bleed air inlet pressure  $P_{hin}$ ; (c) 20°F step increase in ambient temperature  $T_{amb}$ ; (d) 5 psig step increase in bleed air inlet pressure  $P_{amb}$ ; (e) 1% step increase in bypass valve opening  $u_{bypass}$ ; (f) 1% step increase in bypass valve opening  $u_{ram}$**

It can be seen from Fig. 2.12 that the simulation results of the nonlinear and linearized model are very close when the same inputs are applied to the system. Since the linearized model matches the nonlinear model well around the operating condition, the linearized model can be used in the control system design of the ram air and bypass temperature control system working around the operating points.

# CHAPTER 3 TEMPERATURE CONTROL OF BLEED AIR SYSTEM

## 3.1 Ram-Air-Plus-Bypass Control Strategy

The schematic diagram of the ram-air-plus-bypass control strategy for an engine bleed air system is shown in Fig. 3.1. The system is closed with an optimal controller instead of the traditional PI control (Hodal and Liu, 2005) by which the one-loop-at-a-time approach has to be used to design the MIMO system.

In the ram-air-plus-bypass control configuration, the control objective is to maximize the speed of the temperature response with acceptable overshoot through control of the bypass channel, and to minimize the usage of ram air through the ram air channel control.

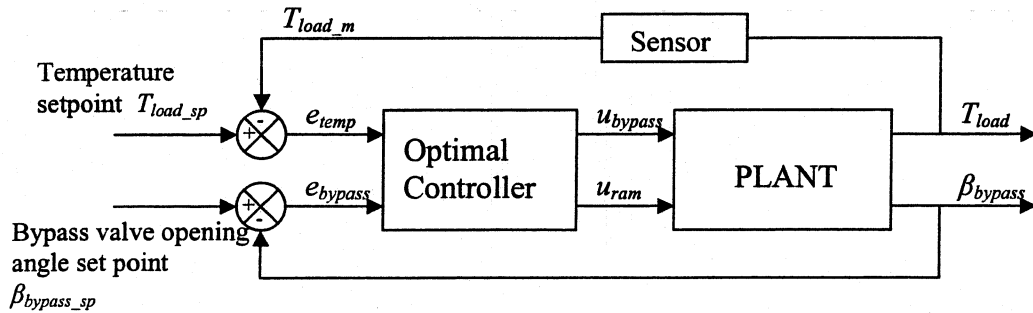


Fig. 3.1 Ram-air-plus-bypass control strategy

To ensure non-excessive ram air usage, the desired amount the bypass bleed flow is kept low (such as 10% of total bleed flow), and the bypass valve opening set-point is set to a value that will yield such bypass ratio at initial conditions. This set-point is regulated during the simulation by the ram air channel controller. Optimizing ram air usage means minimizing the amount of ram air used, which is directly related to choosing

the amount of bleed air bypass – the lower the bypass, the less ram air is being wasted. The bypass valve opening set-point can be re-adjusted by the user, should the use of ram air become more or less of importance. In this way, the ram air usage is optimized by the user, so to speak. With the bypass ratio set, and thus the bypass valve opening set-point defined, the task remains to optimize the performance of the temperature transient response for this system. It is the purpose of the bypass controller to bring about temperature regulation efficiently.

### 3.2 Linear Quadratic Regulator (LQR) with Output Feedback

The objective of LQR output feedback control is to use modern control techniques to regulate certain states of the system to zero while obtain desirable closed-loop response characteristics.

Once the performance criterion has been selected, the control gains are explicitly computed by matrix design equations, and the closed-loop system stability will generally be guaranteed.

#### 3.2.1 Optimal Controller Design

As shown in Fig. 3.1, the temperature error is defined as the difference between the load temperature set-point and the load temperature measured by sensor:

$$e_{temp} = T_{load\_sp} - T_{load\_m} \quad (3.1)$$

And the bypass valve error is defined as the difference between the bypass valve opening angle set-point and its current value:

$$e_{bypass} = \beta_{bypass\_sp} - \beta_{bypass} \quad (3.2)$$

The measured load temperature can be considered as an augmented state vector, and the state equation is driven from Eq. (2.17):

$$\dot{T}_{load\_m} = -\frac{1}{\tau_{ts}} T_{load\_m} + \frac{K_{ts}}{\tau_{ts}} T_{load} \quad (3.3)$$

$$\dot{T}_{load\_m} = -\frac{1}{\tau_{ts}}T_{load\_m} + \frac{K_{ts}}{\tau_{ts}}T_{load} \quad (3.3)$$

The change of load temperature set-point and bypass valve opening angle set-point are considered as disturbances.

The corresponding linear augmented state equation is driven as below:

$$\Delta\dot{X}_{aug} = A_{aug}\Delta X_{aug} + B_{aug}\Delta U + H_{aug}\Delta Z_{aug} \quad (3.4)$$

$$\text{where } \Delta X_{aug} = [\Delta X \quad \Delta T_{load\_m}]^T, \quad \Delta Z_{aug} = [\Delta Z \quad \Delta T_{load\_sp} \quad \Delta \beta_{bypass\_sp}]^T,$$

$$A_{aug} = \begin{bmatrix} A & 0 \\ \frac{K_{ts}}{\tau_{ts}}C_1 & -\frac{1}{\tau_{ts}} \end{bmatrix}, \quad B_{aug} = \begin{bmatrix} B \\ 0 \end{bmatrix}, \quad \text{and } H_{aug} = \begin{bmatrix} H & 0 & 0 \\ \frac{K_{ts}}{\tau_{ts}}G_1 & 0 & 0 \end{bmatrix}$$

The output equation for the closed loop system is defined as:

$$E = C_{aug}\Delta X_{aug} + G_{aug}\Delta Z_{aug} \quad (3.5)$$

$$\text{where } E = [e_{temp} \quad e_{bypass}]^T,$$

$$C_{aug} = \begin{bmatrix} 0 & \dots & 0 & 0 & -1 \\ 0 & \dots & 0 & -1 & 0 \end{bmatrix}, \quad \text{and } G_{aug} = \begin{bmatrix} 0 & \dots & 0 & 1 & 0 \\ 0 & \dots & 0 & 0 & 1 \end{bmatrix}$$

For the linear system written in Eq. (3.4) and (3.5), to eliminate the disturbances term, the system state space equation can be written as below:

$$\Delta\dot{X}_{aug} = A_{aug}\Delta X_{aug} + B_{aug}\Delta U \quad (3.6)$$

$$E = C_{aug}\Delta X_{aug} \quad (3.7)$$

The LQR output feedback is to find an feedback control gain  $K_{lq}$ , where

$$\Delta U = -K_{lq}E \quad (3.8)$$

$$J = \frac{1}{2} \int_0^{\infty} (\Delta X_{aug}^T Q \Delta X_{aug} + \Delta U^T R \Delta U) dt \quad (3.9)$$

where  $Q$  and  $R$  are the user specified ‘penalty’ weights associated with respective state deviations and the overall control effort. Some trial and error are usually necessary to determine the  $Q$  and  $R$  values that yield the best results, where  $Q$  and  $R$  are symmetric positive semidefinite weighting matrices.

By substituting the control law, Eq. (3.8), into Eq. (3.6), the closed-loop system equations are found to be

$$\Delta \dot{X}_{aug} = (A_{aug} - B_{aug} K_{lq} C_{aug}) \Delta X_{aug} \equiv A_c \Delta X_{aug} \quad (3.10)$$

The optimal control gain  $K_{lq}$  can be calculated from the equation below:

$$K_{lq} = R^{-1} B_{aug}^T P S C_{aug}^T (C_{aug} S C_{aug}^T)^{-1} \quad (3.11)$$

where  $P$  is a constant, symmetric, positive-semidefinite matrix and  $S$  is a symmetric matrix of Lagrange multipliers. Matrices  $P$  and  $S$  are calculated from two Lyapunov equations:

$$A_c^T P + P A_c + C_{aug}^T K_{la}^T R K_{la} C_{aug} + Q = 0 \quad (3.12)$$

$$A_c S + S A_c^T + \Delta X_{aug}(0) \Delta X_{aug}^T(0) = 0 \quad (3.13)$$

where  $\Delta X_{aug}(0)$  denotes the initial state variables.

### 3.2.2 Selection of Weighting Matrix

The performance index weighting matrices  $Q$  and  $R$  are user specified terms. Once the weight matrices have been selected, the determination of the optimal feedback gain  $K_{lq}$  can be calculated by matrix equations (Eq. (3.11)-Eq. (3.13)). So the weighting matrices  $Q$  and  $R$  may be chosen to yield good time response in the closed loop system.



Since the matrices  $Q$  and  $R$  are symmetric positive semi-definite matrices, they can be selected as an identity matrix times a positive constant:

$$Q = q \times \text{eye}(N \times N + 3) \quad (3.14)$$

$$R = r \times \text{eye}(2) \quad (3.15)$$

where  $q$  and  $r$  are positive constants,  $\text{eye}(2)$  and  $\text{eye}(N \times N + 3)$  and denote  $2 \times 2$  and  $(N \times N + 3) \times (N \times N + 3)$  identity matrices, respectively.  $N$  is the heat exchanger plate partitioning dimension.

Based on Eq. (3.14) and Eq. (3.15), weighting matrices can be selected by only changing the constants  $q$  and  $r$ . Fig. 3.2 shows the load temperature step response under different values of  $q$  and  $r$ .

As shown in Fig. 3.2, larger  $q$  and smaller  $r$  will result in an unstable step response of the load temperature. Thus, the range of  $q$  and  $r$  is narrowed down to a small range.

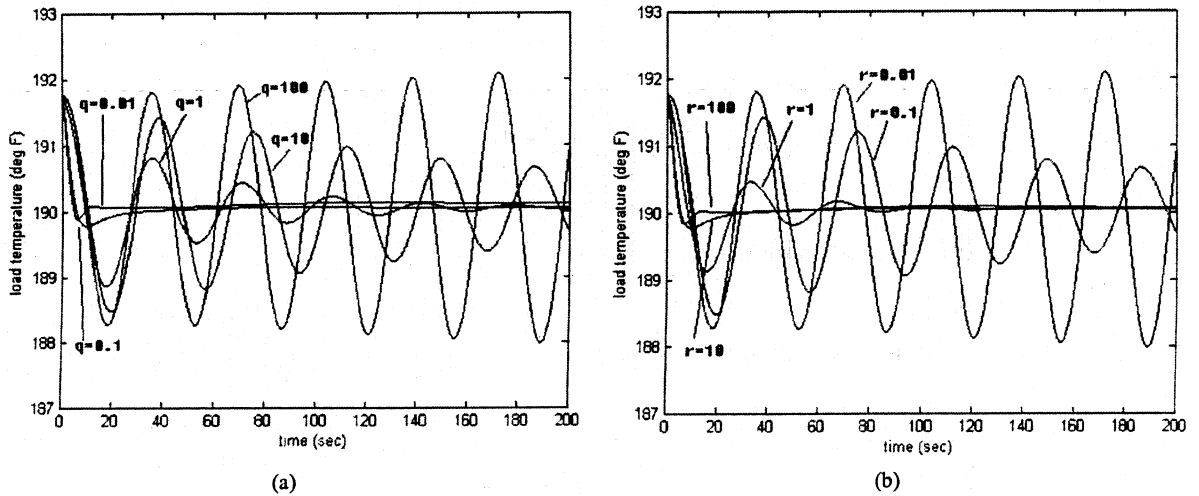
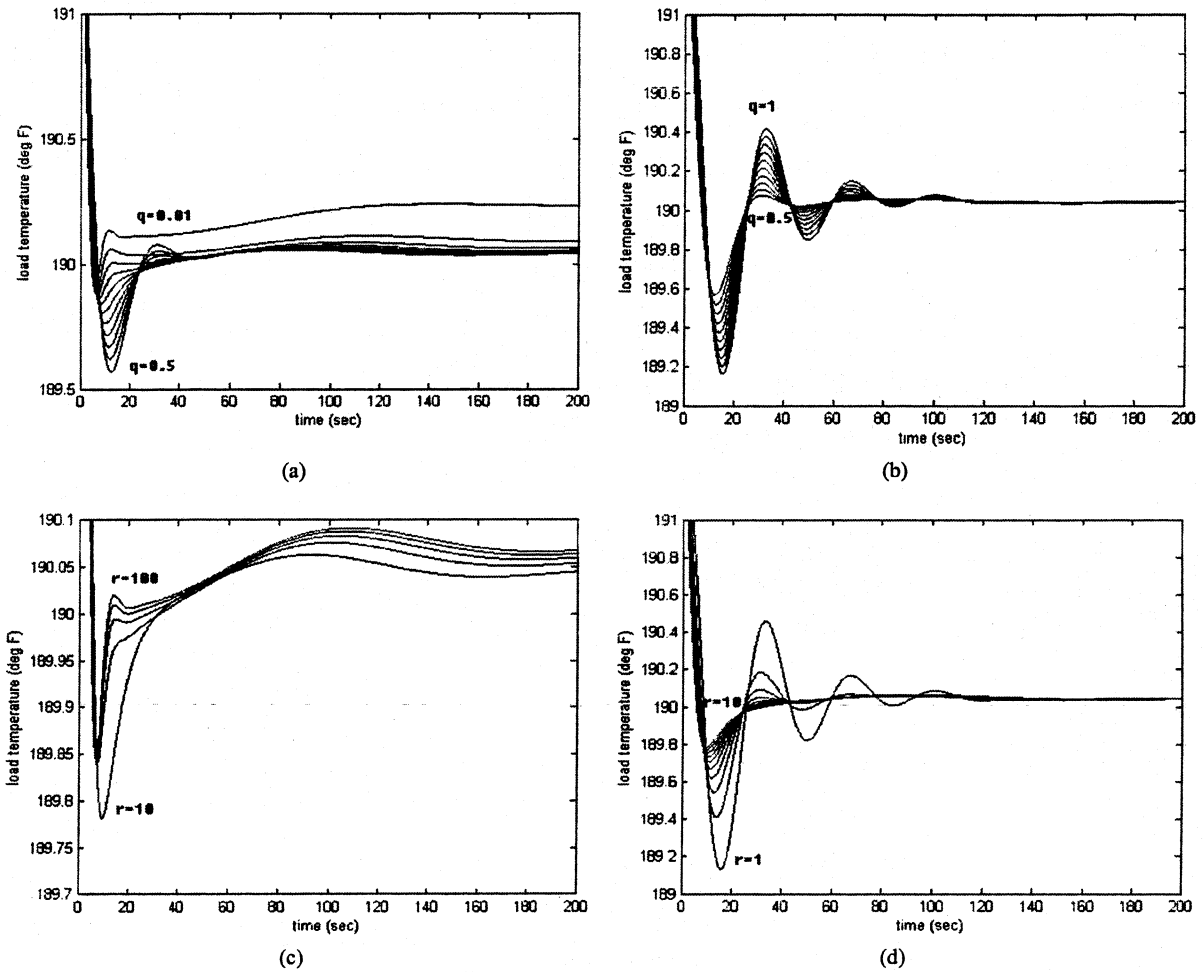


Fig. 3.2 Load temperature response under different  $q$  and  $r$ : (a)  $r = 1$ ; (b)  $q = 1$

The temperature response within a small parameter range is shown in Fig. 3.3. These results show that small  $q$  and large  $r$  will result in a small initial overshoot but large steady-state error and long settling time. In order to balance the overshoot, settling

time and steady-state errors, the values of  $q$  and  $r$  are selected as  $q = 0.5$ ,  $r = 10$ . The output feedback control gain is:

$$K_{lq} = \begin{bmatrix} -11.302 & 0 \\ 6.6625 & -30.98 \end{bmatrix}$$



**Fig. 3.3 Load temperature response under small range of  $q$  and  $r$ : (a)  $r = 1$ ,  $q = 0.01 \sim 0.5$ ; (b)  $r = 1$ ,  $q = 0.5 \sim 1$ ; (c)  $q = 1$ ,  $r = 10 \sim 100$ ; (d)  $q = 1$ ,  $r = 1 \sim 10$**

### 3.3 Simulations

Simulations are conducted using Matlab/Simulink to investigate the effectiveness of the optimal output feedback control based on the ram air and bypass state-space model of the bleed air system developed in Chapter 2.



$c_c=0.24$	$c_h=0.24$	$MC_s=0.65$	$\gamma=1.4$	$g=386.09$
$R=639.6$	$N=10$	$Mach=0.5$	$F_{rec}=0.7$	$d_{ram}=1.5$
$K_v=0.015708$	$\tau_v=1.5$	$\tau_{ts}=24.078$	$K_{load}=104120$	$T_{load\_sp}=190$
$T_{amb}=90$	$T_{hi}=380$	$T_{ci}=117.5$	$T_{ho}=168.89$	$T_{load}=190$
$P_{amb}=10.11$	$Phin=45.11$	$P_{cin}=11.428$	$P_{hi}=45.11$	$d_{bypass}=1.5$
$P_{ho}=45.107$	$P_{co}=10.11$	$P_{load}=45.107$	$\beta_{bypass}=0.38002$	$A_{bypass}=0.12606$
$W_{bleedbypass}=0.0018332$	$W_{ram}=0.019794$	$W_{bleed}=0.018333$	$K_{ts}=1$	$u_{bypass}=24.19$
$W_{bleedmain}=0.0165$	$A_{ram}=0.11932$	$\beta_{ram}=0.36958$	$BR=0.1$	$P_{ci}=10.114$
$u_{bypass\_sp}=24.19$	$u_{ram}=23.529$	$q=0.5$	$r=10$	$K_{lq} = \begin{bmatrix} -11.302 & 0 \\ 6.6625 & -30.98 \end{bmatrix}$

Table 3.1 Initial steady-state conditions

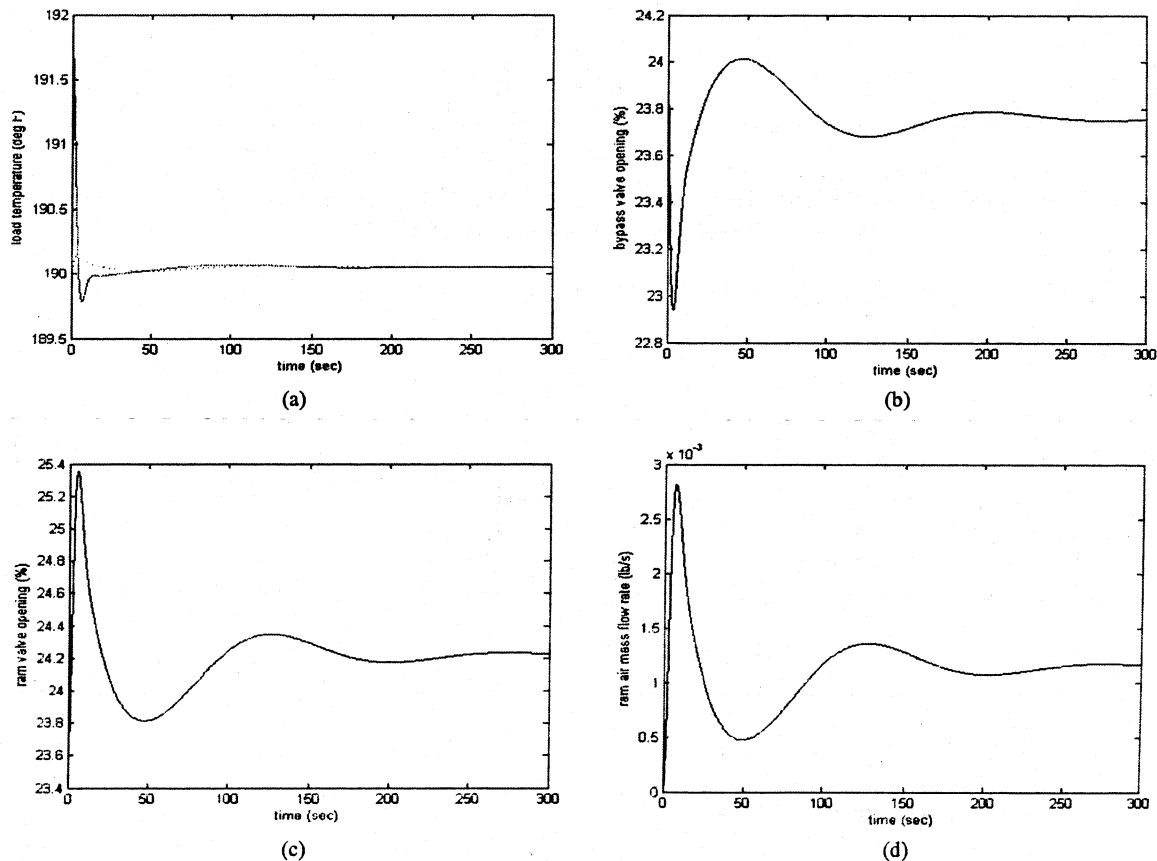
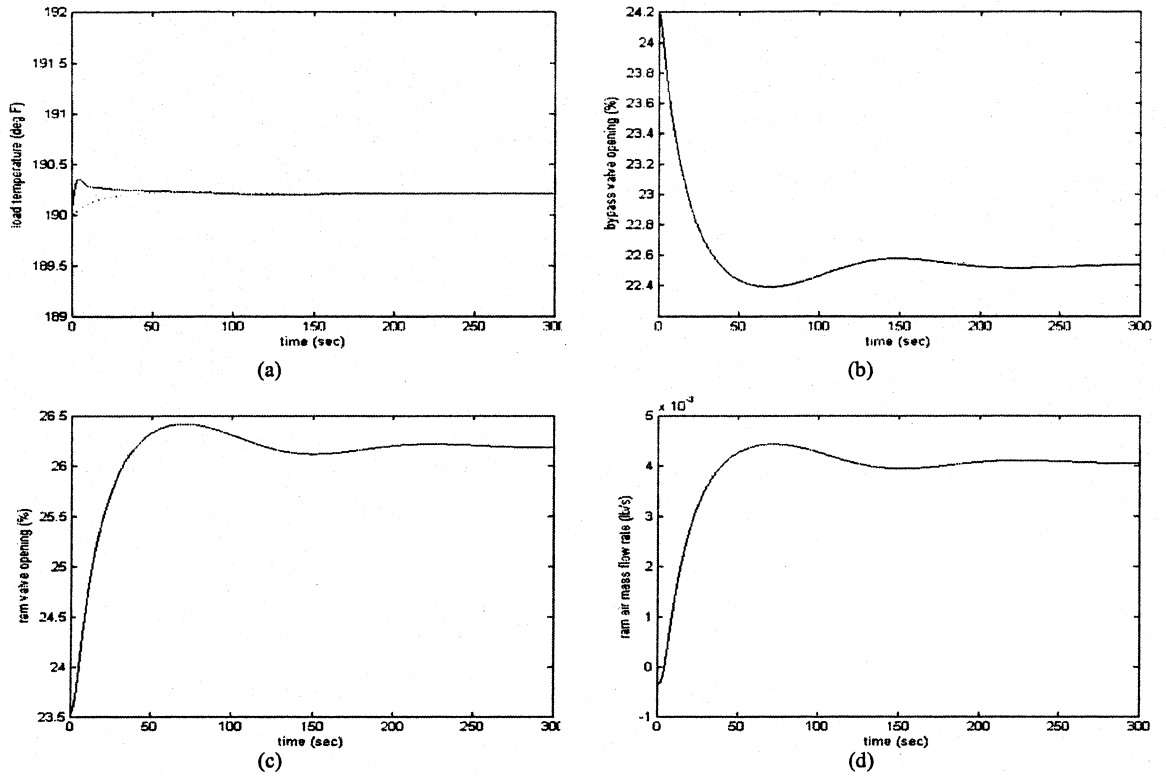
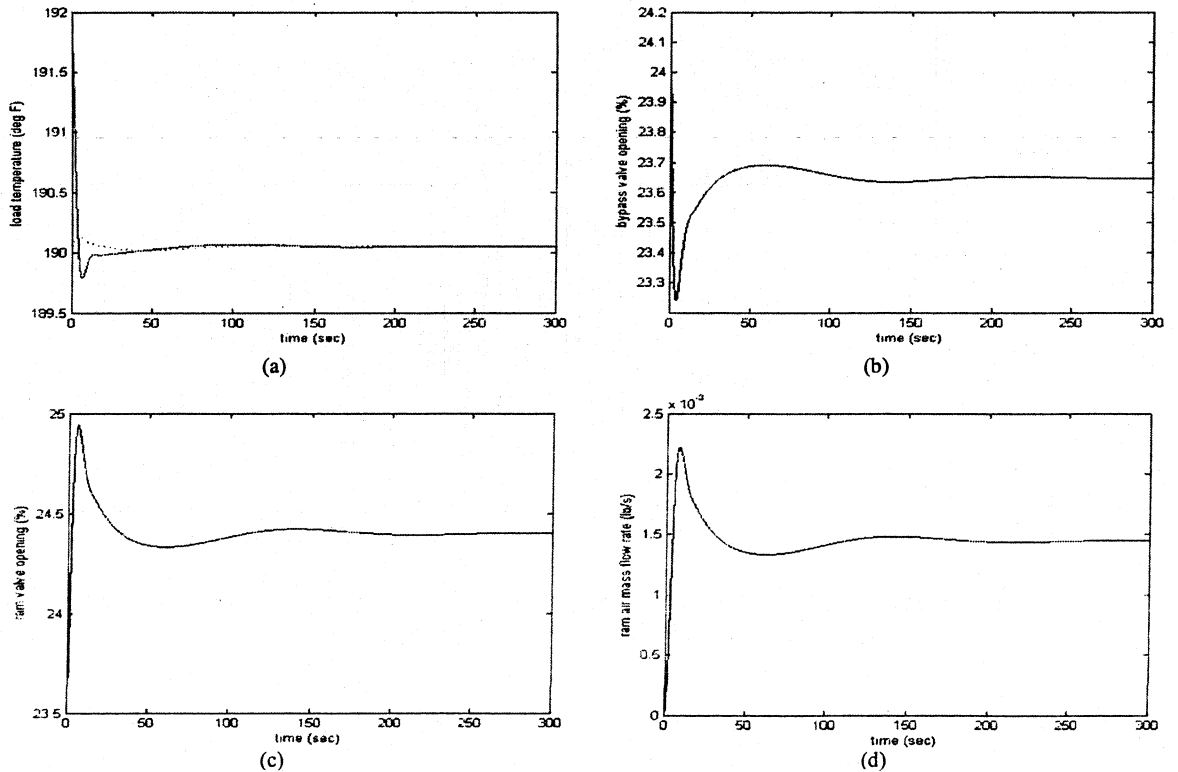


Fig. 3.5 System response to input 1: (a) load temperature; (b) bypass valve opening; (c) ram-air valve opening; (d) ram-air mass flow rate



**Fig. 3.6 System response to input 2: (a) load temperature; (b) bypass valve opening; (c) ram-air valve opening; (d) ram-air mass flow rate**



**Fig. 3.7 System response to input 3: (a) load temperature; (b) bypass valve opening; (c) ram-air valve opening; (d) ram-air mass flow rate**

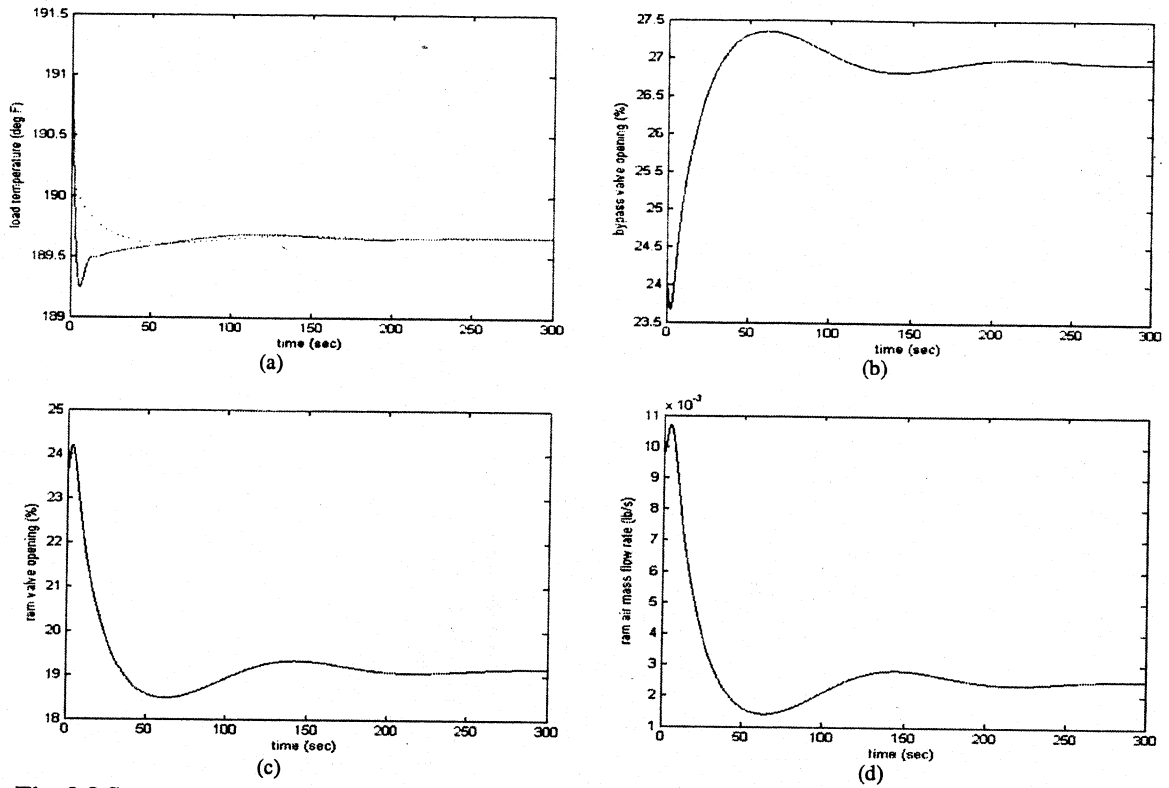


**Fig. 3.8 System response to input 4: (a) load temperature; (b) bypass valve opening; (c) ram-air valve opening; (d) ram-air mass flow rate**

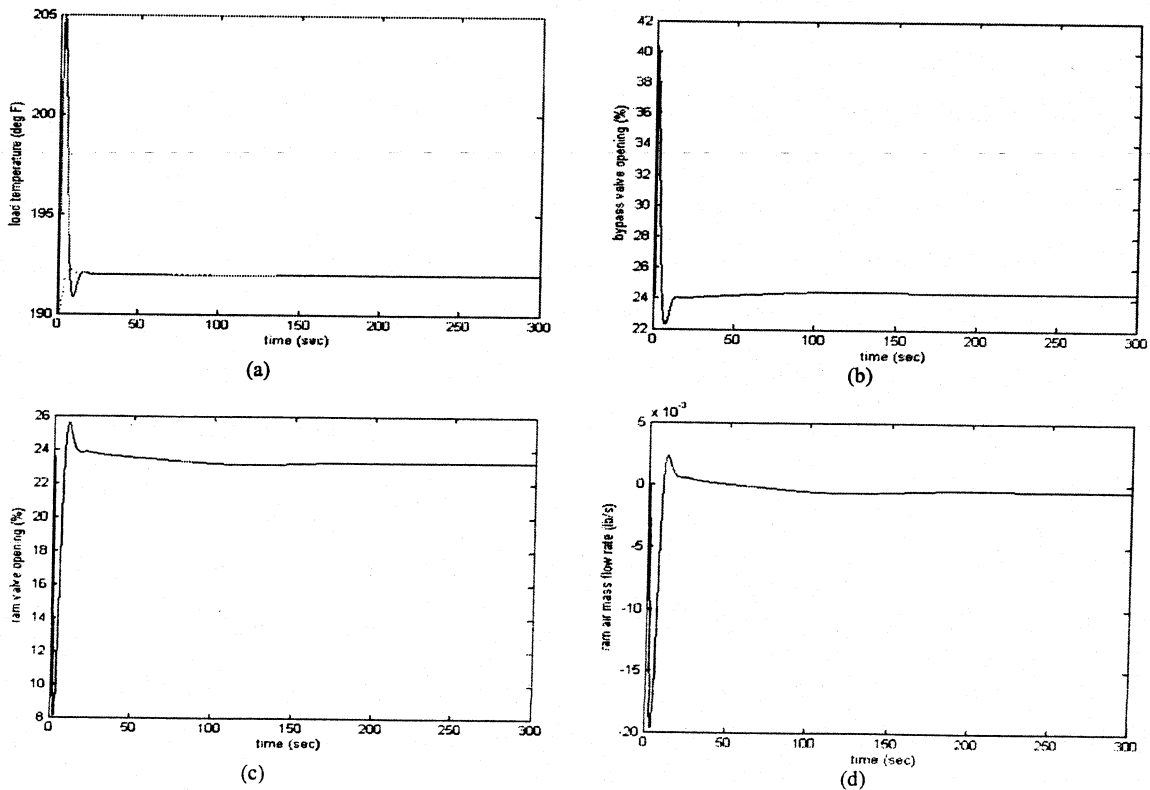


**Fig. 3.9 System response to input 5: (a) load temperature; (b) bypass valve opening; (c) ram-air valve opening; (d) ram-air mass flow rate**

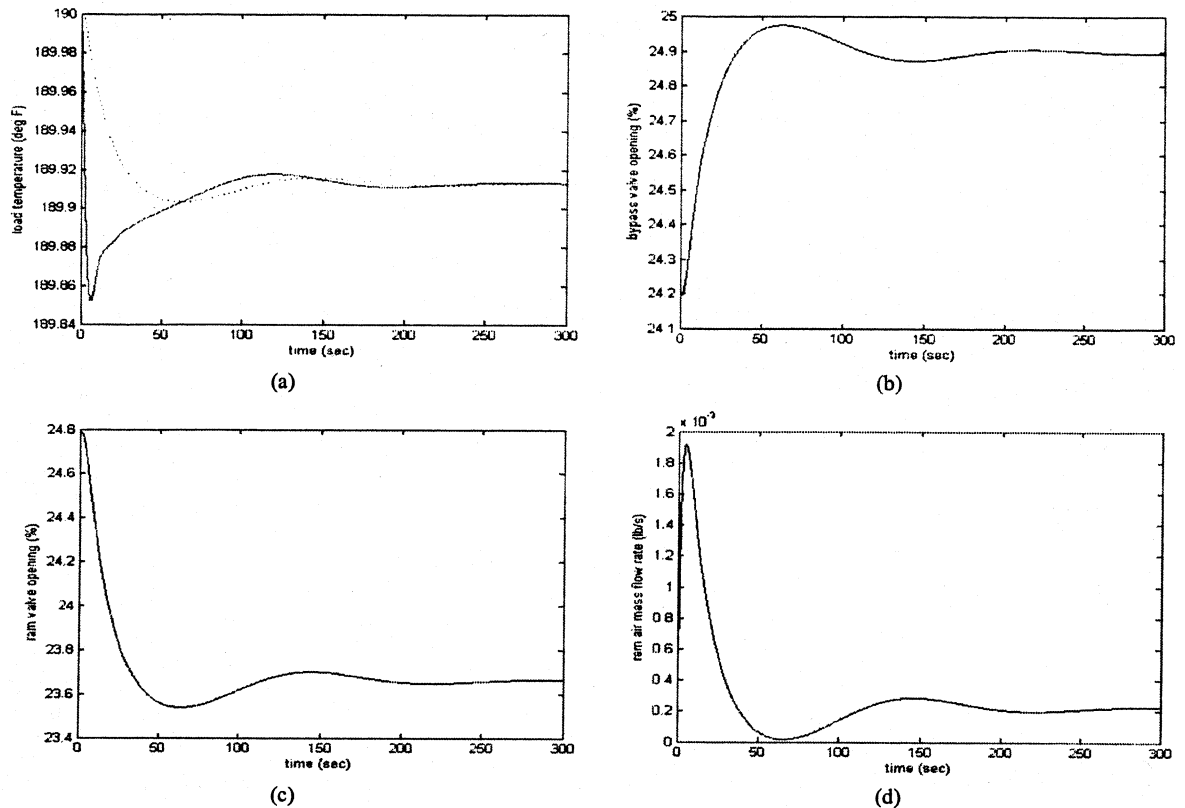


**Fig. 3.10** System response to input 6: (a) load temperature; (b) bypass valve opening; (c) ram-air valve opening; (d) ram-air mass flow rate

### 3.4 Discussions and Conclusions

Increasing the speed of the temperature response is one of the goals in this thesis. From the simulation results, it is seen that this goal can be reached using the LQ output feedback controller. The temperature response with output feedback has small overshoot and little steady error, which is less than 0.2 °F. The output feedback also causes a steady state error in the bypass valve control loop. The matrices  $Q$  and  $R$  may be chosen to yield a better time response.

Reduced ram air usage, which is another goal for thesis project, is also achieved by the optimal controller. As the response to a 20 °F step increase in bleed air inlet temperature, the increment of ram airflow rate is 0.0012 lb/s. As the response to a 1% step increase in bypass valve opening, the increment of ram airflow rate is only 0.0002 lb/s.

# **CHAPTER 4    DEVELOPMENT OF TEST FACILITY AND EXPERIMENTS**

## **4.1 Test Rig Design**

A test rig is developed at the Systems and Control Laboratory of Ryerson University for the flow temperature control studies. The test rig consists of one bleed air channel and a ram air channel. A bypass channel is split from the bleed air channel over the heat exchanger. Electrical control valves are installed in the bypass channel and ram air channel to control the mass flow rate of each channel. A temperature sensor is installed at the end of bleed air channel to measure the load temperature. Mass flow sensors, pressure sensors, temperature sensors and manual valves are equipped for reconfiguring the system.

There are two air sources available for the experiment. The main air source is two parallel-connected high pressure tanks, each having a capacity of 51300 in<sup>3</sup>. The maximum pressure inside the tank is 100 psig, charged by a compressor. Although the compressor can continuously supply the compressed air to the tanks, the pressure of the air feeding to the test rig drops, depending upon the mass flow rate. To solve this problem, a control valve is installed between the tanks and the test rig. The source air pressure for the test rig can be kept approximately constant by regulating this control valve. The second air source is a shared tank with other labs. It can supply air for the ram air channel.

There are two size metal pipes in the test rig. The ¾-inch diameter pipe is used to fit the ¾-inch electrical control valves, which are used to regulate the air source inlet pressure, ram air flow rate and bypass flow rate. The 2-inch diameter pipe is used for installing the flow sensor, which is too long to install in a ¾-inch diameter pipe.



The command unit consist of a Pentium-D PC, a 16 bit A/D board ( PCI 6034E) and a 16 bit D/A board (PCI 6704), both manufactured by National Instruments, Co. The PC serves as the controller that sends out current commands to control valves and collects signals of pressures transducers, flow sensors, and temperature sensors.

The schematic layout and picture of the test rig are shown in Fig. 4.1 and Fig. 4.2, respectively. Main control elements and their locations in the test rig are listed in Table 4.1.

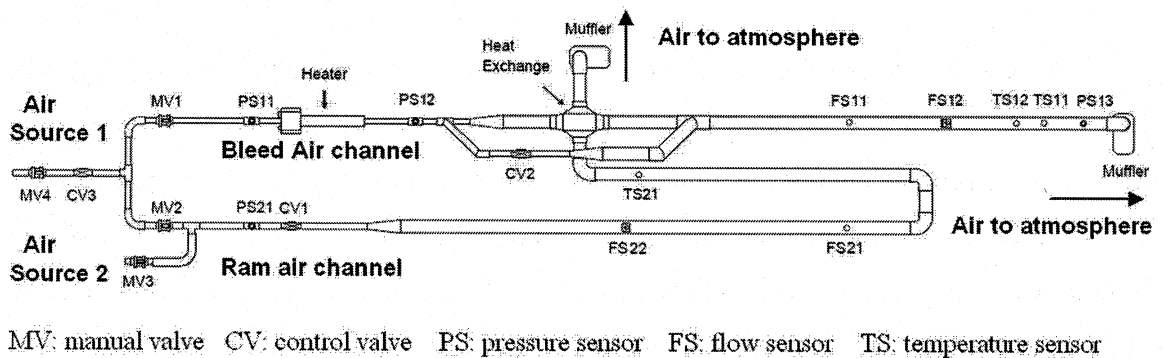


**Fig. 4.1 Bleed air temperature control test fig configuration**

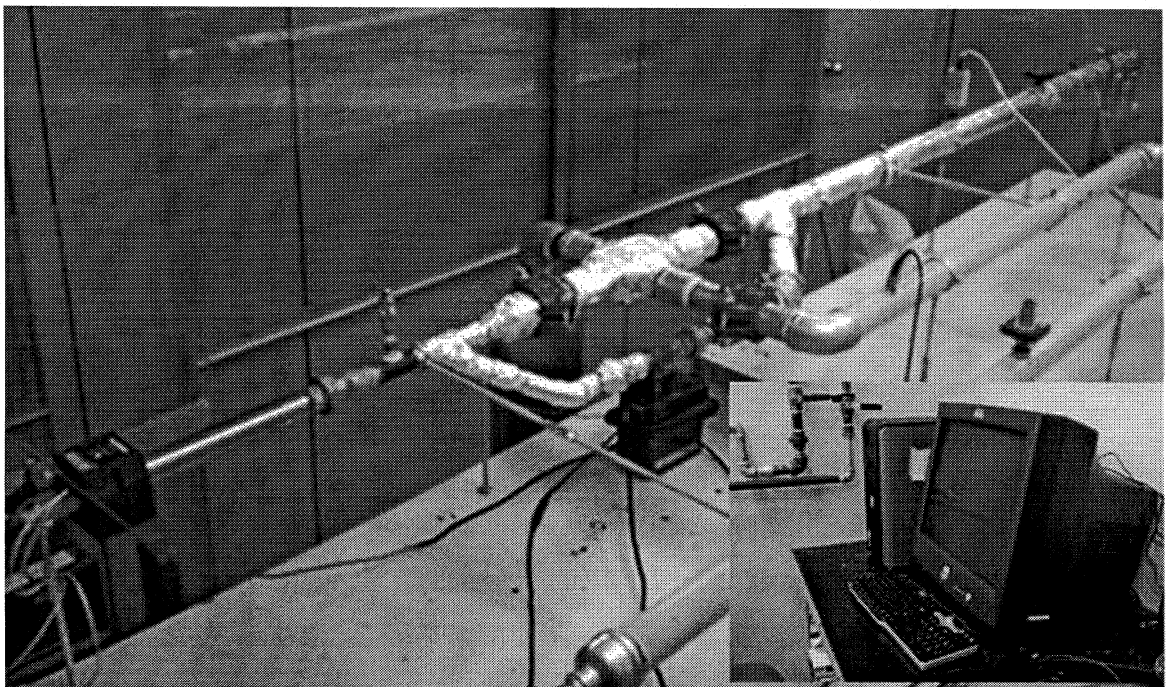


**Fig. 4.2 Picture of the test rig**

Component	Type Part Number	Output/Input	Manufacture	Symbol in Fig. 4.1
Air heater and control cabinet	P/N 074719 & 074722	N/A	SYLVANIA	Heater
Heat Exchanger	A300029060RYU NI	N/A	Bell Intercoolers	Heat Exchanger
Pressure Sensor	PX209-100G10V	0~10V	OMEGA	PS12,PS13
	PX303-100G10V	1~11V		PS11, PS21
Flow sensor	FMA-905-V-S	0~5V	OMEGA	FS11, FS21
Temperature sensor	N/A		Honeywell	TS11, TS21
D/A Board	PCI-6704	0~20mA DC -10~+10V DC	National Instruments	N/A
A/D Board	PCI-6034E	-10~+10V	National Instruments	N/A
PC computer		N/A	DEll	N/A

**Table 4.1 Main components of the test rig**

## 4.2 Main Components

### 4.2.1 Heat Exchanger

The heat exchanger is the core part of the test rig. The high performance air to air heat exchanger (Fig. 4.3) is manufactured by Bell Intercoolers. The size of the heat exchanger core is 3.0"×2.9"×6". Tanks are welded on four sides of the core to connect with pipes. The plate-fin heat exchanger has four bleed air channels and four ram air channels. And it is safe to operate under the pressure of 100 psig.

For the experiments, some parameters for the heat exchanger are unknown to the user. The parameters, such as heat transfer coefficient and thermal mass, are to be identified.

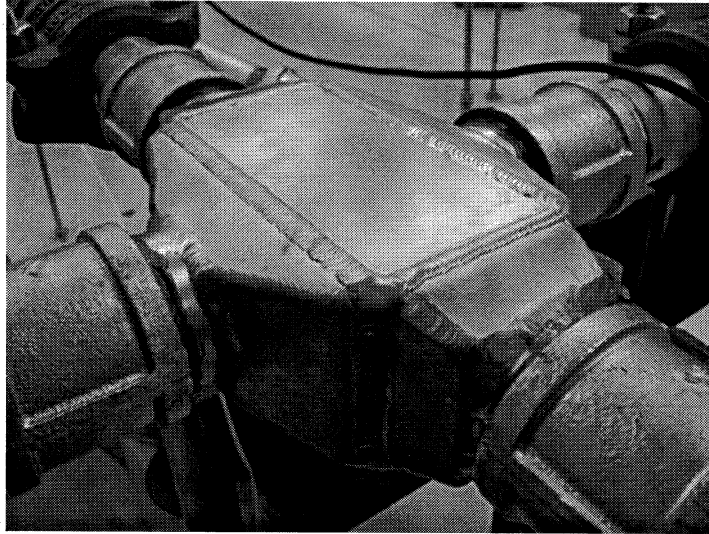


**Fig. 4.3 Air to air plate-fin heat exchanger, manufactured by Bell Intercoolers**

#### **4.2.2 *Heater and Control Systems***

An in-line air heater is installed at the inlet of bleed air channel. The 3 KW heater can heat the flow up to 300 °F (150 °C) at the mass flow rate 0.04 lb/s. The inlet and exit temperature limits are 200 °F (93 °C) and 1400 °F (760 °C), respectively. The maximum air inlet pressure is 60 psig, which is lower than the maximum tank pressure. In order to protect the heater and insure the user's safety, the heater inlet pressure is regulated below 60 psig, and no valve is installed downstream the heater so that the flow will not be blocked.

The closed-loop heater control system contains a temperature controller, power controller, over-temperature protection, and a thermocouple, providing a constant output temperature regardless changes in the airflow. The temperature controller also provides a display of the process air temperature.

Fig. 4.4 shows the heater and its control cabinet. The manufacturer is SYLAVNIA.

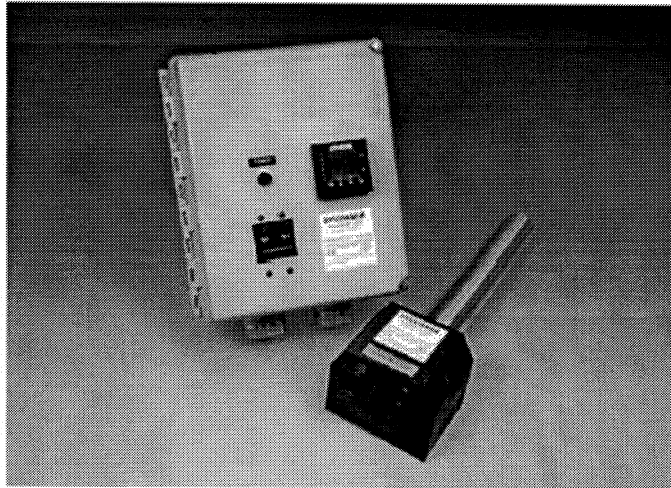


**Fig. 4.4 Air heater control system, manufactured by SYLANVIA**

#### **4.2.3 Control Valve**

The control valve (Fig. 4.5) is a  $\frac{3}{4}$ -inch brass ball valve driven by an electromechanical actuator. Both the valve and actuator are manufactured by BI-TORQ, CARBO-BOND, Inc. The temperature rating for the valve is 297 °F. The control valve used in the test rig has limited sensitivity to the input current. The valve “dead-zone” is about 0.2 mA when the valve keeps going in one direction and about 0.5 mA when the valve changes its movement direction.

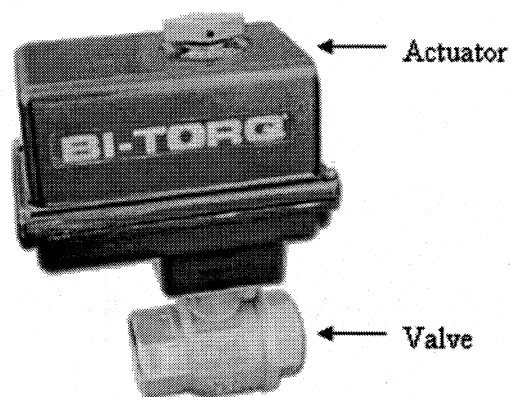


**Fig. 4.5 Control valve manufactured by BI-TORQ, CARBO-BOND, Inc.**

#### 4.2.4 Temperature Sensor

A Honeywell RTD temperature sensor (Fig. 4.6) is used. The response time of the sensor is affected by the air flow rate. For the low flow rate used in the experiment, the response time is considered as a constant.

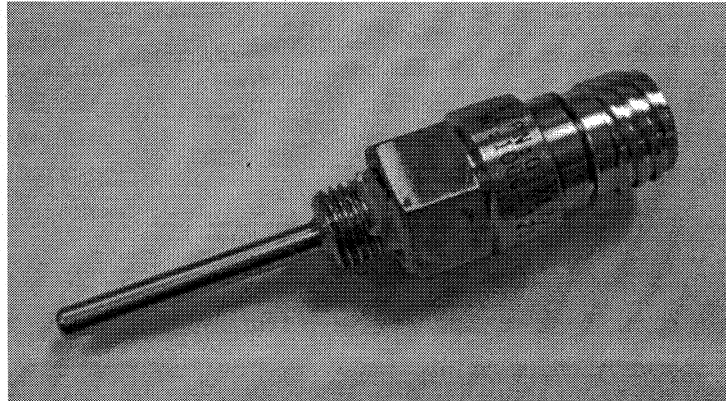


Fig. 4.6 RTD temperature sensor, supplied by Honeywell

#### 4.2.5 Flow Sensor

The air velocity transducer FMA-905 (Fig. 4.7) is manufactured by OMEGA Inc. It utilizes both a velocity sensor and a temperature sensor to accurately measure air velocity  $V$  (in SFPM, standard feet per minute). To obtain mass flow rate  $W$  (lb/s) the SFPM velocity is multiplied by the cross-sectional area of the pipe  $A$  and air density  $\rho$ :

$$W = \rho VA \quad (4.1)$$

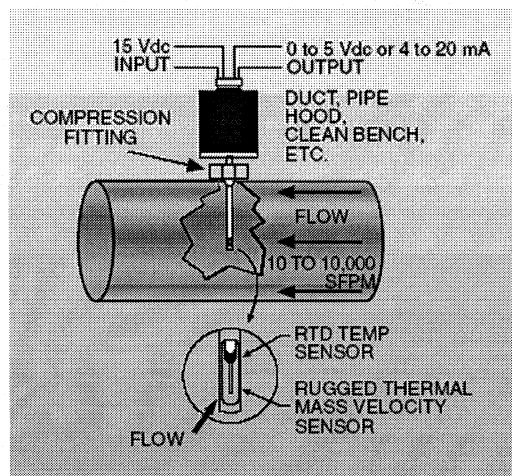


Fig. 4.7 Air velocity transducer, manufactured by OMEGA Inc.

#### 4.2.6 Pressure Sensor

Two types of pressure sensors, PX303 and PX209 (Fig. 4.8) are installed in the test rig to operate in different temperature ranges. Pressure sensors PX303 are used to measure ram air inlet pressure and bleed air inlet pressure before the heater where the operating temperature is relatively low. The inlet pressure of the valve and the load pressure are measured by PX209, which can work at higher temperature. All the pressure sensors are manufactured by OMEGA Inc.

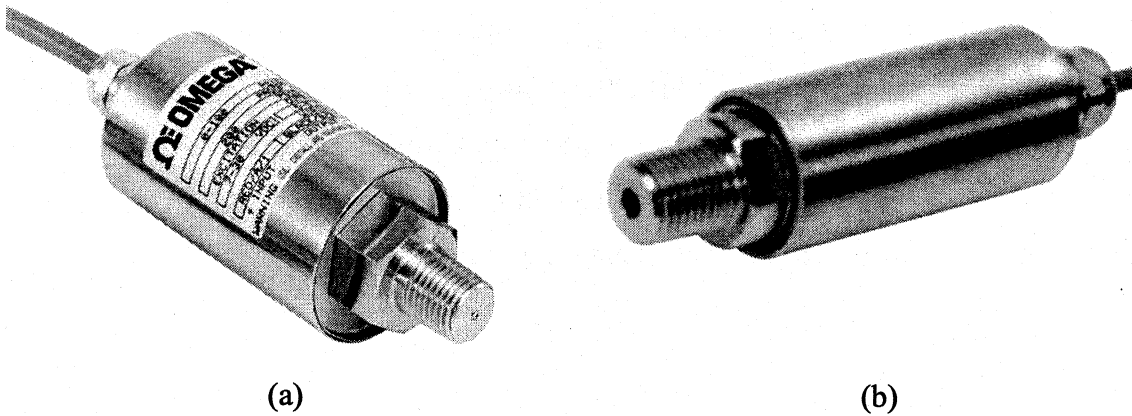


Fig. 4.8 Pressure sensors, manufactured by OMEGA Inc.: (a) PX303; (b) PX209

### 4.3 Operating Conditions of Experiments

The experiment is conducted at a room temperature of about 65 °F and an atmospheric pressure of 14.7 psia. The duration for each test is within 600 seconds. The steady operating conditions can be found by the following steps:

- a. Set the hot air inlet temperature  $T_{hi}$  with heater control box;
- b. Set the hot air inlet pressure  $P_{hin}$ , which can be measured by pressure sensor P11;
- c. Set the bypass valve opening rate  $u_{bypass}$ . For ram air control configuration, the bypass valve opening is zero;
- d. Set the load temperature  $T_{load}$ , which can be measured by temperature TS11;  
and

- e. When the load temperature is set, the desired value of ram air flow rate  $W_{ram}$  can be found by a PI controller. When the system is steady, the steady value of  $W_{ram}$  can be measured by flow sensor FS21.

Since the air sources are from pressure tanks and the capacity for the compressor feeding the tanks is limited, the inlet pressures of ram air and bleed air channels will decrease while the experiment is running. And the mass flow rates will decrease correspondingly. To keep the bleed air inlet pressure constant for a certain period of time, a control valve (CV3) is installed to control the pressure within a certain range. The ram air control valve (CV1) is used for keeping a steady ram air flow rate. The control valve opening rates are regulated by PI controllers. The required mass flow rate of the ram air can be found by another PI controller, the ram air controller. So for the ram air channel, the control input is changed to ram air mass flow rate  $W_{ram}$ , instead of ram air valve opening rate. The discrete PI controllers have the following forms:

CV3 controller:

$$u_{CV3}(k) = u_{CV3}(k-1) + Kp_{CV3} \times \{[e_{CV3}(k) - e_{CV3}(k-1)] + e_{CV3}(k) \times Ts / Ti_{CV3}\} \quad (4.2)$$

$$\text{where } e_{CV3}(k) = P_{hin\_command}(k) - P_{hin\_measured}(k)$$

CV1 controller:

$$u_{CV1}(k) = u_{CV1}(k-1) + Kp_{CV1} \times \{[e_{CV1}(k) - e_{CV1}(k-1)] + e_{CV1}(k) \times Ts / Ti_{CV1}\} \quad (4.3)$$

$$\text{where } e_{CV1}(k) = W_{ram\_command}(k) - W_{ram\_measured}(k)$$

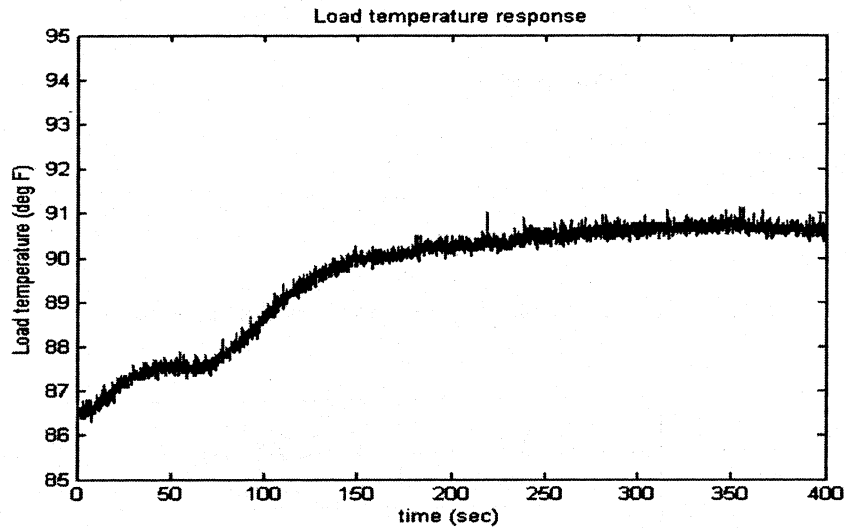
Ram air channel controller:

$$W_{ram\_command}(k) = W_{ram\_command}(k-1) + Kp_{ram} \times \{[e_{ram}(k) - e_{ram}(k-1)] + e_{ram}(k) \times Ts / Ti_{ram}\} \quad (4.4)$$

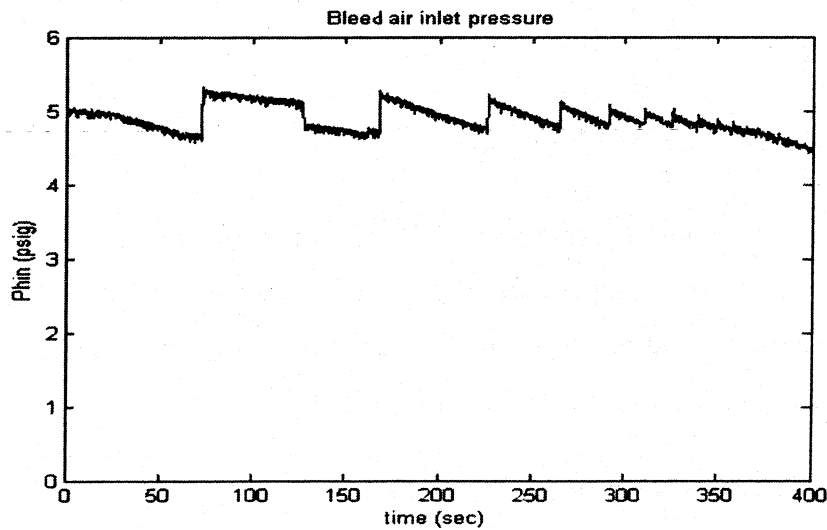
$$\text{where } e_{ram}(k) = T_{load\_sp}(k) - T_{load\_m}(k)$$

where  $u(k)$  is the controller out time at time instant  $k$ .  $K_p$  is the proportional gain,  $T_s$  is the sampling time and  $T_i$  is the integration time.

Fig. 4.9 shows the steady operating condition for ram air control configuration. The controller parameters are listed in Table 4.2.



(a)



(b)

Fig. 4.9 Operating condition for ram air control configuration (to be continued)



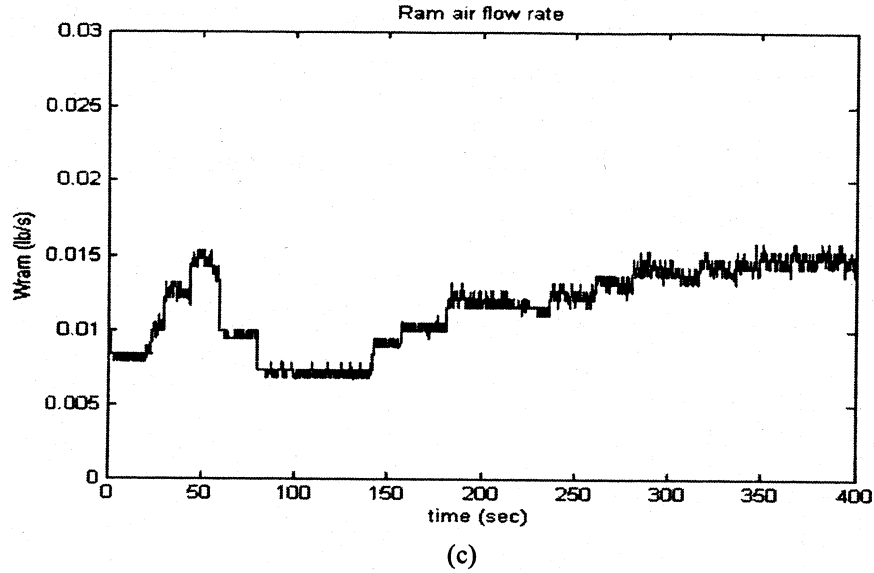


**Fig. 4.9 Operating condition for ram air control configuration**

$T_{hi} = 150\text{ }^{\circ}\text{F}$	$P_{hi} = 5\text{ psig}$	$Kp_{CV3} = 0.1$	$Ti_{CV3} = 2$
$T_{ci} = 65\text{ }^{\circ}\text{F}$	$T_{load} = 90\text{ }^{\circ}\text{F}$	$Kp_{CV1} = 100$	$Ti_{CV1} = 10$
$Kp_{ram} = -0.003$	$Ti_{ram} = 100$	$Ts = 100\text{ ms}$	

**Table 4.2 Initial steady-state conditions and controller parameters for ram air control configuration**

## 4.4 Experiment with PI Controller

In order to demonstrate the advantages of the ram-air-plus-bypass control configuration, a 5 °F load temperature step increase is added at 200 s for the first two control configurations, and at 150 s for the ram-air-plus-bypass control configuration. The operating condition is as given in Table 4.2.

### 4.4.1 Result of Ram Air Control Configuration

In the ram air control configuration, the ram air flow rate is controlled to keep the load temperature at a desired value. The discrete PI control law is stated in Eq. (4.4). The experimental results with ram air control are shown in Fig. 4.10.

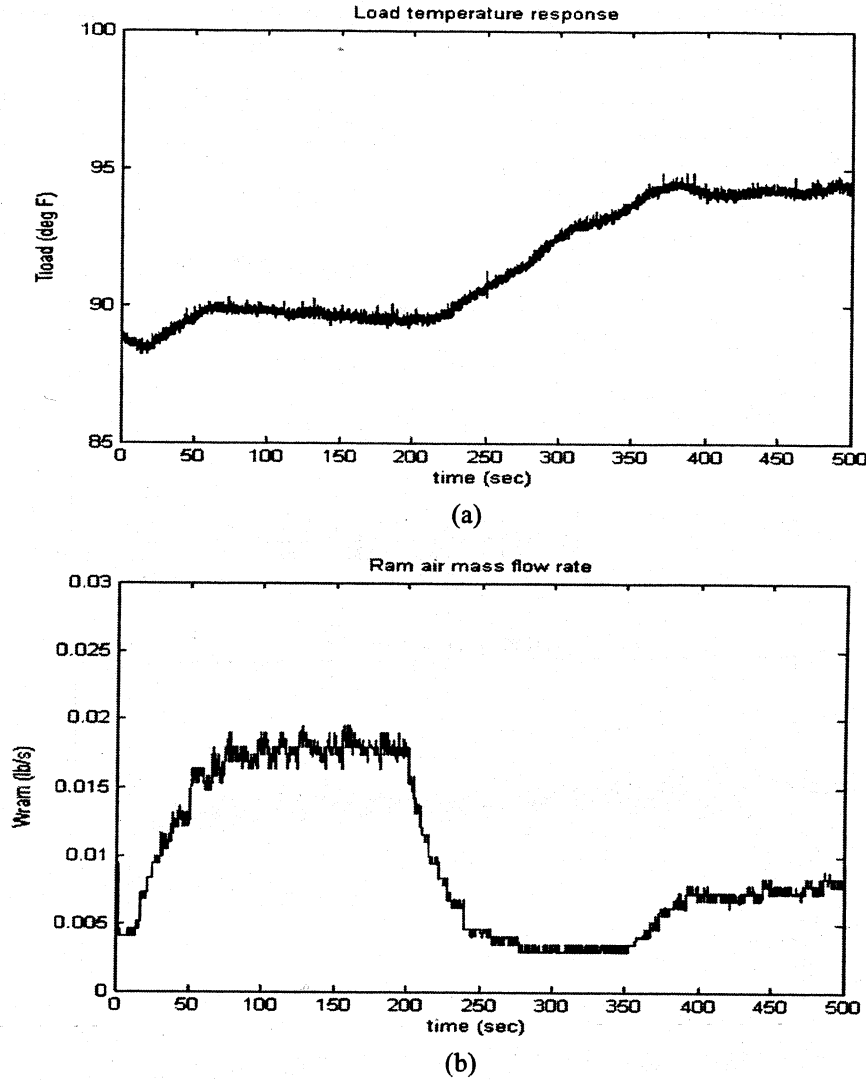


Fig. 4.10 System response to a 5 °F load temperature set point increase using ram air control

#### 4.4.2 Result of Bypass Control Configuration

In the bypass control configuration, ram air flow is kept constant and the load temperature is controlled by the bypass valve (CV2). The discrete PI control law is as follows:

$$u_{bypass}(k) = u_{bypass}(k-1) + Kp_{bypass} \times \{ [e_{bypass}(k) - e_{bypass}(k-1)] + e_{bypass}(k) \times Ts / Ti_{bypass} \} \quad (4.5)$$

where  $e_{bypass}(k) = T_{load\_sp}(k) - T_{load\_m}(k)$ ,  $Kp_{bypass} = 0.5$ ,  $Ti_{bypass} = 20$

Fig. 4.11 shows the system response to a 5 °F load temperature set point increase with bypass control.

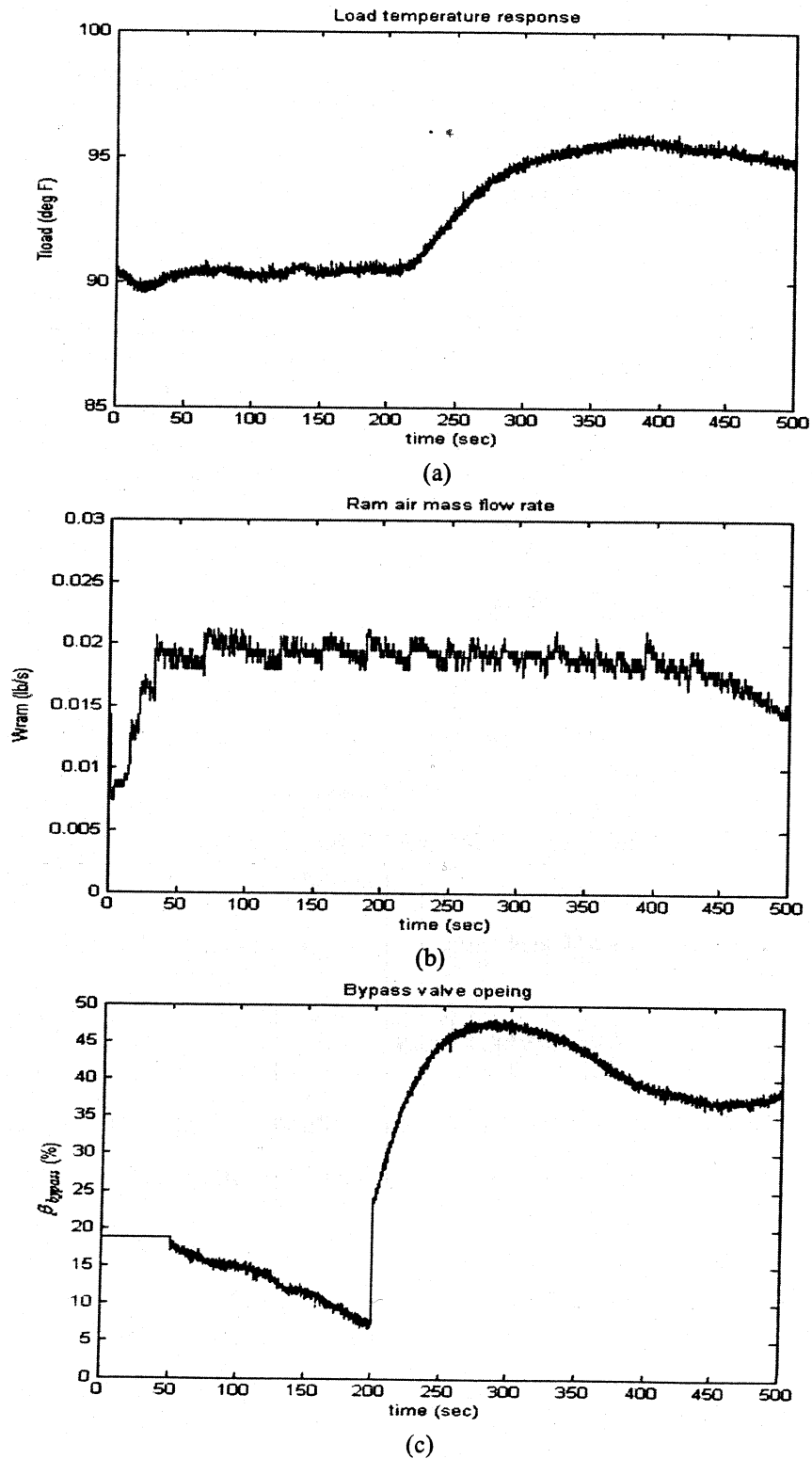


Fig. 4.11 System response to a 5 °F load temperature set point increase using bypass control

#### 4.4.3 Result of Ram-Air-Plus-Bypass Control Configuration

In ram-air-plus-bypass control the bypass channel control law is same as Eq. (4.5). The proportional gain  $Kp_{bypass}$  is 1 and integration time  $Ti_{bypass}$  is 40. The ram air channel control law is:

$$W_{ram\_command}(k) = W_{ram\_command}(k-1) + Kp_{ram} \times \{[e_{ram}(k) - e_{ram}(k-1)]\} + e_{ram}(k) \times Ts_{ram} / Ti_{ram} \} \quad (4.6)$$

where  $e_{bypass}(k) = u_{bypass\_sp}(k) - u_{bypass}(k)$ ,  $Kp_{ram} = 0.001$ ,  $Ti_{ram} = 100$

Fig. 4.12 shows the system response for a 5 °F load temperature set point increase with ram-air-plus-bypass control.

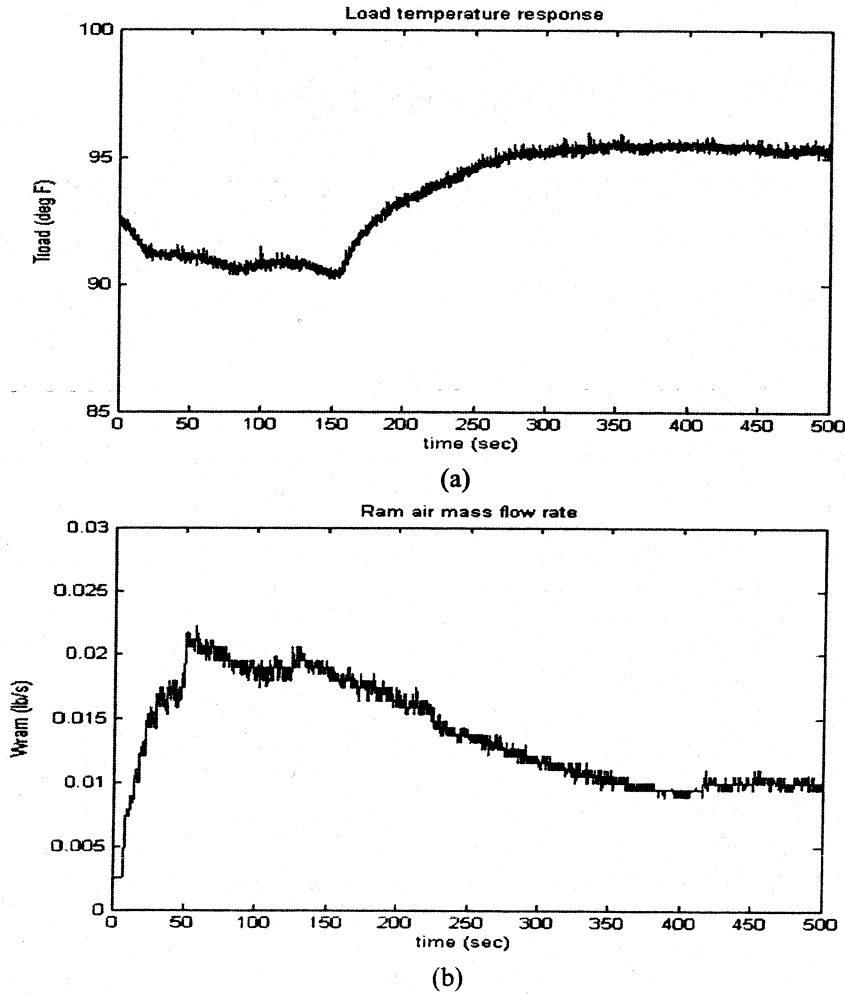


Fig. 4.12 System response to a 5 °F load temperature set point increase using ram-air-plus-bypass control (to be continued)

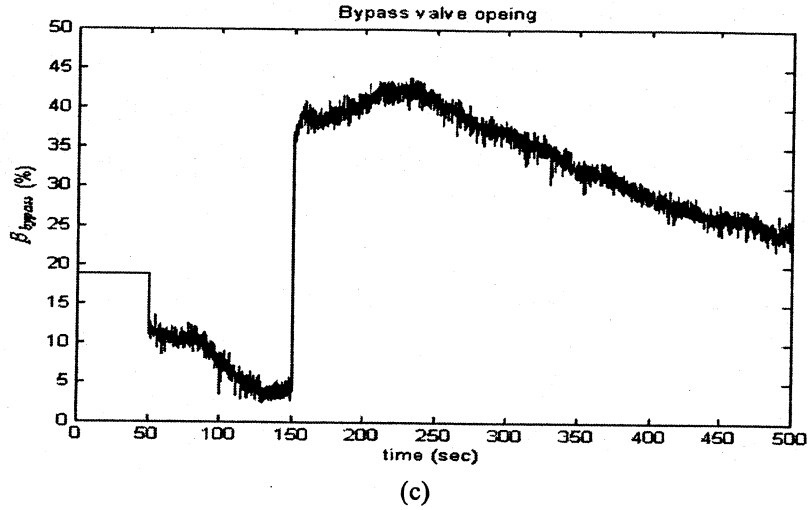


Fig. 4.12 System response to a 5 °F load temperature set point increase using ram-air-plus-bypass control

#### 4.5 Experiment with LQ Output Feedback Controller

Since the optimal control gain is driven based on the system matrices, some system parameters need to be identified. The system operating condition, control gain and parameters are listed in Table 4.3. But some parameters need further identification to get the proper value.

$c_c=0.24$	$c_h=0.24$	$MC_s=0.65$	$\gamma=1.4$	$g=386.09$
$R=639.6$	$N=10$	$Mach=0.4$	$F_{rec}=0.7$	$d_{ram}=0.75$
$d_{bypass}=0.75$	$K_v=0.015708$	$\tau_v=1.5$	$\tau_{ts}=15$	$T_{load\_sp}=90$
$T_{amb}=65$	$T_{hi}=150$	$T_{ho}=75$	$P_{amb}=14.7$	$P_{hin}=18.7$
$P_{ci}=15.7$	$P_{hi}=18.7$	$P_{ho}=14.7$	$P_{co}=14.7$	$P_{load}=14.7$
$W_{bleed}=0.001$	$W_{bleedmain}=0.0004$	$W_{bleedbypass}=0.0006$	$W_{ram}=0.002$	$u_{bypass\_sp}=18.75$
$K_{lq} = \begin{bmatrix} -0.9 & 0 \\ 0.001 & -0.005 \end{bmatrix}$				

Table 4.3 Initial steady-state condition for optimal feedback control

Three types of inputs are applied to the system, and they are defined as follows:

**Input A:** A +5 step increase in load temperature set point  $T_{load\_sp}$  at 100 s.

**Input B:** A 20 °F step increase in bleed air inlet temperature  $T_{hi}$  (from the initial steady state value) at 150 s. Run optimal control at 200 s.

**Input C:** A 6.25% step increase (1 mA input current increase) in bypass valve-opening set-point  $u_{bypass\_sp}$  at 150 s.

The experimental results are in Fig. 4.13 – 4.15.

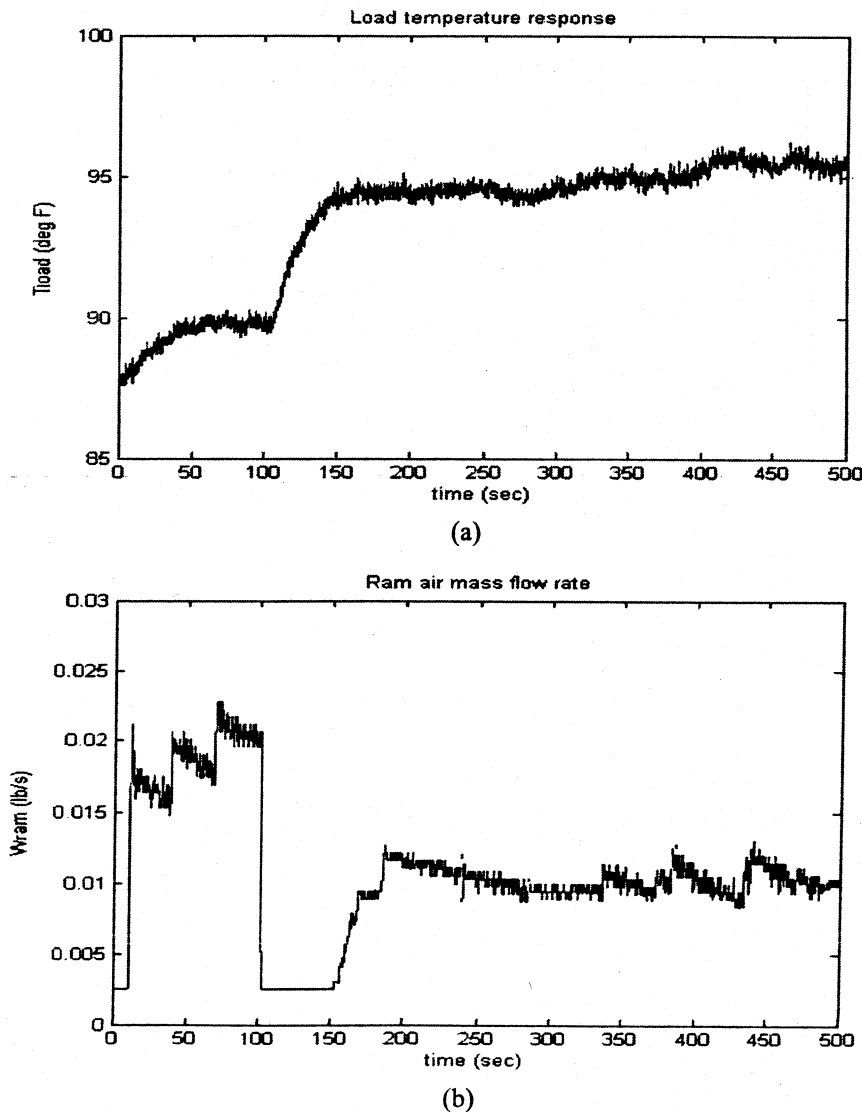


**Fig. 4.13 System response to Input A (to be continued)**

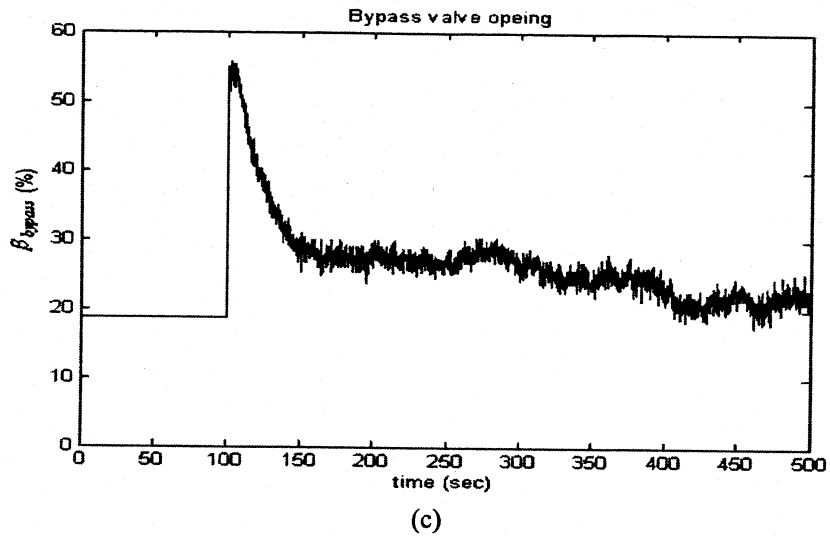


Fig. 4.13 System response to Input A

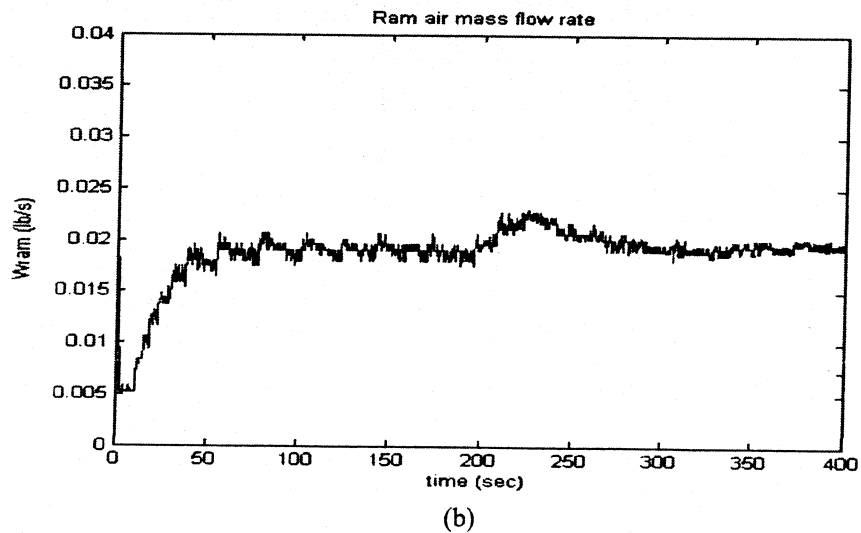
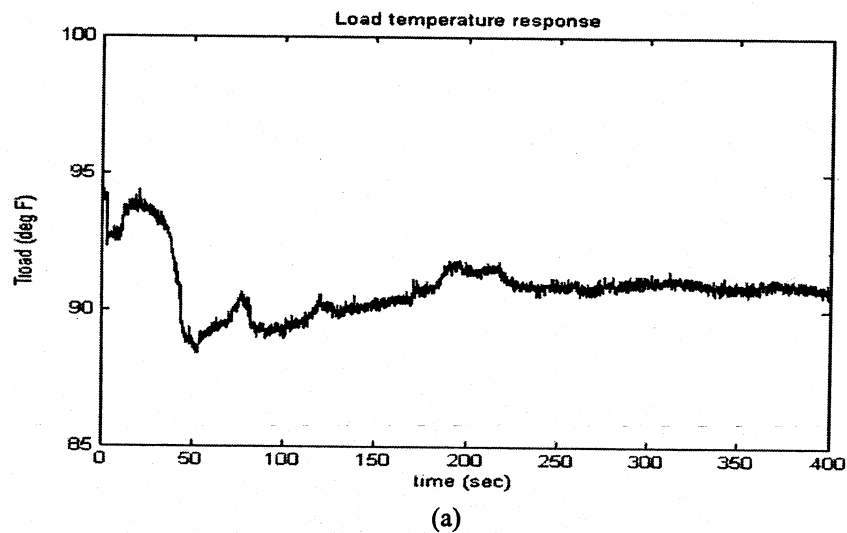
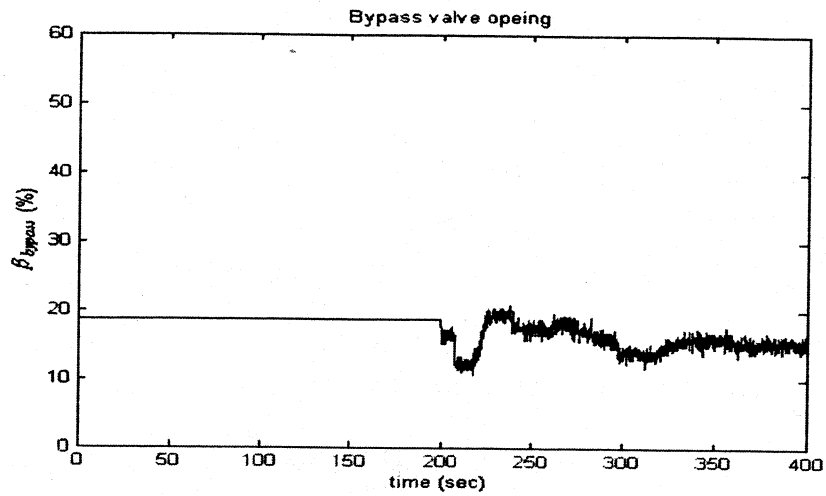
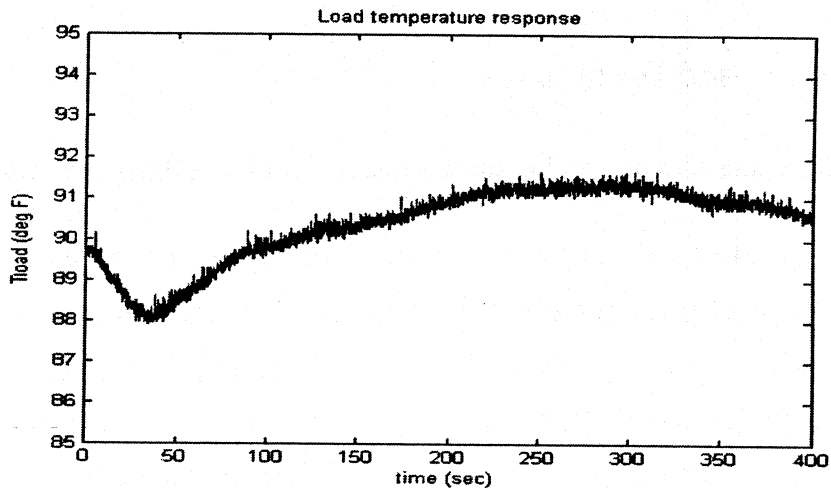


Fig. 4.14 System response to Input B (to be continued)

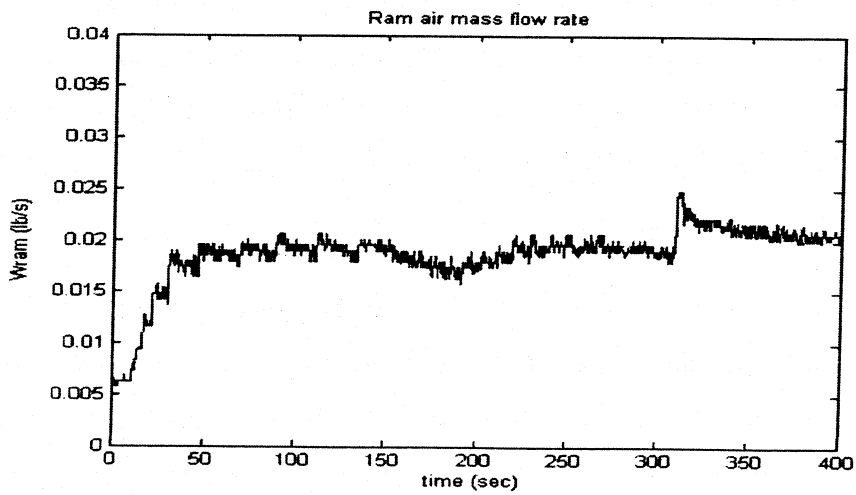


(c)

Fig. 4.14 System response to Input B



(a)



(b)

Fig. 4.15 System response to Input C (to be continued)



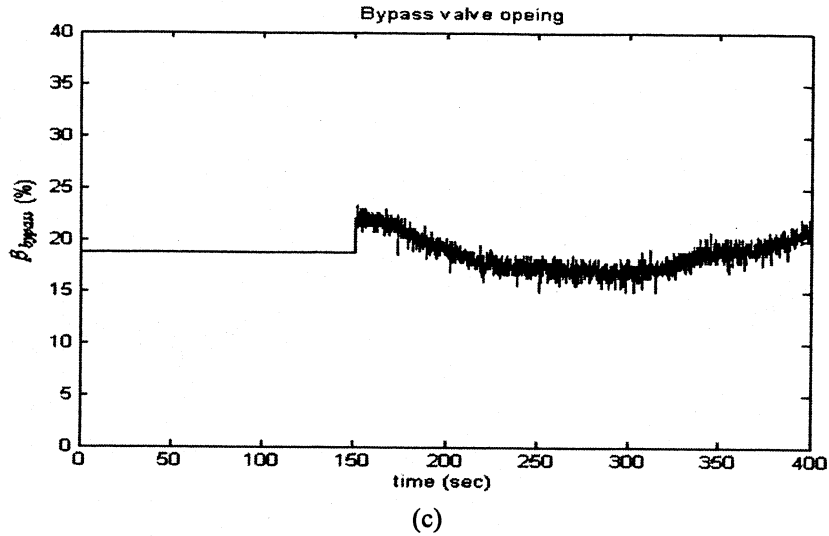


Fig. 4.15 System response to Input C

## 4.6 Conclusions and Discussions

From the experimental results, some conclusions can be drawn as follows:

First, efficient ram air usage and good load temperature response can be achieved by ram-air-plus-bypass control configuration. As shown in Fig. 4.10 to Fig. 4.12, for the system responses to a 5 °F step increase of load temperature, the ram air control has the slowest response, taking about 200 s to reach steady-state. The ram air usage is only 0.008 lb/s when the system is in steady-state. For bypass control, it has the fastest time response, but the corresponding ram air flow rate is significantly higher, about 0.02 lb/s in steady-state. The steady-state ram air mass flow rate for ram-air-plus-bypass control is 0.01 lb/s. Compared to bypass control, this configuration shows sufficient saving of ram air. The response time is about 150 s, and the performance can be improved by optimal control theory.

As mentioned above, PI control gains should be tuned to achieve better system response. For the ram-air-plus-bypass control configuration, which is a two-inputs-two-outputs system, it is difficult to place the poles at the best locations at the same time. Optimal control is suitable for this MIMO system. Fig. 4.13 shows the system time response with optimal output feedback control. It only takes about 50 s to reach the

steady-state of the temperature response. And the ram air flow rate reduces significantly at the beginning and keeps at 0.01 lb/s when the system is in steady-state.

The steady-state error and small swing of the system response can be seen from the experimental results. It may be caused by many factors. Some system parameters are not identified accurately. The optimal control gain that is calculated based on assumed system parameters may not be the best for this system. The temperature errors and small variation may also be caused by sensor measuring error, heat loss through the metal pipes, and low sensitivity of the control valves.

# **CHAPTER 5 CONCLUSIONS AND FUTURE WORK**

## **5.1 Conclusions**

This thesis was concerned with the temperature control of an aircraft engine bleed air system. A simplified bleed air system model was developed first. Based on the developed model, simulation investigation of the ram-air-plus-bypass control strategy with optimal output feedback controller was performed. A test rig system was built and the temperature control for the bleed air system was tested experimentally. The main contents of this thesis can be summarized as follows:

In Chapter 1, the use of engine bleed air in aircraft environment control system was explained. A ram-air-plus-bypass bleed air temperature control strategy was described. The basic concepts of temperature control and optimal control were introduced and the relevant literatures in these research areas were reviewed.

In Chapter 2, a nonlinear dynamic model of a simplified bleed air temperature control system was developed. The nonlinear model was linearized around an operating point, and then a linear state-space representation was derived. Simulations were conducted for both the nonlinear and linearized models and the simulation results were compared.

In Chapter 3, the optimal controller for an engine bleed air temperature control system was formulated mathematically. The application of the ram-air-plus-bypass control strategy for the bleed air temperature control was described in detail. Based on the simplified model, simulations were conducted for different input signals and the simulation results were presented.

In Chapter 4, the experimental setup built for studying the bleed air temperature control system was described. Tests were carried out and the experimental results on the test rig were given for the bleed air temperature control system. The experimental results were presented and discussed at the end of this chapter.

In conclusion, the ram-air-plus-bypass control strategy with optimal output feedback control was applied to the engine bleed air temperature control system. Both simulation and experimental results have demonstrated the effectiveness of this application. Fast temperature control response and efficient ram air usage were achieved by the proposed control strategy.

## **5.2 Future Work**

For the temperature control of the engine bleed air system, the following future works are recommended.

1. Some uncertain system parameters, especially the parameters of the heat exchanger model should be identified to calculate the best optimal feedback control gain.
2. Sensor and actuator faults will significantly degrade the system performance. Some research about sensor and actuator faults detection and tolerance should be conducted.
3. More research work should be carried out to continue investigating some of the practical issues. The condition based maintenance of aircraft, which requires prediction of sensor and actuator faults, will be carried out in the future.

## REFERENCES

- [1] B. T. Burchett, M. F. Costello, "Optimal Output Feedback Using Dyadic Decomposition," *Proceedings of the American Control Conference*, Albuquerque, New Mexico, vol.3, pp.1447-1452, 1997.
- [2] T. Ensign, J. Gallman, "Energy Optimized Equipment Systems for General Aviation Jets," AIAA-2006-228, *44th AIAA Aerospace Sciences Meeting and Exhibit*, Reno, Nevada, 2006.
- [3] S. Forrest, M. Johnson, M. Grimbale, "LQG Self-Tuning Control of Super-Heated Steam Temperature in Power Generation," *Second IEEE Conference on Control Applications*, Vancouver, B.C., vol.2, pp. 805-810, 1993.
- [4] A. P. Fraas, "Heat Exchanger Design, 2<sup>nd</sup> Edition," John Wiley & Sons, New York, 1989.
- [5] P. Hodal, G. Liu, "Bleed Air Temperature Regulation System: Modeling, Control, and Simulation," *Proceedings of the 2005 IEEE International Conference on Control Applications*, Toronto, Canada, pp. 1003-1008, 2005.
- [6] E. H. Hunt, D. H. Reid, D. R. Space, F. E. Tilton, "Commercial Airliner Environmental Control System," *Engineering Aspects of Cabin Air Quality Aerospace Medical Association annual meeting*, Anaheim, California, 1995.
- [7] R. E. Kalman, "When is a Linear Control System Optimal?" *Transactions of the ASME, Journal of Basic Engineering*, Series D, pp. 81-89, 1964.
- [8] T. Katayama, T. Itoh, M. Ogawa, H. Yamamoto, "Optimal Tracking Control of a Heat Exchanger with Change in Load Condition," *Proceedings of the 29<sup>th</sup> Conference on Decision and Control*, Honolulu, Hawaii, pp. 1584-1589, 1990.
- [9] D.E. Kirk, *Optimal Control Theory: An Introduction*, Englewood Cliffs, N.J., Prentice-Hall, 1970.

- [10] M. Kutz, Temperature Control, John Wiley & Sons, Inc., New York, 1968.
- [11] H. Kwakernaak, R. Sivan, Linear Optimal Control Systems, Wiley-Interscience, 1972.
- [12] F. L. Lewis, V. L. Syrmos, Optimal Control, 2<sup>nd</sup> Edition, John Wiley & Sons, Inc. 1995.
- [13] I. Moir, A. Seabridge, Aircraft Systems: Mechanical, Electrical, and Avionics Subsystems Integration, AIAA Education Series, 2001.
- [14] J. Mikles, M. Fikar, Process Modelling, Identification, and Control I: Models and Dynamic Characteristics of Continuous Processes, STU Press, Bratislava, Slovak Republic, 2000.
- [15] W. H. Newman, M. R. Viele, F. J. Hrach, "Reduced Bleed Air Extraction for DC-10 Cabin Air Conditioning," *SAE, and ASME, Joint Propulsion Conference, 16th*, Hartford, Conn., 1980.
- [16] M. Orzylowski, T. Kaluzniacki, Z. Rudolf, G. Nowicki, "Precise temperature control for measurement purposes," *Instrumentation and Measurement Technology Conference, Proceedings of the 16th IEEE*, Volume 1, pp. 16-21, 1999.
- [17] L. Shang, G. Liu, "Optimal Control of a Bleed Air Temperature Regulation System," *IEEE International Conference on Mechatronics and Automation*, Harbin, China, pp. 2610-15, 2007.
- [18] C. A. Smith, A. B. Corripio, Principles and Practice of Automatic Process Control, 2<sup>nd</sup> Edition, John Wiley & Sons Inc., New York, 1997.
- [19] L. Xia, J. A. De Abreu-Garcia, T. T. Hartley, "Modelling and Simulation of a Heat Exchanger," *IEEE International Conference on Systems Engineering, (Ohio)*, pp. 453-456, 1991.
- [20] K. Yeoman, "Efficiency of a bleed air powered inlet icing protective system," *Aerospace Sciences Meeting and Exhibit*, 32nd, Reno, NV, 1994.

- [21] L. Zhang, J. Mao, "An Approach for Selecting The Weighting Matrices of LQ Optimal Controller Design Based on Genetic Algorithms," *Proceedings of IEEE TENCONencon'02*, pp.1331-1334, 2002.

# APPENDIX

## 1. MATLAB Script for the Nonlinear Simulations for the Ram-Air-Plus-Bypass Control Configurations

```

clear all;
clc;

OperatingCondition=[% Pin Ta Pa M Wh Thi
    30 130 14.70 0.0 1.1 380; % mission segment data #1
    35 30 14.70 0.0 1.1 250; % mission segment data #2
    20 130 14.70 0.0 1.1 300; % mission segment data #3
    0 0 14.70 0.0 1.1 0; % mission segment data #4
    35 130 14.70 0.4 1.1 380; % mission segment data #5
    35 20 14.70 0.4 1.1 380; % mission segment data #6
    35 90 10.11 0.5 1.1 380; % mission segment data #7
    35 10 10.11 0.5 1.1 380; % mission segment data #8
    35 50 6.76 0.7 1.1 380; % mission segment data #9
    35 -10 6.76 0.7 1.1 380; % mission segment data #10
    35 10 4.37 0.8 1.1 380; % mission segment data #11
    35 -25 4.37 0.8 1.1 380; % mission segment data #12
    20 -40 2.15 0.85 1.1 380; % mission segment data #13
    10 -25 2.15 0.85 1.1 380; % mission segment data #14
    30 -40 2.15 0.85 1.1 380; % mission segment data #15
    13 -30 2.15 0.85 1.1 380; % mission segment data #16
    35 -40 2.15 0.85 1.1 380; % mission segment data #17
    20 -40 2.15 0.85 1.1 380; % mission segment data #18
    20 10 4.37 0.85 6.5 380; % mission segment data #19
    25 -30 4.37 0.85 6.5 380; % mission segment data #20
    20 50 6.76 0.7 6.5 380; % mission segment data #21
    30 -10 6.76 0.7 6.5 380; % mission segment data #22
    25 90 10.11 0.5 6.5 380; % mission segment data #23
    35 10 10.11 0.5 6.5 380; % mission segment data #24
    35 110 12.23 0.4 6.5 380; % mission segment data #25
    35 15 12.23 0.4 6.5 380; % mission segment data #26
    35 130 14.70 0.4 5.5 380; % mission segment data #27
    35 20 14.70 0.4 5.5 380; % mission segment data #28
    30 130 14.70 0.0 5.5 380; % mission segment data #29
    35 30 14.70 0.0 5.5 250; % mission segment data #30

OpConNum=input('\nCHOOSE THE OPERATING CONDITION NUMBER (1-30): ');
N=input('\nINPUT THE NxN HEAT EXCHANGER DIMENSION: N = '); % for steady-state calculations, we use 15x15 for accuracy

Pin=OperatingCondition(OpConNum,1); % Bleed inlet pressure in psig
T_amb=OperatingCondition(OpConNum,2); % Ambient temperature
P_amb=OperatingCondition(OpConNum,3); % Ambient pressure
Mach=OperatingCondition(OpConNum,4); % Mach number
W_H=OperatingCondition(OpConNum,5)/60; % Total bleed flow in lb/sec
T_HI=OperatingCondition(OpConNum,6); % Bleed air inlet temp. in deg. F

T_H=190; % temperature setpoint at the load
%Bypass_setpoint=0.03824; % BR=0.1 for op#5
%Bypass_setpoint=0.04012; % BR=0.1 for op#7
%Bypass_setpoint=0.07735; % BR=0.1 for op#14
%Bypass_setpoint=0.08205; % BR=0.1 for op#22

%Bypass_setpoint=0.1529; % BR=0.1 for op#5
Bypass_setpoint=0.1605; % BR=0.1 for op#7
%Bypass_setpoint=0.3282; % BR=0.1 for op#22
Kv=(pi/2)/100; % valve gain to convert percentage to angle

d_ram=1.5; % ram channel valve diameter in inch
d_bypass=1.5; % bypass channel diameter
R = 639.6; % Gas constant, inch/Rankine
g=9.80665/0.0254; % Gravity inch/sec^2
Gamma = 1.4;

```



```

C_H=0.24;
C_C=0.24;
C_v=sqrt(2*Gamma*g/((Gamma-1)*R)); % check

% System other variables
M=1;
C_M=0.65;
T_V=1.5;

% *****
% Steady-state (initial condition) calculation starts here *
% *****

P_HI=Pin+P_amb; % Bleed inlet pressure in psia
A_opened_ram=pi*d_ram*d_ram/4; % ram valve full-open area in inch^2
A_opened_bypass=pi*d_bypass*d_bypass/4; % bypass valve full-open area in inch^2
P_CO=P_amb; % dumping ram air into the atmosphere
T_CI=(T_amb+460)*(1+0.2*Mach^2) - 460; % Ram air temperature (deg. F)
F_rec=0.7; % Recovery factor pressure differential=0.7
P_C_inlet=(P_amb*((1+0.2*Mach^2)^3.5)-P_amb)*F_rec+P_amb; % Ram air pressure (psia)

A_bypass=Bypass_setpoint*A_opened_bypass; % force the bypass to be 20% opened at steady state

% NOTE: there is a certain percentage of bypass valve opening beyond which
% the system cannot achieve T_H=190, because the ram air needed is over the maximum value

% iteration to calculate the main & bypass flowrates

W_H1_upper=W_H;
W_H1_lower=0;
flowsum=0;
while abs(W_H-flowsum)>0.000001
    W_H1=(W_H1_upper+W_H1_lower)/2;
    P_H=P_HI-1.8*W_H1^2-0.168*W_H1; % hot side hx pressure drop
    ratio_bypass=P_H/P_HI;
    if ratio_bypass < 0.5283
        ratio_bypass = 0.5283;
    end
    term_bypass=sqrt(((2*Gamma*g)/((Gamma-1)*R))*(ratio_bypass^(2/Gamma)-ratio_bypass^((1+Gamma)/Gamma)));
    W_H2=(A_bypass*P_HI*term_bypass)/sqrt(T_HI+460);
    flowsum=W_H1+W_H2;
    if flowsum>W_H
        W_H1_upper=W_H1;
    else
        W_H1_lower=W_H1;
    end
end

% just for comparison, this is the maximum possible ram flowrate (as
% governed by the pressure loss through the heat exchanger)
W_C_max=-0.04300291545+0.0002429543246*sqrt(31329+(P_C_inlet-P_CO)*0.8232e7);

% we have T_HI, T_CI, W_H1, and the desired T_H, and hence need to calculate
% the corresponding W_C that agrees with the steady-state heat exchanger
% results

W_C_upper=W_C_max;
W_C_lower=0;
T_load=0;

while abs(T_load-T_H)>0.001
    W_C=(W_C_upper+W_C_lower)/2;
    [T_HO,X]=HX_Steady(T_HI,T_CI,W_H1,W_C,N); % call heat exchanger subroutine
    T_load=(T_HO*W_H1+T_HI*W_H2)/W_H;
    if T_load>T_H
        W_C_lower=W_C;
    else
        W_C_upper=W_C;
    end
end
end

```

```

% calculate the corresponding initial valve angles
Beta_bypass=acos(1-((4*A_bypass)/(pi*d_bypass^2)));
Beta_bypass_initial=Beta_bypass;
Beta_bypass_setpoint=Beta_bypass;
U_bypass_setpoint=Beta_bypass/(pi/2)*100;;

W_Ho=W_H;
BRatio=W_H2/W_H
BRatio_setpoint=BRatio;

% ram air channel
P_CI=2.058*W_C^2+0.177*W_C+P_CO; % cold side hx pressure drop
ratio_ram=P_CI/P_C_inlet;
if ratio_ram < 0.5283
    ratio_ram = 0.5283;
end
term_ram=sqrt(((2*Gamma*g)/((Gamma-1)*R))*(ratio_ram^(2/Gamma)-ratio_ram^((1+Gamma)/Gamma)));
A_ram=(W_C*sqrt(T_CI+460))/(P_C_inlet*term_ram);
Beta_ram=acos(1-((4*A_ram)/(pi*d_ram^2)));
Beta_ram_initial=Beta_ram;

% calculate the impedance at the load
K=(P_H-P_amb)/W_H^2;

fprintf('\n');
disp('Steady state temperature at the load:');
T_load
fprintf('\n\n');
disp('Steady state ram air flow rate:');
W_C
fprintf('\n\n');

% calculate the A,B,C,D matrices for the chosen flow regime
if (W_H1 < 0.25 && W_C < 0.1083333)
    C1=0.993415638;
    C2=0.8718;
    C3=0.52682216;
    C4=0.4041;
    [A,B,C,D]=ABCD(T_HI,T_CI,W_H1,W_C,X,C1,C2,C3,C4,N);
elseif (W_H1 > 0.25 && W_C < 0.1083333)
    C1=0.780612787;
    C2=0.6979;
    C3=0.52682216;
    C4=0.4041;
    [A,B,C,D]=ABCD(T_HI,T_CI,W_H1,W_C,X,C1,C2,C3,C4,N);
elseif (W_H1 < 0.25 && W_C > 0.1083333)
    C1=0.993415638;
    C2=0.8718;
    C3=0.822244343;
    C4=0.6044;
    [A,B,C,D]=ABCD(T_HI,T_CI,W_H1,W_C,X,C1,C2,C3,C4,N);
elseif (W_H1 > 0.25 && W_C > 0.1083333)
    C1=0.780612787;
    C2=0.6979;
    C3=0.822244343;
    C4=0.6044;
    [A,B,C,D]=ABCD(T_HI,T_CI,W_H1,W_C,X,C1,C2,C3,C4,N);
end

% *****
% The nonlinear model simulation initialization *
% *****

Interval=input('\nENTER THE DURATION OF THE SIMULATION [SECOND] :');
fprintf('\n');
disp('ENTER THE INPUT NUMBER:');
disp('1. +40 deg. F step in bleed temperature');

```

```

disp('2. -20 deg. F step in ram air temperature');
disp('3. +1 deg. F step in temperature setpoint');
Simu=input('\n');

T_H_setpoint=T_H;
T_HS=T_H;

DT=0.01;
Print_Interval=1/DT;
t=0:DT*Print_Interval/2:Interval;
t=t';
record_index=0;

Y_valve_R=0;
Y_valve_B=0;

% ram air controller proportional controller constant
%Kp_bypass=0.2;

% op7
Kp_bypass=6;
Ti_bypass=15;
Kp_ram=3;
Ti_ram=30;

% op22
%Kp_bypass=1;
%Ti_bypass=15;
%Kp_ram=0.3;
%Ti_ram=60;

M2b=0;
M2r=0;
U_bypass=0;

% introduce steady state variables
T_HI_ss=T_HI;
T_CI_ss=T_CI;
W_H1_ss=W_H1;
W_C_ss=W_C;
X_ss=X;
del_X=X-X_ss;
T_HO_ss=T_HO;

% *****
% The nonlinear model simulation starts here      *
% *****

plot_index=1;
time=0;
T_H_P(plot_index)=T_H;
T_HS_P(plot_index)=T_HS;
Beta_ram_P(plot_index)=Beta_ram;
Beta_bypass_P(plot_index)=Beta_bypass;
W_H2_P(plot_index)=W_H2;
W_C_P(plot_index)=W_C;
BR_P(plot_index)=W_H2/W_H;
%T_H_setpoint_P(plot_index)=T_H_setpoint;
%T_HI_P(plot_index)=T_HI;
%P_HI_P(plot_index)=P_HI;
%error_ram_P(plot_index)=0;
%error_bypass_P(plot_index)=0;

% setup the disturbance
if Simu==1
    T_HI=T_HI+20;
elseif Simu==2
    T_CI=T_CI+20;

```

```

elseif Simu==3
    T_H_setpoint=T_H_setpoint+1;

end

for loop_counter=0:DT:Interval;

    % -----
    % core program (executes every time step) starts here

    A_ram =(pi*d_ram^2)/4*(1-cos(Beta_ram));
    A_bypass =(pi*d_bypass^2)/4*(1-cos(Beta_bypass));

    % Calculate cold side flow and pressure
    ratio_ram = P_CI/P_C_inlet;
    if ratio_ram < 0.5283
        ratio_ram = 0.5283;
    end
    term_ram=sqrt(((2*Gamma*g)/((Gamma-1)*R))*(ratio_ram^(2/Gamma)-ratio_ram^((1+Gamma)/Gamma)));

    WC1 = (A_ram*P_C_inlet*term_ram)/sqrt(T_CI+460);
    WC2 = ((0.177^2+4*(P_CI-P_CO)*2.058)^0.5-0.177)/(2*2.058);

    while (abs(WC1-WC2)>0.00001);
        ratio_ram = P_CI/P_C_inlet;
        if ratio_ram < 0.5283
            ratio_ram = 0.5283;
        end
        term_ram=sqrt(((2*Gamma*g)/((Gamma-1)*R))*(ratio_ram^(2/Gamma)-ratio_ram^((1+Gamma)/Gamma)));
        WC1 = (A_ram*P_C_inlet*term_ram)/sqrt(T_CI+460);
        WC2 = ((0.177^2+4*(P_CI-P_CO)*2.058)^0.5-0.177)/(2*2.058);
        if WC1>WC2
            P_CI=P_CI+0.000002;
        else
            P_CI=P_CI-0.000002;
        end
    end
    W_C=(WC1+WC2)/2;

    % Calculate HX hot side flow
    W_H1=(-0.168+sqrt(0.028224+7.2*(P_HI-P_H)))/3.6;

    ratio_bypass=P_H/P_HI;
    if ratio_bypass < 0.5283
        ratio_bypass = 0.5283;
    end
    term_bypass=sqrt(((2*Gamma*g)/((Gamma-1)*R))*(ratio_bypass^(2/Gamma)-ratio_bypass^((1+Gamma)/Gamma)));
    W_H2=(A_bypass*P_HI*term_bypass)/sqrt(T_HI+460);

    % Calculate W_H
    W_H=((abs(P_H-P_amb))/K)^(1/2)*sign(P_H-P_amb);
    del_flow=(W_H1+W_H2)-W_H;

    if abs(del_flow)>0.00001

        if del_flow > 0
            P_H=P_H+0.000001;
        else
            P_H=P_H-0.000001;
        end

        % Calculate HX hot side flow
        W_H1=(-0.168+sqrt(0.028224+7.2*(P_HI-P_H)))/3.6;

        % Calculate Bypass flow
        ratio_bypass=P_H/P_HI;
        if ratio_bypass < 0.5283
            ratio_bypass = 0.5283;
        end
        term_bypass=sqrt(((2*Gamma*g)/((Gamma-1)*R))*(ratio_bypass^(2/Gamma)-ratio_bypass^((1+Gamma)/Gamma)));

```

```

W_H2=(A_bypass*P_HI*term_bypass)/sqrt(T_HI+460);

% Calculate W_H
W_H=((abs(P_H-P_amb))/K)^(1/2)*sign(P_H-P_amb);

del_flow=(W_H1+W_H2)-W_H;
end

BRatio=W_H2/W_Ho;

% heat exchanger model -----

% calculate the A,B,C,D matrices for the current flow regime
[A,B,C,D]=ABCD(T_HI,T_CI,W_H1,W_,N);

% deviations in the input matrix from steady state values
del_THI=T_HI-T_HI_ss;
del_TCI=T_CI-T_CI_ss;
del_WH1=W_H1-W_H1_ss;
del_WC=W_C-W_C_ss;

% setup the input matrix U
U(1,1)=del_THI;
U(2,1)=del_TCI;
U(3,1)=del_WH1;
U(4,1)=del_WC;

del_X=del_X+(A*del_X+B*U)*DT; % update the state, ie. T_M

% calculate the output, T_HO
Y=C*del_X+D*U;
T_HO=T_HO_ss+Y;

% end of heat exchanger model -----

% Calculate the temperature of the mixed flow
T_H=(T_HO*W_H1+T_HI*W_H2)/(W_H1+W_H2);

T_S=5.94/(0.001+W_H^0.351); % sensor time constant
T_HS=T_HS+(T_H-T_HS)*DT/T_S;

u_bypass=Beta_bypass/(pi/2)*100;

%Temp_Error=(T_H_setpoint-T_HS);
%Bypass_Error=-U_bypass;

%error_ram=(Bypass_Error); % need to investigate the cancelling property of this statement,
% temp_error can be negative,
% while bypass_error can be
% positive
%error_bypass=Temp_Error;

% ram air controller -----

% PI ram controller -----

%M1r=Kp_ram*error_ram;

%M2r=M2r+((Kp_ram*error_ram)/Ti_ram)*DT;

%U_ram=M1r+M2r;

% Valve dynamics
%Y_valve_R=Y_valve_R+(Kv*U_ram-Y_valve_R)*DT/T_V; % ??? (inside the bracket)
%Beta_ram=Beta_ram+(RamControllerOutput-Beta_ram)*DT/T_V;

```

```

% ram air valve opening angle
%Beta_ram=Beta_ram_initial+Y_valve_R;
%if Beta_ram>pi/2
% Beta_ram=pi/2;
%end
%if Beta_ram<0
% Beta_ram=0;
%end

% -----

% bypass controller -----

%M1b=Kp_bypass*error_bypass;

%M2b=M2b+((Kp_bypass*error_bypass)/Ti_bypass)*DT;

%U_bypass=M1b+M2b;

% Valve dynamics
%Y_valve_B=Y_valve_B+(Kv*U_bypass-Y_valve_B)*DT/T_V; % ??? (inside the bracket)
%Beta_bypass=Beta_bypass+(BypassControllerOutput-Beta_bypass)*DT/T_V;

% Valve opening angle
%Beta_bypass=Beta_bypass_initial+Y_valve_B;
%if Beta_bypass>pi/2 Beta_bypass=pi/2; end
% if Beta_bypass<0 Beta_bypass=0; end

% -----

% core program ends
% -----

time=time+DT;
record_index=record_index+1;

if record_index==Print_Interval/2
disp('Time simulated (%)');
disp(round(time/Interval*100));
plot_index=plot_index+1;
record_index=0;
% Record data for plot
T_H_P(plot_index)=T_H;
T_HS_P(plot_index)=T_HS;
Beta_ram_P(plot_index)=Beta_ram;
Beta_bypass_P(plot_index)=Beta_bypass;
W_H2_P(plot_index)=W_H2;
W_C_P(plot_index)=W_C;
BR_P(plot_index)=BRatio;
%T_H_setpoint_P(plot_index)=T_H_setpoint;
%T_HI_P(plot_index)=T_HI;
%P_HI_P(plot_index)=P_HI;
%error_ram_P(plot_index)=error_ram;
%error_bypass_P(plot_index)=error_bypass;

end

end

fprintf('\nSIMULATION DONE\n');

% *****
% Plot simulation results
% *****

figure;
plot(t,T_H_P,'r-',t,T_HS_P,'b:');
xlabel('Time (sec)')
ylabel('Load Temperature (deg F)')

```

```
%figure;  
%plot(t,Beta_bypass_P,'r-');  
%xlabel('Time (sec)')  
%ylabel('Beta_b_y_p_a_s_s (rad)')  
%title('Bypass Valve Opening Angle');
```

```
%figure;  
%plot(t,W_C_P,'r-');  
%xlabel('Time (sec)')  
%ylabel('Mass flow rate (lb/s)')  
%title('Ram Air Channel Flow Rate');
```

```
%figure;  
%plot(t,BR_P,'r-');  
%xlabel('Time (sec)')  
%ylabel('BR')  
%title('Bypass Ratio');
```

## 2. MATLAB Scripts for the Linear Simulations for the Ram-Air-Plus-Bypass Control Configurations—system initialization

```

clear all;
clc;

OperatingCondition=[%Pin Ta Pa M Wh Thi
30 130 14.70 0.0 1.1 380; % mission segment data #1
35 30 14.70 0.0 1.1 250; % mission segment data #2
20 130 14.70 0.0 1.1 300; % mission segment data #3
0 0 14.70 0.0 1.1 0; % mission segment data #4
35 130 14.70 0.4 1.1 380; % mission segment data #5
35 20 14.70 0.4 1.1 380; % mission segment data #6
35 90 10.11 0.5 1.1 380; % mission segment data #7
35 10 10.11 0.5 1.1 380; % mission segment data #8
35 50 6.76 0.7 1.1 380; % mission segment data #9
35 -10 6.76 0.7 1.1 380; % mission segment data #10
35 10 4.37 0.8 1.1 380; % mission segment data #11
35 -25 4.37 0.8 1.1 380; % mission segment data #12
20 -40 2.15 0.85 1.1 380; % mission segment data #13
10 -25 2.15 0.85 1.1 380; % mission segment data #14
30 -40 2.15 0.85 1.1 380; % mission segment data #15
13 -30 2.15 0.85 1.1 380; % mission segment data #16
35 -40 2.15 0.85 1.1 380; % mission segment data #17
20 -40 2.15 0.85 1.1 380; % mission segment data #18
20 10 4.37 0.85 6.5 380; % mission segment data #19
25 -30 4.37 0.85 6.5 380; % mission segment data #20
20 50 6.76 0.7 6.5 380; % mission segment data #21
30 -10 6.76 0.7 6.5 380; % mission segment data #22
25 90 10.11 0.5 6.5 380; % mission segment data #23
35 10 10.11 0.5 6.5 380; % mission segment data #24
35 110 12.23 0.4 6.5 380; % mission segment data #25
35 15 12.23 0.4 6.5 380; % mission segment data #26
35 130 14.70 0.4 5.5 380; % mission segment data #27
35 20 14.70 0.4 5.5 380; % mission segment data #28
30 130 14.70 0.0 5.5 380; % mission segment data #29
35 30 14.70 0.0 5.5 250]; % mission segment data #30

OpConNum=input('nPLEASE CHOOSE THE OPERATING CONDITION NUMBER (1-30, typical No.#7):');
N=input('nPLEASE INPUT THE NxN HEAT EXCHANGER DIMENSION: N = '); % for steady-state calculations, we use 15x15
for accuracy

disp('ENTER THE INPUT NUMBER:');
disp('1. +20 deg. F step in bleed temperature');
disp('2. +20 deg. F step in ram air temperature');
disp('3. +5 psig step in bleed air inlet pressure');
disp('4. +5 psig step in ram air inlet pressure');
disp('5. +1% step in bleed air valve opening');
disp('6. +1% step in ram air valve opening');
Simu=input('n');

Pin=OperatingCondition(OpConNum,1); % Bleed inlet pressure in psig
T_amb=OperatingCondition(OpConNum,2); % Ambient temperature
P_amb=OperatingCondition(OpConNum,3); % Ambient pressure
Mach=OperatingCondition(OpConNum,4); % Mach number
W_H=OperatingCondition(OpConNum,5)/60; % Total bleed flow in lb/sec
T_HI=OperatingCondition(OpConNum,6); % Bleed air inlet temp. in deg. F

T_sp=190; % temperature setpoint at the load

% setup the disturbance
d_T_HI=0;
d_T_amb=0;
d_Pin=0;
d_P_amb=0;
bypass_change=0;
ram_change=0;
if Simu==1
    d_T_HI=20; % Bleed air inlet temp. in deg. F

```



```

elseif Simu==2
    d_T_amb=15; % Ambient temperature
elseif Simu==3
    d_Pin=5; % Bleed inlet pressure in psig
elseif Simu==4
    d_P_amb=5; % Ambient pressure
elseif Simu==5
    bypass_change=1 % percentage change of bypass valve opening
elseif Simu==6
    ram_change=1 % percentage change of ram valve opening
end

d_bypass=1.5; % Valve diameter of bypass in inch
d_ram=1.5; % Valve diameter of ram in inch
R=639.6; % Gas constant, inch/Rankine
g=9.80665/0.0254; % Gravity inch/sec^2
Gamma=1.4;
C_H=0.24;
C_C=0.24;
T_V=1.5; % Valve time constant
K_V=pi/2/100;

% System other variables
M=1;
m=M/(N*N);
c_m=0.65;
BR=0.1; % bypass ratio
F_rec=0.7; % Recovery factor pressure differential=0.7
A_opened_bypass=pi*d_bypass^2/4; % bypass Valve full-open area in inch^2
A_opened_ram=pi*d_ram^2/4; % ram valve full-open area in inch^2
P_HI=Pin+P_amb; % Bleed inlet pressure in psia
P_CO=P_amb; % dumping ram air into the atmosphere
P_CI=(P_amb*((1+0.2*Mach^2)^3.5)-P_amb)*F_rec+P_amb; % Ram air pressure (psia)
T_CI=(T_amb+460)*(1+0.2*Mach^2)-460; % Ram air temperature (deg. F)

d_P_CI=((P_amb+d_P_amb)*((1+0.2*Mach^2)^3.5)-(P_amb+d_P_amb))*F_rec+(P_amb+d_P_amb)-P_CI;
d_T_CI=(T_amb+d_T_amb+460)*(1+0.2*Mach^2)-460-T_CI;
d_P_HI=d_Pin+d_P_amb;

% creation of the averaging matrix AVE
for i=1:N;
    AVE(1,i)=1/N;
end

%*****%
% Initiallization starts here %
%*****%

%=====initialize the hot air bypass set point=====

W_bleedmain=W_H*(1-BR); %hot air main mass flow rate
w_bleedmain=W_bleedmain; %hot air main flow rate for each channel of heat exchanger
W_bleedbypass=W_H*BR; %hot air bypass folw rate

P_load=P_HI-1.8*W_bleedmain^2-0.168*W_bleedmain; % pressure at load

ratio_bypass=P_load/P_HI; % pressre ratio
if ratio_bypass < 0.5283;
    ratio_bypass = 0.5283;
end

term_bypass=sqrt(((2*Gamma*g)/((Gamma-1)*R))*(ratio_bypass^(2/Gamma)-ratio_bypass^((1+Gamma)/Gamma)));
A_bypass=W_bleedbypass/((P_HI*term_bypass)/sqrt(T_HI+460));
Beta_bypass_initial=acos(1-((4*A_bypass)/(pi*d_bypass^2)));
%bypass_setpoint=A_bypass/A_opened_bypass
u_bypass_initial=Beta_bypass_initial*2/pi;
%u_bypass=u_bypass_initial+bypass_change;

%=====initialize the ram air set point=====

```

```

ratio_ram_max=P_CO/P_CI; % pressre ratio
if ratio_ram_max < 0.5283;
    ratio_ram_max = 0.5283;
end

term_ram_max=sqrt(((2*Gamma*g)/((Gamma-1)*R))*(ratio_ram_max^(2/Gamma)-ratio_ram_max^((1+Gamma)/Gamma)));
W_C_max=(A_opened_ram*P_CI*term_ram_max)/sqrt(T_CI+460);
W_C_min=0;
T_load=0;

while abs(T_load-T_sp)>0.001;
    W_C=(W_C_max+W_C_min)/2;
    [T_HO,X_steady]=steadystate(T_HI,T_CI,w_bleedmain,W_C,N); % call heat exchanger subroutine
    T_load=(T_HO*W_bleedmain+T_HI*W_bleedbypass)/W_H;
    if T_load>T_sp;
        W_C_min=W_C;
    else
        W_C_max=W_C;
    end
end

P_Cin=2.058*W_C^2+0.177*W_C+P_CO; % ram air valve downstream pressure
ratio_ram=P_Cin/P_CI;
if ratio_ram < 0.5283
    ratio_ram = 0.5283;
end

term_ram=sqrt(((2*Gamma*g)/((Gamma-1)*R))*(ratio_ram^(2/Gamma)-ratio_ram^((1+Gamma)/Gamma)));
A_ram=(W_C*sqrt(T_CI+460))/(P_CI*term_ram);
Beta_ram_initial=acos(1-((4*A_ram)/(pi*d_ram^2)));
u_ram_initial=Beta_ram_initial*2/pi;
%u_ram=u_ram_initial+ram_change;

%=====Heat Exchanger model=====
for i=1:N;
    for j=1:N;
        Tm(i,j)=X_steady((i*N-N)+j);
    end
end

a=1-exp(-H_H/(N*W_bleedmain*C_H));
b=1-exp(-H_C/(N*W_C*C_C));
psi=(-W_bleedmain*C_H*a/N-W_C*C_C*b/N)/(m*c_m);
theta=W_bleedmain*C_H*a/(N*m*c_m);
phi=W_C*C_C*b/(N*m*c_m);
[A_HX,B_HX,C_HX,D_HX]=ABCD(T_HI,T_CI,W_bleedmain,W_C,X_steady,N);

%=====Other coefficients=====
K1=1.8;
K2=0.168;
C8=1/((K2^2+4*K1*(P_HI-P_load))^(1/2));

K3=2.058;
K4=0.177;
C7=2*K3*W_C+K4;

K_load=(P_load-P_amb)/W_H^2;
C10=2*K_load*W_H;

C11=W_bleedmain/W_H;
C12=W_bleedbypass/W_H;
C13=W_bleedbypass*(T_HO-T_HI)/W_H^2;
C14=W_bleedmain*(T_HI-T_HO)/W_H^2;
C15=-C11*D_HX(3)-C13+C14;
C16=C11*D_HX(4);

%D11=diff(W_bleedbypass,T_HI)
D11=-1/2*A_bypass*P_HI*term_bypass/(T_HI+460)^(3/2);
%D12=diff(W_bleedbypass,P_HI)

```

```

D12=A_bypass*2^(1/2)*(Gamma*g/(Gamma-1)/R*((P_load/P_HI)^(2/Gamma)-
(P_load/P_HI)^((1+Gamma)/Gamma)))^(1/2)/(T_HI+460)^(1/2)+1/2*A_bypass*P_HI*2^(1/2)/(Gamma*g/(Gamma-
1)/R*((P_load/P_HI)^(2/Gamma)-(P_load/P_HI)^((1+Gamma)/Gamma)))^(1/2)/(T_HI+460)^(1/2)*Gamma*g/(Gamma-1)/R*(-
2*(P_load/P_HI)^(2/Gamma)/Gamma/P_HI+(P_load/P_HI)^((1+Gamma)/Gamma)*(1+Gamma)/Gamma/P_HI);
%D13=diff(W_bleedbypass,P_load)
D13=1/2*A_bypass*P_HI*2^(1/2)/(Gamma*g/(Gamma-1)/R*((P_load/P_HI)^(2/Gamma)-
(P_load/P_HI)^((1+Gamma)/Gamma)))^(1/2)/(T_HI+460)^(1/2)*Gamma*g/(Gamma-
1)/R*(2*(P_load/P_HI)^(2/Gamma)/Gamma/P_load-(P_load/P_HI)^((1+Gamma)/Gamma)*(1+Gamma)/Gamma/P_load);
%D14=diff(W_bleedbypass,Beta_bypass)
D14=1/4*pi*d_bypass^2*sin(Beta_bypass_initial)*P_HI*term_bypass/(T_HI+460)^(1/2);
%D15=diff(W_C,T_CI)
D15=-1/2*A_ram*P_CI*term_ram/(T_CI+460)^(3/2);
%D_16=diff(W_C,P_CI)
D16=A_ram*2^(1/2)*(Gamma*g/(Gamma-1)/R*((P_Cin/P_CI)^(2/Gamma)-
(P_Cin/P_CI)^((1+Gamma)/Gamma)))^(1/2)/(T_CI+460)^(1/2)+1/2*A_ram*P_CI*2^(1/2)/(Gamma*g/(Gamma-
1)/R*((P_Cin/P_CI)^(2/Gamma)-(P_Cin/P_CI)^((1+Gamma)/Gamma)))^(1/2)/(T_CI+460)^(1/2)*Gamma*g/(Gamma-1)/R*(-
2*(P_Cin/P_CI)^(2/Gamma)/Gamma/P_CI+(P_Cin/P_CI)^((1+Gamma)/Gamma)*(1+Gamma)/Gamma/P_CI);
%D_17=diff(W_C,P_Cin)
D17=1/2*A_ram*P_CI*2^(1/2)/(Gamma*g/(Gamma-1)/R*((P_Cin/P_CI)^(2/Gamma)-
(P_Cin/P_CI)^((1+Gamma)/Gamma)))^(1/2)/(T_CI+460)^(1/2)*Gamma*g/(Gamma-
1)/R*(2*(P_Cin/P_CI)^(2/Gamma)/Gamma/P_Cin-(P_Cin/P_CI)^((1+Gamma)/Gamma)*(1+Gamma)/Gamma/P_Cin);
%D_18=diff(W_C,Beta_ram)
D18=1/4*pi*d_ram^2*sin(Beta_ram_initial)*P_CI*term_ram/(T_CI+460)^(1/2);

%=====bypass loop=====
%C1b=diff(A_bypass,Beta_bypass)
C1b=1/4*pi*d_bypass^2*sin(Beta_bypass_initial);
%C2b=diff(W_bleedbypass,A_bypass)
C2b=P_HI*term_bypass/(T_HI+460)^(1/2);
%C3b=diff(W_bleedbypass,P_HI)
C3b=D12;
%C4b=diff(W_bleedbypass,P_load)
C4b=D13;
%C5b=diff(W_bleedbypass,T_HI)
C5b=D11;
K_bypass=pi/2;
T_bypass=1.5;

%=====ram air loop=====
%C1r=diff(A_ram,Beta_ram)
C1r=1/4*pi*d_ram^2*sin(Beta_ram_initial);
%C2r=diff(W_C,A_ram)
C2r=P_CI*term_ram/(T_CI+460)^(1/2);
%C3r=diff(W_C,P_CI)
C3r=D16;
%C4r=diff(W_C,P_Cin)
C4r=D17;
%C5r=diff(W_C,T_HI)
C5r=D15;
K_ram=pi/2;
T_ram=1.5;

%flow sensor
T_s=5.94/(0.001+W_H^0.351);%sensor time constant

%*****STATE SPACE MODEL*****%
%      X_dot=AX+BU+HZ      %
%      Y=CX+DU+GZ      %
%*****%

%=====State Variables X at operation opint=====
X_0=[X_steady;Beta_bypass_initial;Beta_ram_initial];

%=====Inputs=====
%U=[u_bypass;u_ram];

%=====Outputs=====

```

```

%Y=[T_load;u_bypass]

%=====Disturbances=====
% d_T_CI=((T_amb+d_T_amb)+460)*(1+0.2*Mach^2)-460)-T_CI;
% d_P_HI=d_Pin+d_P_amb;
% P_load_offset=(P_HI+d_P_HI)-1.8*W_bleedmain^2-0.168*W_bleedmain
% Z=[d_T_HI;d_T_CI;d_W_H;d_P_HI;d_P_load;d_P_CI;d_P_Cin];

%=====Matrix A=====
% calculate the hot & cold heat transfer coefficients, as functions of
% TOTAL hot and cold flow rates
% initialize the A matrix with zeros
% A is (N*N+2)*(N*N+2) matrix
% term_diff_bypass=diff(W_bleedmain,Beta_bypass)
% term_diff_bypass=D14;
% term_diff_ram=diff(W_ram,Beta_ram)
% term_diff_ram=D18;
% first chunk
A=A_HX;
% Do the last two column
% N*N+1 column (wrt Beta_bypass)
A(:,N*N+1)=-B_HX(:,3)*D14;
% N*N+2 column (wrt Beta_ram)
A(:,N*N+2)=B_HX(:,4)*D18;
% Beta_bypass and Beta_ram
A(N*N+1,:)=0;
A(N*N+2,:)=0;
A(N*N+1,N*N+1)=-1/T_V;
A(N*N+2,N*N+2)=-1/T_V;

%=====Matrix B=====
for i=1:(N*N+2);
    for j=1:2;
        B(i,j)=0;
    end
end
B(N*N+1,1)=K_V/T_V;
B(N*N+2,2)=K_V/T_V;

%=====Matrix H=====
% T_HI
H(:,1)=B_HX(:,1)-B_HX(:,3)*D11;
% T_CI
H(:,2)=B_HX(:,2)+B_HX(:,4)*D15;
% W_H(W_bleedmain)
H(:,3)=B_HX(:,3);
% P_HI
H(:,4)=-B_HX(:,3)*D12;
% P_load
H(:,5)=-B_HX(:,3)*D13;
% P_CI
H(:,6)=B_HX(:,4)*D16;
% P_Cin
H(:,7)=B_HX(:,4)*D17;
% last two rows
H(N*N+1,:)=0;
H(N*N+2,:)=0;

%=====Matrix C=====
C_row1=[C11*C_HX,C15*D14,C16*D18];
C_row2=zeros(1,N*N+2);
C_row2(N*N+1)=1;
C=[C_row1;C_row2];

%=====Matrix D=====
D=[0,0,0,0];

```

```

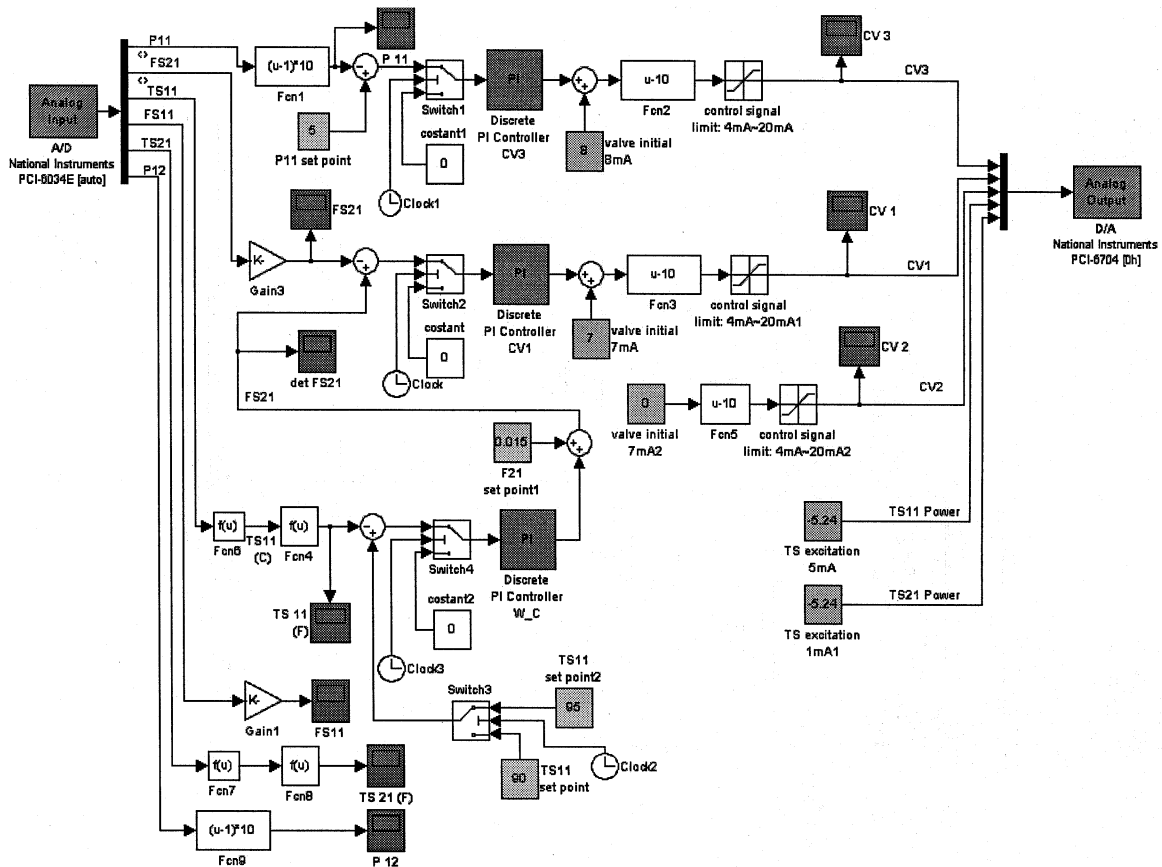
%=====Matrix G=====
G_row1=[C15*D11+C12+C11*D_HX(1), C16*D15+C11*D_HX(2), C11*D_HX(3)+C13, C15*D12, C15*D13, C16*D16,
C16*D17];
G_row2=zeros(1,7);
G=[G_row1;G_row2];

% response time of temperature sensor
T_S=5.94/(0.001+W_H^0.351)

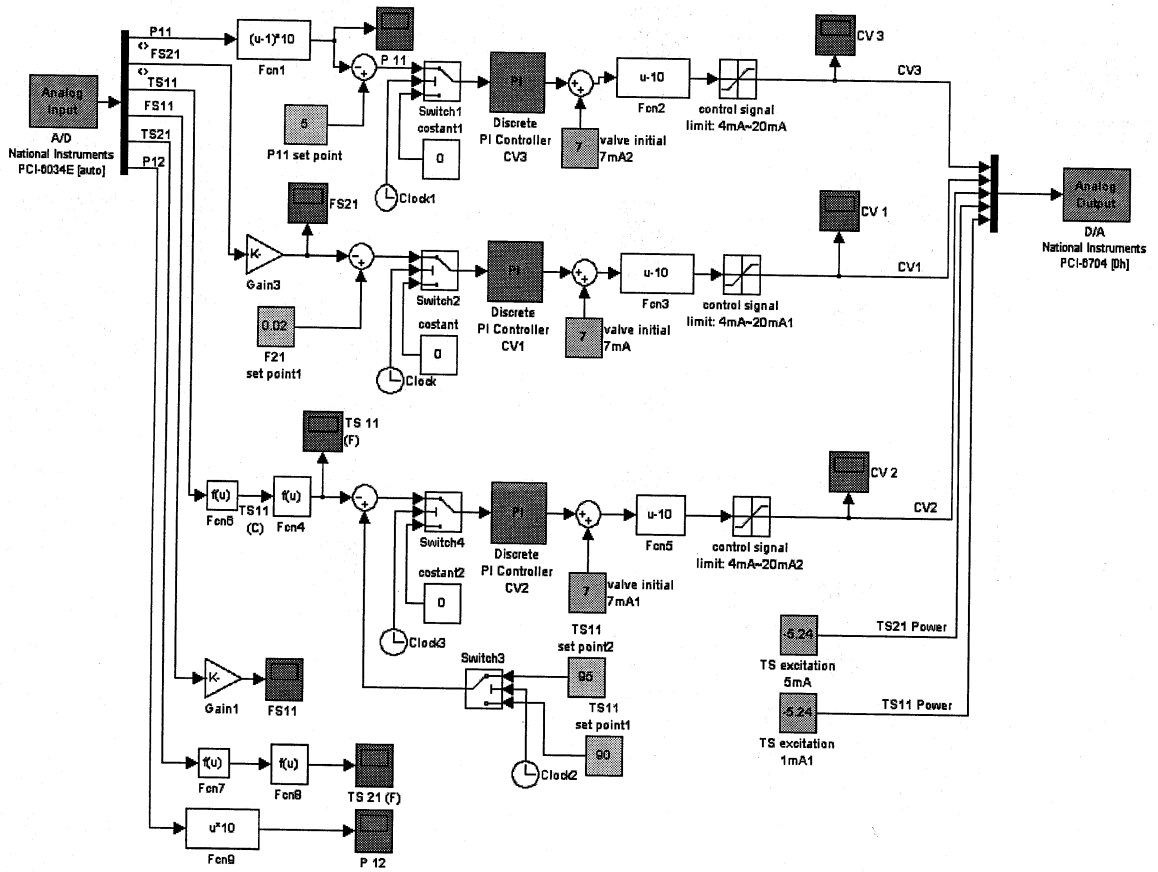
sim('rambypass_linear_openloop',300)

```

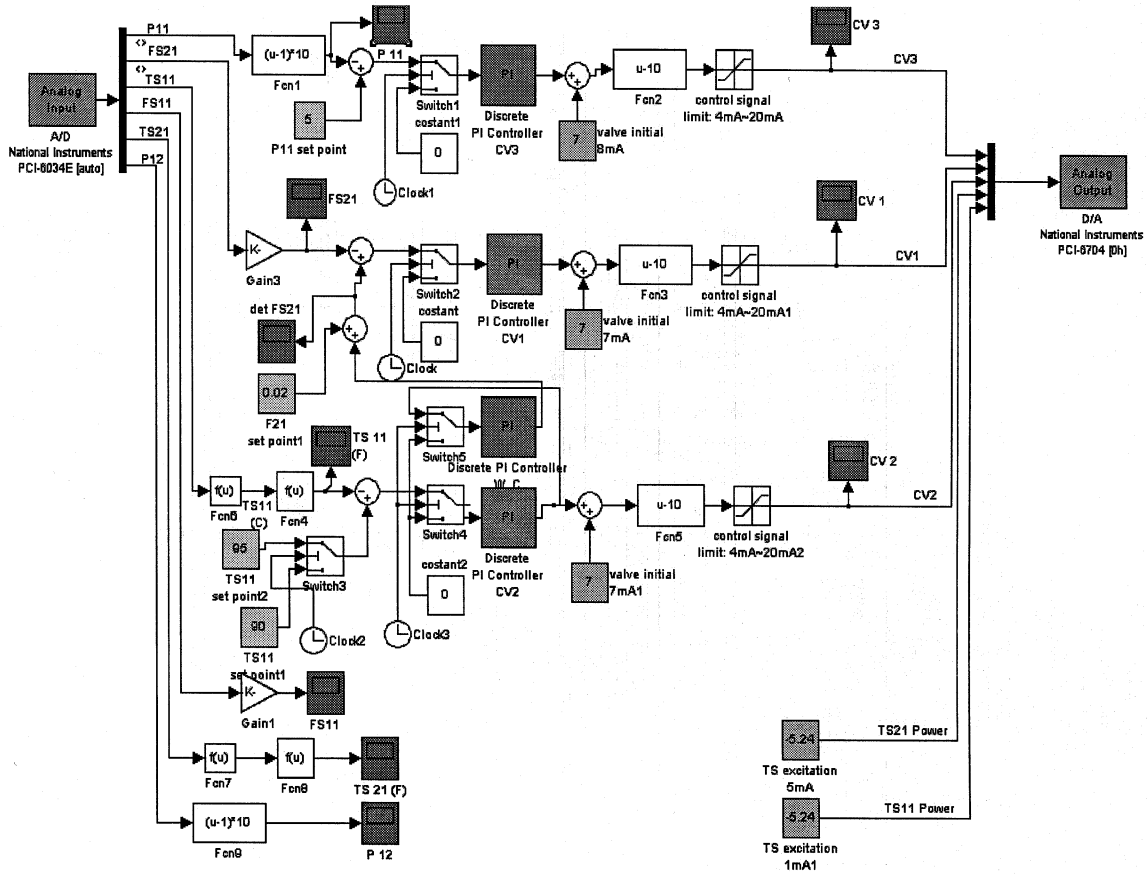
### 3. Simulink Scripts for Ram Air Control Experiments



#### 4. Simulink Scripts for Bypass Control Experiments

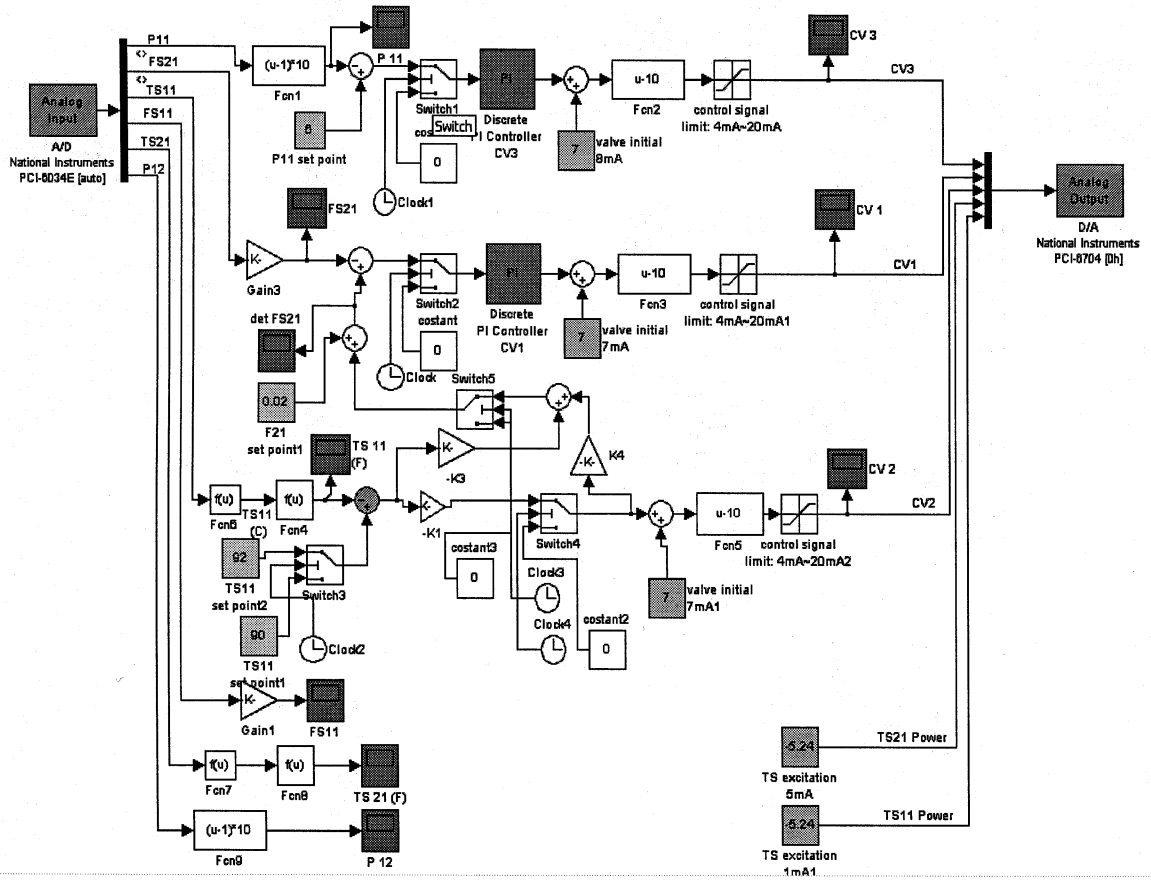


## 5. Simulink Scripts for Ram-Air-Plus-Bypass Control Experiments with PI Controller





## 6. Simulink Scripts for Ram-Air-Plus-Bypass Control Experiments with Optimal Output Feedback Control



## CURRICULUM VITAE

Name: Lan Shang

Post-secondary Educaiton and Degrees: Ryerson University  
Toronto, Ontario, Canda  
2005-2007, M.A.Sc

Beijing University of Technology  
Beijing, P.R.China  
2000-2004, B.Eng.

Honors and Awards

Ryerson Graduate Award, 2005-2007

Excellent Undergraduate Thesis Award,  
Beijing University of Technology, 2004

Excellent Graduating Student Award, Beijing  
University of Technology, 2004

Related Work Experience

Research Assistant  
Ryerson University  
2005-2007

Teaching Assistant (Part-time)  
Ryerson University  
2005-2007

Publication:

L. Shang and G. Liu, "Optimal Control of a Bleed Air Temperature Regulation System," *IEEE International Conference on Mechatronics and Automation*, Harbin, China, pp. 2610-15, Aug 2007.

